Automatic Generation of Residential Thermal Network Models for Predictive Control from Smart Thermostat Data

Charalampos Vallianos

A Thesis

In the Department

of

Building, Civil and Environmental Engineering

Presented in Partial Fulfillment of the Requirements

for the Degree of

Doctor of Philosophy (Building Engineering) at

Concordia University

Montréal, Québec, Canada

September 2023

CONCORDIA UNIVERSITY
SCHOOL OF GRADUATE STUDIES

This is to certify that the thesis prepared

By: Charalampos Vallianos

Entitled: Automatic Generation of Residential Thermal Network Models for Predictive Control from Smart Thermostat Data

and submitted in partial fulfillment of the requirements for the degree of

Doctor Of Philosophy Building Engineering

complies with the regulations of the University and meets the accepted standards with respect to originality and quality.

Signed by the final examining committee:

Dr. Charalambos Poulis — Chair

Dr. Rongling Li — External Examiner

Dr. Chunyan Lai — Examiner

Dr. Radu Zmeureanu — Examiner

Dr. Mohamed Ouf — Examiner

Dr. Andreas Athienitis — Thesis Supervisor (s)

Dr. José Candanedo

Approved by

Dr. Chunjiang An — Chair of Department or Graduate Program Director

21-Nov-23
Date of Defence

Dr. Mourad Debbabi — Dean, Faculty of Engineering and Computer Science

Abstract

Automatic Generation of Residential Thermal Network Models for Predictive Control from Smart Thermostat Data

Charalampos Vallianos, Ph.D.

Concordia University, 2023

Model Predictive Control (MPC) can help a building achieve specific objectives, such as reducing operating cost, minimizing energy consumption, or implementing demand response measures. As its name indicates, MPC relies on an accurate building model. However, determining the model structure and level of detail can be challenging. An extensive analysis on a building-by-building basis is typically required, involving significant time and cost. The task of creating a model remains a critical hurdle for the large-scale uptake of MPC.

This thesis contributes a systematic method to generate control-oriented residential building thermal models with focus on day-ahead predictions for MPC. The method relies on data from smart thermostats, since their widespread adoption provides a unique opportunity to develop advanced control strategies. The method presented here can be categorized into two main approaches: single-zone and multi-zone models.

When detailed data are available for each room, multi-zone models may provide better estimates of comfort and flexibility. Québec presents an excellent opportunity for testing multi-zone models because of its widespread utilization of decentralized electric baseboards that allow for individual room control. This research introduces a novel automatic method for multi-zone model generation and selection. The methodology starts with a very simple model and iteratively increases the complexity of the model until the model quality cannot increase further. It is then applied on data from an unoccupied experimental house in Shawinigan, Québec. The resulting 13^{th}-order model can accurately predict all 9 zone temperatures 24 hours in advance, with a Root Mean Squared Error of less than 0.5 °C and its parameters reflect the layout of the house, previously unknown to the methodology.

The method was applied in a real-time MPC framework to the experimental house during demand response events and compared to MPC using low-order models and a "business-as-usual"

(BAU) reference approach. The MPC employing the multi-zone model modeled the building thermal mass separately and managed to leverage it better to preheat more before demand response events compared to the low-order models. The MPC controller with the multi-zone model reduced electricity costs by 55% compared to the BAU scenario; it also outperformed the 40% cost reduction achieved by MPC controllers based on low-order models.

On the other hand, a single thermal zone representation can produce sufficiently accurate predictions when coupled with (uncertain) weather and occupancy forecasts. Second-order single-zone models of 7,800 houses in Ontario and Québec were used to investigate the most suitable data length, data interval and calibration horizon of building models for use in an MPC framework. Overall, models with a calibration horizon of 24 hours, data length of 7 days and time interval of 15 minutes provided the best balance between accuracy and computational resources. The models were then used to assess the large-scale deployment of MPC strategies under existing time-of-use tariffs and dynamic pricing. Results showed that the adoption of MPC can reduce the daily electricity cost on average by 16% in Ontario and by 31% in Québec, respectively.

Lastly, this thesis used smart thermostat data to model and characterize 60,000 homes across North America (the resulting model parameters have been made publicly available, enabling building archetypes and building-to-building knowledge transfer). The results showed that just modeling the indoor air temperature of the building may not suffice. Instead, single-zone models need additional states (e.g., for effective temperature of the exterior and/or interior building materials) for accurate predictions. The building time constants were computed as a means to assess building thermal storage ability.

Acknowledgements

I want to thank my supervisors Professors Andreas Athienitis and José Candanedo for their guidance and support. Your knowledge, experience, feedback, and trust in me and my work were instrumental to this PhD thesis and my growth as an academic. Thank you for giving me access to resources that honed my skills, including but not limited to: experimental facilities and setups, case studies, real measurement data, and large datasets. Thank you for giving me the opportunity to present my work in multiple international meetings and conferences.

I would like to acknowledge the financial support I received during my PhD: the doctoral research scholarship from Fonds de recherche du Québec - Nature et technologies (FRQNT), the Concordia International Tuition Award of Excellence, the Concordia Merit Scholarship, as well as funding received through the NSERC/Hydro-Québec Industrial Research Chair in Optimized Operation and Energy Efficiency: Towards High Performance Buildings held by Professor Andreas Athienitis.

I would also like to thank the whole team at Le Laboratoire des technologies de l'énergie (LTE) at Shawinigan for our fruitful collaboration, and Benoit Delcroix and Luis Rueda specifically for their help with the Experimental House for Building Energetics.

My biggest thanks to all the members, (former and current) colleagues, and friends at Concordia's Centre for Zero Energy Building Studies (CZEBS) and Solar laboratory. There is not enough space to name each one of you separately, but you all know the impact you had to my life. A special shout-out to Costa Kapsis, Vasken Dermardiros, and Matin Abtahi. I appreciate the help of Jiwu Rao and Lyne Dee.

Finally I would like to thank my family and friends for tolerating me through my PhD life. I cannot express enough gratitude for the support of my mother, father, and sister, both while growing up and during the years we lived in different continents; I am the person I am because of you. Last but not least, I want to thank Vickie Vainionpää for supporting me during the hardest times and encouraging me to follow my dreams. With you, I am a better person.

Contribution of Authors

This section explains the contribution of any author other than the author of this thesis. In all papers, Professors Andreas Athienitis and José Candanedo contributed in the form of general supervision, providing resources, reviewing and editing the final work, funding acquisition and took part in the conceptualization of the projects.

More specific contributions of coauthors of journal articles used in this thesis are explained below:

- Chapter 3: The work presented in Chapter 3 was developed as part of a larger project in collaboration with le Laboratoire des technologies de l'énergie Shawinigan and Université du Québec à Trois-Rivières. Dr. Benoit Delcroix took part in the project administration and distribution of resources. He assisted with the conceptualization of the project and provided the data and documentation on the Experimental House for Building Energetics (EHBE).

- Chapter 4: Matin Abtahi developed and calibrated the two low-order models used in the study. Drs Benoit Delcroix and Luis Rueda were in charge of the experimental setup, which is located in le Laboratoire des technologies de l'énergie in Shawinigan. They took care of the Raspberry Pi in the experimental house, its communication with the smart thermostats, as well as the data collection.

"Quotes are inherently misleading; they are often used out of context and can be twisted to support any argument at hand."

Harry, Grumpy's Bar, 2019

Contents

List of Figures

List of Tables

Nomenclature

Acronyms

ACF	Auto-Correlation Function
AIC	Akaike Information Criterion
API	Application Programming Interface
BAU	Business as usual
BEF	Building Energy Flexibility
BEFI	Building Energy Flexibility Index
BIC	Bayesian Information Criterion
CEC	Commission for Environmental Cooperation
CP	Cumulative Periodogram
CTSMR	Continuous Time Stochastic Modeling in R
DR	Demand Response
DSM	Demand Side Management
DYD	Donate Your Data
EBC	Energy in Buildings and Communities
EHBE	Experimental House for Building Energetics
FDD	Fault Detection and Diagnosis
FIT	Goodness of fit
FMI	Functional Mockup Interface
GHG	Greenhouse Gas
HVAC	Heating, Ventilation and Air-Conditioning
IEA	International Energy Agency

KPI	Key Performance Indicators
LoD	Level of Detail/Development
MAE	Mean Absolute Error
MI	Mission Innovation
MPC	Model Predictive Control
MRI	MPC Relevant Identification
NARX	Non-linear Auto-Regressive with Exogenous inputs
nCPBES	normalized Cumulative Periodogram Boundary Excess Sum
NN	Neural Network
NRMSE	Nornmalized Root Mean Squared Error
PID	Proportional Integral Derivative
PLS	Partial Least Squares
PV	Photovoltaic
R^2	Coefficient of Determination
RBF	Radial Basis Function
RC	Resistor Capacitor
RL	Reinforcement Learning
RMSE	Root Mean Squared Error
SIMEB	SIMulation Energétic des Bâtiments
TOU	Time of Use
UBEM	Urban Building Energy Model

Latin letters

A	State matrix
B	Input matrix
C	Output matrix
u	Inputs
x	States
Y	Proceeding observations
y	Outputs

$\mathcal{L}$	Likelihood function
C	Thermal capacitance (J/K)
c	Cost of heating per W installed (¢/W_{inst})
CH	Control Horizon
d	Discomfort (°Chr)
G_t	Global horizontal irradiance (W/m^2
J	Cost function
N	Number of thermostats
Nd	Total number of datapoints
p	Total number of parameters
PH	Prediction Horizon
$pole$	Real and positive pole
Q	Heating output (W)
q	Heating energy consumption per W installed (Wh/W_{inst})
R	Thermal resistance (K/W)
T	Temperature (°C)
t	Time (s)
U	Thermal conductance (W/K)

Greek Letters

α	Effective solar factor (m^2)
β	"Cost" of discomfort (¢/Khr)
Δt	Simulation timestep (s)
δ	Heating or cooling system runtime (s)
ω	Standard Wiener process
σ	Incremental variance of the Wiener process
τ	Time constant (s)
θ	Parameter vector

Subscripts

a	Ambient
c	Cooling
e	Building envelope mass
$flex$	Flexible
h	Heater/heating
i	Indoor
$inst$	installed
m	Interior thermal mass
ref	Reference
s	Sensor
set	Setpoint
sol	Solar

Superscripts

k	k-th timestep

1 Introduction

1.1 Problem statement and motivation

Reducing electricity consumption of buildings is an established research topic in the engineering field, gaining more popularity as the fight against climate change intensifies [1]–[5]. Sustainable solutions, like renewable energy sources, are a preferred alternative to polluting fossil fuel power plants. The price of photovoltaic (PV) solar panels has decreased exponentially since 1980 and continues to drop; this is mainly due to manufacturing advancements and governmental financial incentives [6], [7]. As a result, PV panels have become a familiar feature of building design and are now often found in residential areas [8], [9]. However, one of the limitations of large-scale integration of PV is the challenges it presents to the electricity grid, due to a mid-day drop of electricity demand followed by a high evening peak when the sun sets [10], [11]. An example of the effect of PV penetration on the grid is the utility grid of California and the so-called "duck curve" shown in Figure 1.1a. To handle this disparity, utilities are often forced to turn on gas-based power plants, dramatically increasing their environmental footprint.

In addition, electrification of space and water heating, along with widespread use of electric vehicles, is a practical way to reduce Greenhouse Gas (GHG) emissions and has been attracting interest in the last years [13], [14]. Heating electrification, in particular, can result in energy savings of up to 20% and GHG emissions reduction of up to 30% [15]. The electrification of space heating, however, means an increased electricity demand across the building sector, especially in cold climates. Such an increase in demand can put a strain on the electrical grid infrastructure and pose a similar challenge for the utilities. Figure 1.1b shows the effect of electric space heating in Québec, where approximately 80% of residential buildings use electricity for heating in the winter. Although electrification of space heating can dramatically increase the winter peak power

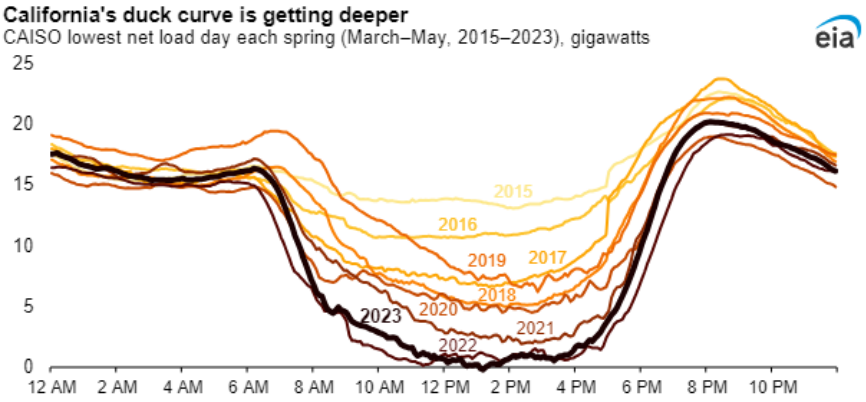

(a) The case of California and the effect of PV penetration [11]

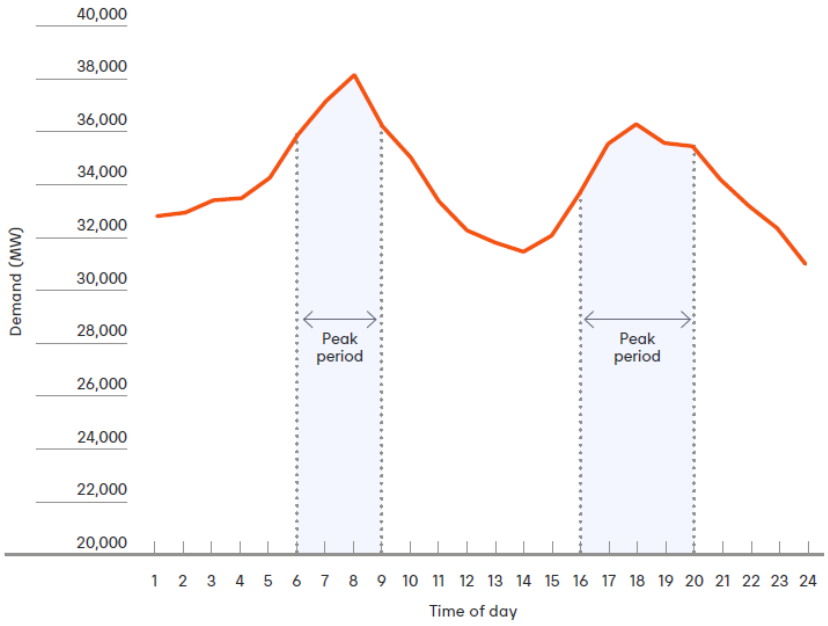

(b) The case of Québec and the effect of electric space heating (2019) [12]

Figure 1.1: The "duck curve": Grid power demand profile

demand [16], advanced controllers for space conditioning have been identified as a potential way to mitigate the problem [17].

One way to tackle this problem is to optimize the profile of the consumption side, using Demand Response (DR) programs. This can happen through incentives from the utility to the customer. Hydro-Québec recently introduced the rates flex D and Winter credit option, starting from the winter of 2019-2020 [18]. These programs increase the cost of electricity during peak hours of especially cold days (6 to 9 a.m. and/or 4 to 8 p.m.); it is up to the residents to take measures to reduce their consumption. Instead of burdening the customer with a series of actions that may decrease their thermal comfort, the building could automatically leverage energy flexible concepts, such as the electrical and thermal storage of the building [19]–[23].

Building Energy Flexibility (BEF) is defined as "the ability to manage the demand and generation according to climate conditions, user needs, and energy network requirements" [24]. The need to quantify the BEF in respect to a reference profile has led to the definition of the Building Energy Flexibility Index (BEFI), which represents the ability of a building to change its power demand during a specific period requested by the grid [25].

Currently, most buildings are equipped with a thermostat that attempts to keep the indoor temperature close to a deterministic temperature setpoint [26]. In some cases, that setpoint can be manually adjusted by the occupant [27]. The smart thermostats available on the market still use the same control method, but they make it easier for the owner to change said setpoint, either remotely via the Internet or with preset weekly schedules. However, with the increased adoption of smart thermostats, there is an opportunity to use the building data of homeowners to develop advanced and smarter control strategies. These strategies optimize the setpoint throughout the season, allowing the building to match supply and demand on days with different weather and occupancy conditions. Smart thermostats can provide access to data of unprecedented detail. Not only is the approximate location of the home available to the thermostats company, but also the thermostats can log temperature and humidity readings of multiple zones inside a house. The occupancy of the building (as a result of a motion sensor) is often available, as well as the output or the runtime of the installed heating/cooling systems.

The importance of data in energy modeling has been recognized by the global research community, and an International Energy Agency (IEA) Energy in Buildings and Communities Programme

(EBC) Annex is in progress: IEA EBC Annex 81: Data-Driven Smart Buildings. The Annex aims to increase access to low-cost high-quality data and develop software analytics and applications that provide real time optimization. This Annex is a result of expert discussions during Innovation Challenge 7: Affordable Heating and Cooling of Buildings of the Mission Innovation Programme (MI), a global initiative of 24 countries and the European Commission, working to accelerate clean energy innovation [28].

The importance of building thermal models, and their role in estimating energy flexibility, as well as energy flexibility itself has been the topic of IEA EBC Annex 67: Energy Flexible Buildings, which concluded in 2019, and IEA EBC Annex 82: Energy Flexible Buildings Towards Resilient Low Carbon Energy Systems, which focuses on large-scale applications, such as clusters of buildings or communities.

1.2 Objectives

In light of the above considerations, this thesis investigates how data from smart thermostats can be leveraged to develop models of residential buildings in an automated way for use in control applications. It follows two main parallel directions: one based on detailed multi-zone models of houses equipped with multiple smart thermostats and one based on more simplified single-zone models of houses with central heating.

Detailed multi-zone models can predict the indoor temperature and energy consumption of separate zones in a house, providing better insight into the thermal comfort conditions of each zone and enabling a more accurate estimation of energy flexibility. Space electrification and smart thermostats now provide individual zone control in many houses; a common sight in Québec are rooms heated by separate baseboards with their own setpoints. However, multi-zone models can have very complicated structures and require the expertise of an engineer to develop and calibrate. In this direction, the thesis aims to:

Objective 1.1 Propose a novel methodology for automated thermal model generation aimed for 24-hour predictions for MPC applications using smart thermostat data. The automated methodology will be evaluated on measured data from an experimental house in Québec.

Objective 1.2 Compare the performance of the detailed multi-zone RC model to simple low-order models for real-time online MPC. The performance of the models will be evaluated in a real-time MPC framework during demand-response events in Québec using with real weather forecasts.

However, many houses lack the ability to control the heating output of different zones individually, either because of the nature of the heating system itself (e.g., central heating) or because of a lack if instrumentation. In these cases, the house can be represented as a single zone. The single-zone representation of a house assumes that the whole house indoor air is well mixed and at the same temperature. The resulting building models have low resolution but are simple, interpretable and fast. This representation is also useful in large-scale district or community simulations, where the sheer number of models requires them to be simple and computationally efficient. In this research direction, the thesis aims to:

Objective 2.1 Calibrate single-zone RC building models aimed for 24-hour predictions for MPC applications using smart thermostat data. It will investigate the effect of data resolution, data length and calibration horizon on the model accuracy and assess the effect of large-scale application of MPC in the residential sector.

Objective 2.2 Create a database of single-zone building models calibrated on measured data from smart thermostats. This database will be publicly available for large-scale applications by the scientific community. The thermal storage ability of the models will be evaluated by estimating the time constants of each house.

1.3 Thesis structure

This is a manuscript-based thesis. It is an alternative to the traditional chapter-based thesis, and it contains multiple chapters based on accepted or submitted manuscripts. More specifically, the layout of the thesis is as follows:

Chapter 1 Introduction: The chapter presents the problem and motivation behind the thesis. It shows the current state of the grid, how renewable energy sources and electrification are affecting it and the role of buildings and building control.

Chapter 2 Literature review: The chapter presents the state-of-the-art literature and identifies research questions and gaps, which this thesis will address and attempt to answer. It starts with the current building control practices and shows the need for advanced control strategies, introducing Model Predictive Control (MPC). The chapter connects MPC to energy flexibility and presents the different types of building models. The challenges resisting the widespread implementation of MPC in the residential sector are identified, as well as the role of smart thermostats. Finally, the chapter presents recent studies regarding large-scale modeling of buildings and automated model generation, development and evaluation. ***Although the literature review is presented in a holistic and comprehensive manner, its contents include sections from the literature review of each separate published manuscript.***

Chapter 3 Automatic generation of multi-zone RC models using smart thermostat data from homes: The chapter presents a novel automated methodology for multi-zone model generation of residential buildings. The multi-zone models are calibrated with smart thermostat data and predict the indoor air temperature up to 24 hours ahead. The methodology starts with a very simple model and iteratively increases the complexity of the model until the model quality cannot increase further. It is then applied on data from an unoccupied experimental house. The resulting model can accurately predict all 9 zone temperatures 24 hours in advance, and its parameters reflect the layout of the house, previously unknown to the methodology. This chapter is a published manuscript[1].

Chapter 4 Online model-based predictive control with smart thermostats: Application to an experimental house in Québec: The chapter tests the impact of model resolution and structure on the performance of MPC implementation in an unoccupied experimental house equipped with smart thermostats. A high-order multi-zone model is developed using the automated methodology presented in Chapter 3, and is compared to two low-order models. The three models are used to apply real-time MPC. While all three models successfully preheat the house before demand-response events, outperforming the reference reactive controller, the high-order model reduced electricity cost and energy consumption the most. This chapter is a published manuscript[2].

Chapter 5 Application of a large smart thermostat dataset for model calibration and

[1] C. Vallianos, A. Athienitis, and B. Delcroix, "Automatic generation of multi-zone RC models using smart thermostat data from homes," *Energy and Buildings*, vol. 277, p. 112 571, 2022. DOI: 10.1016/j.enbuild.2022.112571.

[2] C. Vallianos, M. Abtahi, A. Athienitis, *et al.*, "Online model-based predictive control with smart thermostats: Application to an experimental house in Québec," *Journal of Building Performance Simulation*, pp. 1–17, 2023. DOI: 10.1080/19401493.2023.2243602.

Model Predictive Control implementation in the residential sector: The chapter uses smart thermostat data from 7,800 houses in Ontario and Québec to investigate the most suitable data length, data interval and calibration horizon of building models for use in an MPC framework. It then uses the most suitable models to apply MPC on a large scale, showing a systematic reduction in electricity cost and improvement of thermal comfort by successful preheating. This chapter is a published manuscript[3].

Chapter 6 Application of a large smart thermostat dataset for model calibration and Model Predictive Control implementation in the residential sector: The chapter uses smart thermostat data from 60,000 houses in North America to calibrate single-zone thermal models. The work adapts an existing automated model selection and evaluation procedure for stochastic building modeling. It analyzes the final model structures and assesses their ability to be used in MPC applications. It investigates the correlation of building parameters with available metadata and it estimates the time constants of the houses as a measure of their thermal storage capabilities. This chapter is based on a submitted manuscript[4].

Chapter 7 Conclusion and future work: The chapter concludes the thesis. Potential for future work is discussed. The research contributions are presented, along with a list of all published journal articles, presented conference papers, and other non-refereed work.

[3]C. Vallianos, J. Candanedo, and A. Athienitis, "Application of a large smart thermostat dataset for model calibration and Model Predictive Control implementation in the residential sector," *Energy*, vol. 278, p. 127 839, 2023. DOI: 10.1016/j.energy.2023.127839.

[4]C. Vallianos, J. Candanedo, and A. Athienitis, "Thermal modeling for control applications of 60,000 homes in north america using smart thermostat data," *Energy and Buildings*, p. 113 811, 2023. DOI: 10.1016/j.enbuild.2023.113811.

2 Literature review

This section will go over the current practices in building control, identify their disadvantages and propose solutions of advanced controls found in the literature. It will discuss these solutions and what is preventing them from becoming the new baseline in building control. It will explain the role of measured data from smart thermostats in potential residential building control. It will conclude by presenting research gaps and questions that the next chapters will fill and answer.

2.1 Current control practices

Currently, a typical building is being controlled in a reactive, closed-loop way, based on the difference between a setpoint and a measured value. These setpoints are deterministic and they are often constant or scheduled based on the time of day (day vs. night) or the output of a sensor (e.g., an occupancy sensor or a CO_2 sensor).

Most heating and cooling systems are controlled using a two-level control structure: the local-loop control and the supervisory control. On the lower level, the local-loop control makes sure that an actuator meets a specific setpoint, e.g., the indoor air temperature of a room may be controlled by turning on or off the heating element in the baseboard heater of that room. In order to meet these setpoints, buildings often rely on cycling on-off controllers and PID controllers, and mainly on the Proportional (P) and the Integral (I) component. Purely proportional control can lead to oscillatory behavior when the system does not reach steady-state after a disturbance. This behavior leads to the system constantly *hunting* for the setpoint. On the other hand, integral control can lead to instabilities when the integral time is reduced to a value comparable to the time constant of the controlled system [29]. As a result, PI controls may struggle when used with slower systems, e.g., when controlling a radiant floor heating system [30].

On the higher level, supervisory control specifies setpoints and time-dependent modes of operation. This usually translates to several setpoints (e.g., air temperatures, duct static pressure setpoints etc.) being chosen with energy usage and power demand minimization in mind, but while maintaining thermal comfort [31]. Supervisory control is particularly useful in demand-response frameworks, when the participants receive a signal from the utility and activate a building "mode" that tries to minimize non-critical operations. An example of supervisory control is when the occupant of a house reduces the indoor temperature setpoint from 21°C to 19°C at night before going to bed. Supervisory control often requires the expert knowledge and experience of building managers or consultant engineers.

The reactive nature of traditional control makes it a bad candidate for DR events and cannot leverage energy flexible concepts in the built environment. Reactive control is defined by current disturbances, such as weather conditions and occupancy patterns. The need to shift peak power demand makes the use of a different, more advanced control strategy necessary. Recently, commercial and industrial buildings have started using model-based control strategies, like MPC as a way to decrease energy consumption or power demand, while maintaining thermal comfort.

2.2 Model-based control and Model Predictive Control (MPC)

Model Predictive Control (MPC) is a control approach that uses a model of a system (e.g., a building) and a forecast of the disturbances to said model (e.g., weather forecast, occupancy etc.) to predict the response of the system and decide on the best action for the near future. To decide on the best action, a cost function J is minimized over a prediction horizon while respecting the constraints and the resulting action is applied on the system for a control horizon. The general mathematical framework is shown in Figure 2.1.

The cost function differs for different building applications and can be the cost of operation, the cost of electricity, the overall energy consumption, the power peak demand, the energy flexibility of the house etc. The most common constraints are temperature range limitations for thermal comfort, equipment capacity limitations and equipment runtimes. Thermal comfort can be implemented as a hard constraint or a soft constraint. Hard constraints cannot be violated and correspond to (2) in Figure 2.1, while soft constraints are included in the cost function, increasing the cost when

$$J(x_0) = \min_{u_0,\ldots,u_{N-1}} \sum_{k=0}^{N-1} l_k(x_k, u_k) \quad \text{Cost function} \quad (1)$$

$$\text{subject to } (x_k, u_k) \in \mathcal{X}_k \times \mathcal{U}_k \quad \text{Constraints} \quad (2)$$

$$x_0 = x \quad \text{Current state} \quad (3)$$

$$x_{k+1} = f(x_k, u_k) \quad \text{Dynamics} \quad (4)$$

Common types of cost functions.

Cost function type	Mathematical description
Quadratic cost	$l_k(x_k, u_k) = x_k^T Q x_k + u_k^T R u_k$
Linear cost	$l_k(x_k, u_k) = c^T u_k$
Probabilistic cost	$l_k(x_k, u_k) = \mathbb{E}[g_k(x_k, u_k)]$

Common types of constraints.

Constraints type	Mathematical description
Linear constraint	$Ax_k \leq b$
Convex quadratic constraint	$(x_k - \bar{x})^T Q (x_k - \bar{x}) \leq 1, Q \succcurlyeq 0$
Chance constraint	$\mathbb{P}[Ax_k \leq b] \geq 1 - \alpha, \alpha \in (0, 0.5]$
Second order cone constraint	$\|Ax_k + b\|_2 \leq Cx_k + d$
Switched constraint	if *condition*, then $A_1 x_k \leq b_1$ else $A_2 x_k \leq b_2$
Nonlinear constraint	$h(x_k, u_k) \leq 0$

Figure 2.1: Generic mathematical MPC framework with common cost functions and constraints. Source: Oldewurtel, Parisio, Jones, *et al.* [32]

thermal comofrt criteria are not met. They are multiplied by a large factor in the cost function, often called *cost of discomfort*, to ensure that they are prioritized over energy savings or demand reduction. In general, soft constraints are preferable, because they are more practical and do not hinder optimization convergence. Both hard and soft constraint approaches have been used by many studies. For example, Huchuk, Sanner, and O'Brien [33] and Seal, Boulet, and Dehkordi [34] included thermal comfort as a soft constraint, with the former penalizing it when the indoor temperature deviated from the (heating or cooling) setpoint by more than 2 °C and the latter using a temperature setpoint range of 1 °C when the house was occupied and 5.5 °C when the house was unoccupied. On the other hand, Cole, Powell, Hale, *et al.* [35] and Bianchini, Casini, Vicino, *et al.* [36] used a hard constraint, with the former having a setpoint range of 4 °C when the house was occupied and 8 °C when the house was unoccupied and the latter a range of 2 °C (occupied) and 6 °C (unoccupied). An in-depth discussion on thermal comfort constraints used in building control can be found in [37].

When the MPC algorithm can account for disturbances that are bounded to a specific range the procedure is called robust MPC (rMPC), whereas when the distribution of the disturbance in that range is also known and used in the MPC, then the procedure is called stochastic MPC (sMPC) [38].

MPC requires building energy modeling [39], in order to capture the dynamics of the high thermal inertia of their building materials [30], [40]. Challenges regarding the building energy model have been described as the "bottleneck of the whole procedure" of MPC by Prívara, Váňa, Žáčeková, *et al.* [41]. Henze [42] estimates that model creation and calibration accounts for 70% of project costs.

2.3 Building energy flexibility

Advanced or "smart" controllers, and MPC controllers specifically, have been identified as a potential way to reduce peak power demand and facilitate Demand Response (DR) measures by utilizing concepts that leverage energy flexibility, such as electrical [20] and thermal [23] storage of a building, or by interacting with the grid in a transactive way [17].

Building energy flexibility has been defined by International Energy Agency's Energy in Buildings and Communities (IEA-EBC) Annex 67 "Energy Flexible Buildings" [24] as "the ability to manage the demand and generation according to climate conditions, user needs, and energy network requirements". Dozens of Key Performance Indicators (KPIs) can be used to characterize energy flexibility. In most cases, this quantification takes place in comparison with a baseline or benchmark [43]. Energy and demand flexibility are tightly connected to Demand Side Management (DSM), an encompassing name given to techniques that aim to modify customer load patterns, and more specifically to its Demand Response aspect, which offers incentives to the customers to encourage change in their consumption patterns [44].

For example, Athienitis, Dumont, Morovat, *et al.* [25] have defined a Building Energy Flexibility Index (BEFI), which measures and compares the flexible power demand over a specific period to a reference power demand for the business-as-usual case. The average dynamic BEFI at time t and for duration Δt is calculated using Equation (2.1), where Q_{ref} is the total power consumption under a reference energy consumption profile and Q_{flex} is the total power consumption of the flexible strategy (in this case the MPC strategy).

$$BEFI_{\Delta t}(t) = \frac{\int_t^{t+\Delta t} Q_{ref}(t)dt - \int_t^{t+\Delta t} Q_{flex}\,(t)\,dt}{\Delta t} \tag{2.1}$$

2.4 Building thermal modeling

Both MPC strategies and energy flexibility applications rely on building models. In the former case, the building model is necessary to obtain the optimal control; in the latter, the model is used to establish the baseline energy demand profile needed to quantify energy flexibility [45].

Building thermal energy models are used to predict the thermal response of a building. Dur-

ing the design stage they are used to simulate the behavior of the building for different design parameters and observe their effect on energy demand, thermal comfort and control strategies [46]. Depending on the objective and the problem at hand, the whole building may be modeled, or just the section of interest. Thermal models can vary in complexity, accuracy and computational demand.

According to the ASHRAE Handbook of Fundamentals [47], there are two distinct approaches to modeling: forward (classical) and data-driven (inverse), based on the objective of the investigation. The models created with the forwards approach, also called white-box models, use detailed physics-based mathematical equations to model the building and its components. On the other hand, the models created with the data-driven approach, called black-box models, are based completely on available data.

2.4.1 White-box models

White-box models are based on physical principles like the conservation of mass and energy and their parameters are often identified from the geometry and materials of the building and its equipment. White-box models are mainly used during the design stage of the building. White-box models can be further subdivided into simplified and elaborate or detailed [48], based on the number of assumptions and simplifications (e.g., linearizations) that take place during the modeling stage. There is no clear boundary about the number of simplifications that differentiate simple and detailed models.

White-box models are the product of a lot of popular building simulation tools or engines (EnergyPlus, TRNSYS, DOE-2, etc.). These models produce high-detail models and (a) require a great deal of knowledge about the building, which is often not available but assumed [49]–[52], (b) demand expertise to create and are time consuming to calibrate [53], or (c) the available building data are insufficient to calibrate these models [54]–[57]. Their complexity makes them poor candidates for control applications, when computational resources are of importance [58].

Coakley, Raftery, and Keane [59] presented a detailed review of model development and calibration. They highlight the inability of detailed Building Energy Performance Simulation software to properly predict the actual metered building energy use.

2.4.2 Black-box models

A rising technique, both in popularity and accuracy, is using artificial intelligence and neural networks to model, predict and control the thermal behavior of buildings. Black-box models rely on statistics and machine learning. They are trained with measured data, they can be highly accurate, and they do not require the expertise of a building engineer [60]. They have the advantage that no information is needed about the physical properties of the buildings [61]. They can also be adaptive and self-learning [62].

Many different types of neural networks have been tried, like simple multi-layer perceptrons [62]–[64] or Radial-Basis Function networks (RBF) [65]. The main parameter that has to be defined is the number of neurons for each network. In most cases this number results either from heuristics or from a self adjusting mechanism implemented in the algorithm. Time series models have also been used to model buildings, most commonly some kind of variation of Non-linear AutoRegressive models with eXogenous inputs (NARX) [66], [67].

Data-driven models represent a correlation, a mapping of sorts between the inputs and the outputs. To establish this mapping the model is trained on data (called the training set). As the number of neurons and layers increases, so does the degrees of freedom of the model. More degrees of freedom increase the capacity to capture the various factors correlating the inputs to the outputs, but also increase the amount of data needed in the training set. Since this mapping is established using the training set, the ability of the model to extrapolate is limited.

A limitation of black-box models is overfitting: the network yields good results during the training phase, but it is performs well only on the training data. This approach results in lower accuracy when new data are presented, and leads to poor generalization ability. There are multiple techniques developed to to avoid overfitting. In some cases the available training set is divided into two batches. One is used to train the data and the other one is used to validate the generalization ability of the network. Another method is to apply some kind of pruning and/or growing mechanism to determine the proper size of the network [67].

Although black-box models can describe non-linear phenomena with great accuracy, they have low generalization between different buildings, which makes building-to-building comparisons of models difficult, and are not an ideal candidate to optimize operation, because they are trained with

data derived from conventional control strategies [30]. They require to be trained using a large number of "good quality" data and can be very computationally intensive [68]–[74].

During the last years there has been significant effort to constrain the parameters of a black-box models to "physical" bounds and improve their interpretability, but such research is still at the early stages [75], [76].

2.4.3 Grey-box models

Grey-box models are a combination of white- and black-box models. They implement low-order building physics and use statistical methods to calibrate their parameters form measured data. A very common representation of grey-box models is the resistance-capacitance (RC) model, or thermal network [77]. They have fewer parameters than white-box models, making them much faster to calibrate, and at the same time they have a better extrapolation ability than black-box models [78]. Grey-box models are relatively accurate for energy performance predictions and control applications, despite their reduced order structure [79]. Their simple structure makes them preferred candidates to be used in MPC and flexibility assessment applications [58], [80] and district-level applications [81]; compared to white-box models, they are easier to integrate into an MPC framework; compared to black-box models, grey-box models require fewer data and have the significant advantage of providing insight into the thermal behaviour of the building [82].

Harish and Kumar [83] reviewed modeling and simulation techniques of building energy systems. They identify the grey-box approach as one with great potential, especially for fault detection and diagnosis (FDD) and online control, but with a limited applicability to whole-building energy use. They conclude that the effectiveness of a control strategy depends greatly on the development and calibration of building models and that what the state-of-the-art is lacking is a systematically developed simplified building model dealing with temperature, heat and relative humidity.

Killian and Kozek [84] answered 10 questions regarding MPC in energy efficient systems. They identify the lack of a commercial tool to easily generate MPC models and the lack of modeling expert knowledge in building automation as the main disadvantage of MPC. They conclude that grey-box models represent a good trade-off between physics, expert knowledge, and data-driven approaches, and explain that building model parameterization has to happen in a building-to-building basis.

Arendt, Jradi, Shaker, *et al.* [85] compared white-, grey-, and black-box models using a real case study and different cross-validation datasets. They calibrated an EnergyPlus model, a Nonlinear AutoRegressive eXogenous model (NARX), a Neural Network (NN), and a first-, second-, and third-order RC model on data from a single room study zone (125 m^2) and a classroom (139 m^2), both unoccupied. They show that the NARX model outperforms all other models when the validation period is long (longer than 10 days) due to the accumulation of error for the RC models. For shorter horizons (3 days) the RC models accuracy is comparable to the NARX, with the second-order model outperforming it in 1 of the 4 cases.

Li, O'Neill, Zhang, *et al.* [86] wrote a critical review of grey-box modeling. They explain the fundamental aspects of grey-box models in detail and go through the most common assumptions and applications. They identify RC grey-box models as the best available choice for control applications and a good choice for building-grid interaction. The authors pinpoint the lack of a unified software solution as one of the reasons why RC models are not widely applied. They conclude that the structure and order of the model, more often than not, is chosen based on the experience of the engineer without hard proof that it is the best model for the system at hand.

Drgoňa, Arroyo, Cupeiro Figueroa, *et al.* [37] wrote a detailed review of the MPC framework. Initially they discuss the motivation behind MPC. They identify the main benefits of MPC for existing buildings as the systematic improvement of thermal comfort, with a simultaneous reduction of building energy consumption and grid flexibility services. They list 6 challenges opposing the wide-spread application of MPC. Three of those are concerned with the automated development of building energy models, automated deployment of MPC and its automated robust operation. They conclude that grey-box models are more likely to be suitable for MPC, because they require less data, are less prone to overfitting, and have higher building-to-building generalizabilty.

2.5 MPC in the residential sector and smart thermostats

Many studies identify the lack of a practical and automated methodology for the development and tuning of accurate building energy models as one of the gaps in the literature and one of the challenges hindering the wide-spread adoption of MPC [30], [37], [83], [84], [86]–[88].

The automated development of building energy models would have a great impact on residential

buildings. The residential sector accounts for 12% of the energy consumption in Canada [89], 16% in the United States [90] and 26% in the European Union [91], and could account for up to 50% of power peak consumption of countries [92]. However, applying MPC on a house would require the development of a building energy model, which in turn requires the expertise of building operators and consultant engineers, and involves significant time and resources. The high consultancy fees are not cost-efficient for the homeowners, especially when compared with the modest savings from electricity consumption reduction. This consideration stresses the need for an inexpensive solution that can be massively applied in residential buildings, eliminating the cost for individual analysis and the cost and inconvenience of retrofitting. The question then becomes whether there is an appropriate building modeling approach that can be used for mass deployment.

A secondary challenge is the data availability, quality and resolution. Zhan and Chong [93] identify three major gaps in the current literature: a holistic review of model performance evaluation and its relationship with control performance, a comparison of modeling methods within the same category (white-, grey-, and black-box) and a quantitative investigation of different modeling methods. They highlight the importance of data in quality and management in MPC. They suggest that the Level of Detail/Development (LoD) is extended to include data time series information. LoD defines the overall state of a Building Information Model during the design and construction phase. LoD is a three-digit number that corresponds to a design stage (100 as a conceptual placeholder to 500 as-built). They propose an additional 3 levels for commission (5xx), historical (6xx), and real-time operational data (7xx), where the last two digits indicate the measurement granularity and temporal resolution.

With the adoption of Internet-of-Things and smart thermostats, big data sources are becoming increasingly available. The abundance of data brought by smart thermostats can help in automated model development in multiple ways. Smart thermostats provide a valuable opportunity to develop building energy models on a large scale; these models can then be used to evaluate the aggregated impact of their control strategies on the grid. On the other hand, the data can be used on a local level to develop higher-order multi-zone models that would be used to control the heating and cooling of the house in an optimal way while maintaining thermal comfort.

MPC implementation in smart thermostats is a very promising topic in the province of Québec, Canada specifically, where electric space heating is already widely adopted in the residential sector.

According to the 2023 "State of Energy in Québec" report [94], electricity accounts for 77% of the total energy consumption of the residential building sector. When examining the distribution of energy consumption by category, space heating emerges as the primary factor, accounting for 61%. Most houses are equipped with decentralized electric baseboards, which can potentially provide high energy flexibility potential, since they allow for individual control of each room according to its purpose and need. Therefore, space heating in the residential sector is detrimental in shaping the whole province's demand profile in the winter, putting the grid under stress on very cold weekday mornings and evenings (before and after a typical work schedule).

Hydro-Québec, which is the public utility that manages the generation, transmission, and distribution of electricity in Québec, has introduced a dynamic tariff (Rate Flex-D) [95], and a smart home service with tailored instructions for energy efficiency through their subsidiary Hilo. These services provide an opportunity for homeowners to reduce their cost of electricity by shifting their load to off-peak periods and, as a result, relieve some of the pressure on the grid.

2.6 Large-scale modeling of buildings

A critical challenge when modeling buildings at a district or community level is the characterization of the dynamic response of buildings on a large scale. In this case the models are called Urban Building Energy Models (UBEM), and they are bottom-up, physics-based models that simulate the thermal performance usually on a building-to-building basis [96]. UBEMs rely on the development of architectural building archetypes, which are physics-based representations (usually a high-fidelity white-box models) that simulate single buildings as generalizable typical samples of an entire building stock [97]. Such a building archetype is often generated by sampling building parameters from available distributions or databases [98]. For example, several studies (e.g., [99]–[101]) have used the TABULA database [102], which clusters residential buildings based on size and age and includes typical building material values for various European countries. Similar studies in North America (e.g., [103], [104]) use ResStock [105], a building stock energy model based on millions of EnergyPlus simulations. The high computational cost often associated with these large-scale simulations has also created a need for surrogate models, i.e., fast statistical models that emulate high-fidelity simulations and have been trained on their inputs and outputs [106]. More in-

formation on archetype buildings can be found in [107] and a detailed literature review on existing residential high-fidelity building stock classification studies can be found in [108].

Even with archetypes, however, building model parameters often rely on a certain amount of guesswork, e.g., the wall materials and insulation are estimated based on the location and the year of the house. However, with the development of novel technologies, such as the Internet of Things and smart thermostats in particular, a substantial amount of operational data has recently become available. These data can be used to develop and calibrate fast, reduced-order models for control applications (also known as control-oriented models) or UBEM for district-level applications. Using real data to calibrate UBEMs has been proposed as a means to ensure that archetype buildings are in fact representative of a district and to estimate the actual simulation error [109]. Moreover, the lack of control-oriented models has been identified as a significant hurdle for the widespread adoption of MPC solutions on a building level [37].

John, Vallianos, Candanedo, *et al.* [110] used smart thermostat data to identify time constant values of more than 10,000 residential buildings in North America. They used an exponential decay method based on the solution of a simple 1R1C in a steady-state condition. They used only periods during the night (no solar gains), when the HVAC systems were off, and the outdoor temperature stayed relatively constant. They found that the time constants vary seasonally, being lower in the summer likely due to open windows.

Baasch, Wicikowski, Faure, *et al.* [111] used smart thermostat dataset of 4,646 houses in Ontario, Canada and New York, USA to compare different grey-box methods to derive building properties. They used 3 different methods to identify the time constant τ of a house: the energy signature, exponential decay, and an overall energy balance. They concluded that the first method showed the most unreliable results, and that the energy balance method systematically overpredicts the time constants τ compared to the exponential decay method.

Hossain, Zhang, and Ardakanian [112] used smart thermostat data from 8,884 in Canada to identify grey-box models with Bayesian neural networks. They used 3 months of data to train a Bayesian Neural Network (NN) based on a nRnC structure for each house, and they showed that the 2R2C model has the best performance. They also explored the idea of transfer learning across seasons for the same house and across different houses with similar characteristics and they showed that the models can achieve the same or better accuracy with much less data.

Doma, Ouf, Newsham, *et al.* [113] used smart thermostat data to investigate the thermal performance of 11,000 Canadian houses. They represented each house with a simple 1R1C model and used two methods to identify the model parameters: least-squares fitting of exponential decay curves and of the overall energy balance. The two methods resulted in time constant values with a median of 60 and 59 hours respectively. The authors identified the building age as the most influential parameter on the time constant and the number of floors the least.

Huchuk, Sanner, and O'Brien [33] used smart thermostat data to develop and evaluate data-driven models for residential buildings. They used ResStock [105] to generate 500 representative single-family houses in the United States. They modified the houses to match the metadata of the available houses and used EnergyPlus to simulate one year of operation. They tested three different types of control for each house: a simple deadband control, MPC using a ridge regression with history of 20 minutes and a Reinforcement Learning (RL) model-free control. The MPC controller managed to reduce the costs compared to the deadband controller, while the RL controller showed poor performance.

In a different study, Huchuk, Sanner, and O'Brien [114] used smart thermostat data from 1,000 houses in the United States to evaluate data-driven thermal models for multi-hour predictions. They compared simple 1R1C grey-box models and various black-box models, including Lasso and Ridge Regression, Random Forest and Autoregressive models with exogenous variables, to a baseline model that consisted of a constant temperature (the one of the last timestep). They showed that the first-order models were outperformed by the other models, and they suggested the order and structure of the model as the most likely explanation.

Leprince, Madsen, Miller, *et al.* [115] used data from 247 Dutch houses to calibrate stochastic single-zone models. They used the method presented in [116] and they proposed a new evaluation metric, the normalized Cumulative Periodogram Boundary Excess Sum (nCPBES), which indicates the residual auto-correlation. Based on nCPBES they classified their models as good (38%), close (38%), and poor (24%). They used the identified parameters to benchmark the building envelope insulation performance. They also published the calibrated model parameters [117].

Doma and Ouf [118] used smart thermostat data from 60,000 houses in North America to target buildings for retrofits. They calibrated a 1R1C model for each house using two methods: least-squares fitting of exponential decay curves and of the energy balance. The resulting models had

time constant values with a median of 52 hours. Then they clustered the model parameters and ranked each cluster to indicate the need for retrofit.

As the number of houses increases, methods that generate models of a higher order or with "varying" structures require significant computational resources. As a result, most of the aforementioned studies used a fixed model structure. For instance, most studies have calibrated first-order models [110], [111], [113], [114], [118]. However, these studies focused mostly on time constant estimation, most of them neglecting the effect of solar radiation in the process ([110], [111], [113], [118]).

2.7 A note on model zoning

Generally, a building should be modelled with enough thermal zones so that each zone represents a region of the building with distinct boundary or operating conditions [119]. Representing a building with only a few zones —— or even just one —— is common when using simplified or reduced-order grey-box models for control applications [80], [110], [120]–[122]. For example, studies [41], [115], [116] used a single-zone model, while [123] assumed one zone for each of the basement, first floor and second floor. Representing a large space with one thermal node may estimate correctly the overall energy consumption, but modeling a house with a higher number of zones can be beneficial in situations in which quantifying occupant thermal comfort is important. One of these cases is the estimation of the energy flexibility of a house in a smart-grid interaction framework [25], where the zoning definition can influence the estimation of energy flexibility potential [124].

However, deciding the structure of the multi-zone model is not as straightforward as with the low-order models. Not all zones exchange heat or interact with each other, nor are all of them affected by solar radiation. On one hand, including all parameters in the calibration process would over-parameterize the model and pose identifiability problems, while, on the other hand, creating a model by identifying which zones exchange heat through studying the floor plans has to be done manually and requires the time and expertise of an engineer.

2.8 Automatic model generation for MPC

In Section 2.4.3, grey-box models were identified as the best candidates for control and district level applications. However, choosing the model structure and order (i.e., the thermal capacitances and resistances) is not a straightforward task and doing it without help from an engineer with consistent and accurate results is necessary for the development of an automated methodology for MPC.

2.8.1 Model identifiability

A major challenge arises as the complexity of the model increases: the problem of parameter identifiability [125]–[127]. Identifiability can be divided into structural identifiability and local (or data-dependent) identifiability [128].

Structural identifiability refers to the appropriateness of a given model structure for the problem at hand. It relates the identifiability of a model to its structure and it depends only on the model order and the parameter set [128]. A model with very few parameters and low order may lack the ability to accurately describe the physical phenomena that define the system. On the other hand, a model with too many parameters — or equivalently of too high an order — is an over-parameterized model. This parameter redundancy makes multiple combinations of parameter values correspond to the same model output, therefore having multiple "optimal" parameter set solutions. Coakley, Raftery, and Keane [59] call this effect "equifinality" or "model indetermancy", meaning that the calibration of different models with available data can result into models with accurate predictions, but with different structures with each other, or even structures "incompatible" with reality. Over-parameterization is the most common reason for identifiability problems in building thermal modeling [123], [125]–[127].

Data-dependent identifiability relates the identifiability of a model to the data it is calibrated with and it only depends on the initial state of the system and its inputs [128]. It expresses that even if a model is structurally identifiable, the dataset used may be of poor quality and not contain enough thermal dynamics information for the model calibration. Ljung [129] proposes to excite the system with a variety of inputs in an open-loop fashion in order to ensure that the dataset will contain enough information for the system identification.

The sampling time of the measured data used in the calibration should result from the purpose of the prediction of the model and be short enough to encompass enough thermal dynamics information, but not too short to be subject to high measurement errors and noise. In general, for successful calibration, the dataset needs to include sufficient dynamic information, i.e., to have many datapoints dispersed in the model input dimensional space [116]. For models that predict the therrmal dynamics of buildings there are studies that suggest 15-minutes intervals are sufficient [80].

In practice, both the structural and data-dependent identifiability of a model are not a binary state, i.e., they extend over the whole range from identifiable to non-identifiable. Moreover, structural and data-dependent identifiability are not independent to each other; for example, models of higher order generally need to be trained on larger datasets.

2.8.2 Automated model selection

Bacher and Madsen [116] developed a model selection methodology for building heat dynamics and applied it on an experimental setup. They proposed a forward selection procedure that iteratively adds complexity to the model, stopping when the more complex model does not statistically increase the quality of the model.

Prívara, Váňa, Žáčeková, *et al.* [41] introduced a two-stage procedure to choose building models for MPC applications. They start by iteratively increasing the number of inputs until the prediction ability of the model cannot be improved. Then, with the inputs set fixed, they identify the minimum order of the model that maximizes model quality. They validated their method using a TRNSYS model.

Prívara, Cigler, Váňa, *et al.* [130] used Partial Least Squares (PLS) as an answer to structural identifiability challenges. PLS is a frequently used solution in situations with multicollinearity problems. The number of principal components is a case-specific hyperparameter that is often evaluated using cross-validation. They applied their methodology both on a TRNSYS model and on a real campus building, showing increased model quality.

Reynders, Diriken, and Saelens [131] compared the robustness of identified black-box and grey-box models for day-ahead predictions and simulations of the thermal response of a dwelling. They compared black-box models with different inputs and grey-box models with different structures. The data used in the calibration come from a detailed model developed in Modelica. They conclude

that the best models are the 3rd-order grey-box model and the black-box model with all the available inputs, having satisfactory accuracy for day-ahead predictions. They emphasize the importance of the data used in the calibration, showing that free-floating conditions do not allow the identification of robust reduced-order models.

Coninck, Magnusson, Åkesson, *et al.* [132] developed a toolbox for grey-box identification and tested it on data from 2 experiments. It is written in Python, but it is based on a Modelica library with thermal building models and HVAC models. The toolbox compares different models and finds the one that fits the measured data the best. The building models have to be manually developed. The tested models were tested for models of up to two thermal zones.

Wang, Chen, and Li [123] proposed a model development methodology for RC models. Their methodology starts with a very complex model and iteratively deletes parameters based on their ratio of standard error over the identified parameter estimate. The methodology works better as the number of data points increases and the simplifications greatly reduce the number of model calibrations needed for the final model. They applied the methodology on measured data from a low-energy house. They used on zone for each floor of the house and showed that the final model can accurately predict the temperature of the house.

Arroyo, Spiessens, and Helsen [133] presented a methodology for the identification of multi-zone grey-box models. They compare a centralized model to a decentralized one (where each zone is identified independent of the others) and a single-zone model. They used an emulator building of BOPTEST to compare the three strategies and showed that the centralized model outperforms the decentralized and has similar accuracy as the single-zone model. When performing MPC with the identified models the centralized model showed the best results with the minimum possible comfort violations.

Leprince, Madsen, Miller, *et al.* [115] presented a method for automatic model selection of residential building models. The model selection tries a number of pre-set models structures and the metric used was the normalized Cumulated Periodogram Boundary Excess Sum, which expresses how much the cumulative periodogram of the response of a model deviates from white noise. They applied the methodology on data from 247 Dutch buildings, creating a model for each, 93 of which were identified as good. They used the resulting models to cluster the buildings based on their thermal characteristics.

2.8.3 A note on MPC-oriented models

Models created to be used in an MPC framework may have a slightly different focus from other control-oriented models, especially when it comes to the evaluation of the models. MPC models need to ensure accurate predictions over the whole prediction horizon, not just one timestep like traditional control models [53]. In most building MPC applications that would mean a model that can consistently and accurately predict indoor temperatures up to 24 hours ahead.

One calibration technique used to ensure accuracy over the prediction horizon is the *MPC Relevant Identification* (MRI), which minimizes the multi-step prediction error [41], instead of the one-step prediction error. During the MRI at timestep k the model uses the temperatures of timestep k and inputs (heating outputs, internal gains and weather conditions) of timestep k to predict the temperatures of timestep $k+1$. The temperatures for the timesteps after $k+1$ are not available at timestep k, therefore the model is using its own predicted temperature for timestep $k+1$ to estimate temperature $k+2$, etc.

Many studies have shown that MRI yields models with better accuracy in the prediction horizon, but significantly increases the computational resources needed [120], [134]–[138]. It has been reported that MRI may not be beneficial when the model order is correct, but the data noisy [139]. Since the calibration horizon affects the parameter estimation, Wang and Chen [87] suggest that it is selected based on the purpose of the model itself.

2.8.4 A note on practical implementation of MPC

Another factor necessary for successful MPC implementation is disturbance forecasts, i.e., the forecast of any non-controllable input to the building system. The most common disturbances are the weather conditions (exterior temperature and solar radiation) and internal heat gains (occupancy schedules, equipment etc.). Carlucci, De Simone, Firth, *et al.* [140] presented a systematic review of occupant behavior models. They concluded that most studies use data-driven methods to predict either occupant presence, occupant interaction with building devices, or both. Weather forecasts can be included in the form of a data-driven linear model [32], with stochastic [141] or adaptive [142] mechanisms to increase their accuracy. However, it is easier to use an online weather forecast service, which usually uses advanced climate models [37].

2.9 Model evaluation and benchmarking

There are multiple metrics for the performance evaluation of building energy models [41], [93]. The most commonly used metrics include the Root Mean Squared Error (RMSE), shown in Equation (2.2), the coefficient of determination R^2, shown in Equation (2.3) and the goodness of fit FIT, shown in Equation (2.4). FIT is equal to $1 - NRMSE$, where NRMSE is the Normalized Root Squared Error.

$$RMSE = \sqrt{\frac{1}{Nd}\sum_{i=1}^{Nd}\left(T_i - \hat{T}_i\right)^2} \tag{2.2}$$

$$R^2 = 1 - \frac{var\left(T_i - \hat{T}_i\right)}{var\left(T_i - \bar{T}\right)} \tag{2.3}$$

$$FIT = 1 - NRMSE = \left(1 - \frac{\sqrt{\sum_{i=1}^{N}\left(T_i - \hat{T}_i\right)^2}}{\sqrt{\sum_{i=1}^{N}\left(T_i - \bar{T}\right)^2}}\right) \cdot 100\% \tag{2.4}$$

To evaluate and compare models during the model selection procedure, the aforementioned metrics would have to be estimated and compared by performing cross-validation. A cross-validation technique would ensure that the model selection procedure is not prone to overfitting. However, such an approach would significantly increase the computational resources needed, as the optimization procedure of the calibration process would have to run multiple times (e.g., 10 times in the case of a 10-fold cross-validation).

Another way to compare models to each other is through the Akaike Information Criterion (AIC) [143] and the Bayesian Information Criterion (BIC) [144]. They are both founded on information theory and they penalize both overfitting and underfitting [145]. They do not provide any insight as to how good the prediction of a model is. Both criteria do not have a physical meaning or a meaning by themselves; they are only meaningful as a comparison between different models that were calibrated using the same dataset [146]. The model with the lower AIC or BIC predicts the model better. The very nature of BIC and AIC does not allow for comparison of a model with

one-step ahead predictions with one with multiple-step ahead predictions.

The BIC and AIC do not need to be used in a cross-validation manner, reducing the computational time significantly. The BIC inherently penalizes complex structures more than AIC. Because of that, the BIC will be used in the following model selection. It is given by Equation (2.5), where *Nd* is the number of datapoints, *p* is the number of calibrated parameters and $\mathcal{L}^*$ is the maximized likelihood function of the model with parameters θ^* given observed temperature data *T*.

$$BIC = -2\ln\left(\mathcal{L}^*\left(\theta^*|T\right)\right) + p\ln\left(Nd\right) \tag{2.5}$$

Assuming that the model errors are independent and sampled by a gaussian distribution, the BIC can be written as shown in Equation (2.6) [147].

$$BIC = Nd\ln\left(\frac{\sum_{i=1}^{Nd}\left(T_i - \hat{T}_i\right)^2}{Nd}\right) + p\ln\left(Nd\right) \tag{2.6}$$

A third way to evaluate whether the model captures building thermal dynamics properly is to test the residuals for whiteness, since the model structure assumes white-noise residuals [87]. This is often done using the auto-correlation function (ACF) and cumulative periodogram (CP) of the residuals. The CP is a Fourier transformation of the autocovariance function of a stationary process. If the model residuals correspond to white noise, then the CP should be a straight line. If the normalized cumulative periodogram differs significantly from the one of white noise, then the null hypothesis that the residuals are white noise can be rejected. In that case the residuals show signs of periodic patterns and indicates that there are thermal dynamics that the model fails to capture. The ACF represents the same concept as the CP, but in the time domain instead of the frequency domain. Leprince, Madsen, Miller, *et al.* [115] introduced the normalized Cumulative Periodogram Boundary Excess Sum, or nCPBES, facilitating the automated evaluation of building models. The nCPBES is essentially the sum of all the instances the CP of the residuals exceeds the boundaries where white-noise residuals would (statistically) reside. If the nCPBES is 0, or in practice less than a small value (e.g., 0.1) then the residuals are considered white noise and the model is considered to capture well the building thermal dynamics.

Drgoňa, Arroyo, Cupeiro Figueroa, *et al.* [37] argue that one of the challenges hindering the

wide adoption of advanced control strategies, and MPC in particular, is the lack of a standard way to benchmark them against each other and against reference reactive control. In the last years there have been multiple studies and frameworks addressing this issue.

Pallonetto, Mangina, Milano, *et al.* [148] developed SimApi, an open source smart grid software infrastructure that enables co-simulation between a building energy model and cloud-based energy management systems. The main contribution of the work is an Application Programming Interface (API) that works as a decoupler between the control algorithm and the building, essentially enabling the development and testing of intelligent controls. The authors tested it using an EnergyPlus model.

Scharnhorst, Schubnel, Fernández Bandera, *et al.* [149] developed Energysym, a building model library to test and benchmark building controls. It is based on python and the building models are based on EnergyPlus and Modelica. The building models developed with Modelica use first-order models for envelopes and the zone temperature limits are constant.

Blum, Arroyo, Huang, *et al.* [150] developed BOPTEST, a building optimization testing framework that integrates high-fidelity building simulation using Modelica and the Functional Mockup Interface Standard (FMI). The framework is similar to Energysym, but provides more flexibility for the user. The building models are very detailed and developed in Modelica.

All these automated and comprehensive frameworks are being developed to be able to test and evaluate control strategies, but they do not deal with the model generation and development itself.

2.10 Research questions

Through careful review of the literature, certain research gaps and research questions have been identified. They are summarized here and this thesis will try to answer them to the best of its ability.

- Is there an automated way to develop and calibrate multi-zone residential models? Are they accurate for 24-hour predictions for MPC applications?
- How can smart thermostats assist the practical implementation of MPC? Are low-order models sufficient for MPC? How do they compare in practice to detailed multi-zone models?

- Do single-zone control-oriented models need a different calibration approach? How much data do they need and at what temporal resolution to produce accurate 24-hour predictions?
- What is the aggregated impact of MPC if it was widely adopted by residential buildings? How much can a homeowner benefit from MPC?
- Urban Building Energy Modeling relies on detailed white-box models of architectural building archetypes. Is it possible to create a database of fast control-oriented models? Can the models be clustered based on their metadata (e.g., age or size of home)?

3 Automatic generation of multi-zone RC models using smart thermostat data from homes[1]

3.1 Abstract

An automated methodology that generates sufficiently accurate building models is essential for both the adoption of advanced control strategies like Model Predictive Control, and the estimation of building energy flexibility required for building-grid interactions. This paper presents such a methodology for the generation of multi-zone resistor-capacitor models of residential buildings. The models are calibrated using smart thermostat data and predict the indoor air temperature up to 24 hours ahead. The methodology starts with a very simple model and iteratively adds one parameter at a time; the parameter that increases the quality of the model the most, as measured with the Bayesian Information Criterion. When the quality of the model cannot be improved any further, the procedure is reversed to delete any redundant parameters. The algorithm concludes when neither adding nor removing a parameter increases the model quality. The algorithm is applied on measured data from an experimental facility, a bungalow house in Québec, Canada. The resulting model can accurately predict all 9 zone temperatures 24 hours in advance with an RMSE of 0.44 °C. An examination of the estimated parameters shows that they reflect the layout of the house, previously unknown to the methodology.

[1] C. Vallianos, A. Athienitis, and B. Delcroix, "Automatic generation of multi-zone RC models using smart thermostat data from homes," *Energy and Buildings*, vol. 277, p. 112 571, 2022. DOI: 10.1016/j.enbuild.2022.112571.

3.2 Introduction

The benefits of advanced heating and cooling strategies have been well researched and verified by multiple studies, with Model Based Control strategies having a prominent role [152]. Specifically, Model Predictive Control (MPC) has been a major topic of research in intelligent building control and operation in the last couple of decades, with studies showing that MPC can reduce energy consumption while simultaneously maintaining thermal comfort [32], [120], [153], [154].

Challenges regarding the building energy model have been described as the "bottleneck of the whole procedure" of MPC by Prívara, Váňa, Žáčeková, *et al.* [41]. Henze [42] estimates that model creation and calibration accounts for 70% of project costs. Many studies identify the lack of a practical and automated methodology for the development and tuning of accurate building energy models as one of the gaps in the literature and one of the challenges hindering the wide-spread adoption of MPC [37], [83], [84], [86].

Building Energy Models are often categorized into white-box, black-box and grey-box models. White-box models are based on physical principles (conservation of mass, energy and momentum), while black-box models rely on statistical treatments of measured data and machine learning [155]. Grey-box models are a combination of the two; they retain some physical meaning, but they are simpler than white-box models. Their parameters are calibrated using measured data, as opposed to being calculated based on assumptions. One of the most common grey-box model representations is the resistance-capacitance (RC) model, or thermal network [77].

Li, O'Neill, Zhang, *et al.* [86] wrote a critical review on grey-box modeling, explaining the fundamental principles. They identify RC models as the best choice for both control and district-level applications — an idea shared by other studies [30], [80], [83], [84], [87], [88]. Li, O'Neill, Zhang, *et al.* present an exhaustive review of studies using grey-box models. They conclude that the structure and order of the model, more often than not, is chosen based on the experience of the engineer without hard proof that it is the best model for the system at hand.

3.2.1 Literature review

Choosing the order and the structure of the model (model selection), without help from the engineer and with consistent and accurate results is necessary for the development of an automated methodology for MPC. However, a major challenge arises as the complexity of the model increases: the problem of parameter identifiability [125]–[127]. Identifiability can be divided into structural identifiability and local (or data-dependent) identifiability [128]. Data-dependent identifiability happens when data do not contain enough information to allow for (accurate) model identification and depends only on the initial state of the system and system inputs, while structural identifiability is related to model structure and depends only on model order and the parameter set [128]. The most common reason for identifiability problems in building energy modeling is an over-parameterized model (or parameter redundancy) [123], [125]–[127]. As a result, there are multiple combinations of parameter values that correspond to the same model output, and therefore multiple "optimal" parameter set solutions.

Bacher and Madsen [116] developed a model selection methodology for building heat dynamics and applied it on an experimental setup. They proposed a forward selection procedure that iteratively adds complexity to the model, stopping when the more complex model does not statistically increase the quality of the model.

Prívara, Váňa, Žáčeková, *et al.* [41] introduced a two-stage procedure to choose building models for MPC applications. They start by iteratively increasing the number of inputs until the prediction ability of the model cannot be improved. Then, with the inputs set fixed, they identify the minimum order of the model that maximizes model quality. They validated their method using a TRNSYS model.

Prívara, Cigler, Váňa, *et al.* [130] used Partial Least Squares (PLS) as an answer to structural identifiability challenges. PLS is a frequently used solution in situations with multicollinearity problems. The number of principal components is a case-specific hyperparameter that is often evaluated using cross-validation. Prívara, Cigler, Váňa, *et al.* applied their methodology both on a TRNSYS model and on a real campus building, showing increased model quality.

Reynders, Diriken, and Saelens [131] compared the robustness of identified black-box and grey-box models for day-ahead predictions and simulations of the thermal response of a dwelling. They

compared black-box models with different inputs and grey-box models with different structures. The data used in the calibration come from a detailed model developed in Modelica. They conclude that the best models are the 3rd-order grey-box model and the black-box model with all the available inputs, having satisfactory accuracy for day-ahead predictions. They emphasize the importance of the data used in the calibration, showing that free-floating conditions do not allow the identification of robust reduced-order models.

Coninck, Magnusson, Åkesson, *et al.* [132] developed a toolbox for grey-box identification and tested it on data from 2 experiments. It is written in Python, but it is based on a Modelica library with thermal building models and HVAC models. The toolbox compares different models and finds the one that fits the measured data the best. The building models have to be manually developed. The tested models were tested for models of up to two thermal zones.

Wang, Chen, and Li [123] proposed a model development methodology for RC models. Their methodology starts with a very complex model and iteratively deletes parameters based on their ratio of standard error over the identified parameter estimate. The methodology works better as the number of data points increases and the simplifications greatly reduce the number of model calibrations needed for the final model. Wang, Chen, and Li applied the methodology on measured data from a low-energy house. They used on zone for each floor of the house and showed that the final model can accurately predict the temperature of the house.

Arroyo, Spiessens, and Helsen [133] presented a methodology for the identification of multi-zone grey-box models. They compare a centralized model to a decentralized one (where each zone is identified independent of the others) and a single-zone model. They used an emulator building of BOPTEST to compare the three strategies and showed that the centralized model outperforms the decentralized and has similar accuracy as the single-zone model. When performing MPC with the identified models the centralized model showed the best results with the minimum possible comfort violations.

Leprince, Madsen, Miller, *et al.* [115] presented a method for automatic model selection of residential building models. The model selection tries a number of pre-set models structures and the netric used was the normalized Cumulated Periodogram Boundary Excess Sum, which expresses how much the cumulative periodogram of the response of a model deviates from white noise. They applied the methodology on data from 247 Dutch buildings, creating a model for each, 93 of which

were identified as good. They used the resulting models to cluster the buildings based on their thermal characteristics.

3.2.2 Objective

All the studies in the existing literature focus on creating low-order models and often use information that is not usually available in a typical residential building from smart meters and thermostats (e.g., wall temperatures). However, modeling a house with a higher number of zones can be beneficial in situations in which quantifying occupant thermal comfort is important. One of these cases is the estimation of the energy flexibility of a house in a smart-grid interaction framework [25], where the zoning definition can influence the estimation of energy flexibility potential [124]. The concept of building energy flexibility is becoming increasingly important as electrification of space and water heating (especially with the use of heat pumps) and electric vehicles can be part of the answer to decreasing Greenhouse Gas Emissions (GHG) emissions [15], [156].

The aim of this study is the automated development of residential building models for control purposes. The focus is on models that can accurately predict the indoor air temperature of the house up to 24 hours in advance. These models can facilitate Model Predictive Control applications, along with quantifying the energy flexibility for building-grid interaction, especially for demand response events.

Section 3.3 explains the algorithm for automatic model development, selection, and evaluation. The case study houses and their measured data are presented in Section 3.4. The results are discussed in Section 3.5 and the article concludes in Section 3.5.3.

3.3 Methodology

This section describes the proposed methodology for the automated development of models using data from smart thermostats. The objective is to create models that can accurately predict indoor air temperatures up to 24 hours ahead. The proposed methodology aims for minimal human intervention, using information that would be available to a typical smart thermostat. These models could then be used by the thermostat alone to optimally control the heating outputs of the house, or in conjunction with a smart grid.

3.3.1 Model description

The study uses an RC model, because it is the most promising choice for control applications, as discussed in Section 3.2. Each house is divided into as many zones as the number of smart thermostats measured. Each zone is modeled with one equivalent air zone capacitance and up to one equivalent envelope node representing the building materials of the zone. Each thermal resistance is considered to be an effective thermal resistance that includes all forms of heat transfer between two zones and is assumed to be constant. The equivalent thermal network is shown in Figure 3.1.

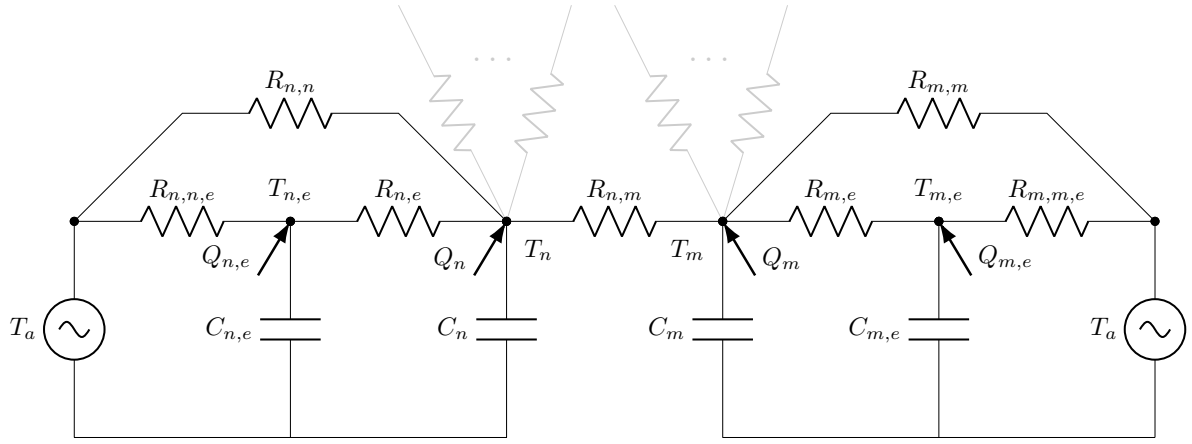

Figure 3.1: Thermal network representation for a random zone n connected to another random zone m. Each zone is modeled with one effective capacitance for the air and one for the envelope

Assuming that a house has N thermostats, it is equivalently divided into N zones. Each zone temperature T_n:

- has a thermal capacitance C_n;
- is heated with a total heating load of Q_n;
- exchanges heat with another zone temperature T_m with a thermal conductance $U_{n,m}$ (or thermal resistance $R_{n,m}$);
- exchanges heat with the exterior temperature T_a with a thermal conductance $U_{n,n}$ (or thermal resistance $R_{n,n}$);

- exchanges heat with its envelope node. The envelope node has a thermal capacitance $C_{n,e}$ with temperature $T_{n,e}$ and is connected to the zone temperature with a thermal conductance $U_{n,e}$ (or thermal resistance $R_{n,e}$). The envelope node itself is heated with a total heating load of $Q_{n,e}$ and exchanges heat with the exterior temperature T_a with a thermal conductance $U_{n,n,e}$ (or thermal resistance $R_{n,n,e}$).

That heating load for a node T_n can be further divided into the load from the heating system $Q_{h,n}$, the internal gains $Q_{i,n}$ the solar heat gains $Q_{sol,n}$: $Q_n = Q_{h,n} + Q_{i,n} + Q_{s,n} = Q_{h,n} + Q_{i,n} + \alpha_n G_t$. α_n is the solar factor of each zone (including its solar aperture) and G_t is the global horizontal irradiance. The heat transfer differential equation for air node *n* is shown in Equation (3.1) and for its respective envelope node in Equation (3.2).

$$C_n \frac{dT_n}{dt} = \sum_{m \neq n} U_{n,m} \left(T_m - T_n\right) + U_{n,e} \left(T_{n,e} - T_n\right) + U_{n,n} \left(T_a - T_n\right) + Q_{h,n} + Q_{i,n} + \alpha_n G_t \tag{3.1}$$

$$C_{n,e} \frac{dT_{n,e}}{dt} = U_{n,e} \left(T_n - T_{n,e}\right) + U_{n,n,e} \left(T_a - T_{n,e}\right) + \alpha_{n,e} G_t \tag{3.2}$$

Table 3.1 shows the number of available parameters for a building with N number of zones. For N zones there is a maximum of $\frac{N}{2}(N + 13)$ potential parameters to be calibrated:

- N thermal capacitances for the air node;
- N thermal capacitances for the envelope node;
- N solar factors for the air node;
- N solar factors for the envelope node;
- N thermal conductances between each air node and its envelope node;
- N thermal conductances between each envelope node and the outdoors;

- and every possible combination of two parameters from a set of N parameters for the thermal conductances of the air nodes: $\frac{(N+1)!}{2 \cdot (N-1)!} = \frac{(N+1)\,N}{2}$.

Table 3.1: Total number of available parameters for a building with N number of zones

	Number of parameters
Thermal capacitance of air node (C_n)	N
Thermal capacitance of envelope node($C_{n,e}$)	N
Solar factor of air node (α_n)	N
Solar factor of envelope node ($\alpha_{n,e}$)	N
Thermal conductance between air and envelope nodes ($U_{n,e}$)	N
Thermal conductance between envelope nodes and outdoors ($U_{n,n,e}$)	N
Thermal conductance between air nodes or air node and outdoors (U)	$\frac{(N+1)\,N}{2}$
Total	$\frac{N}{2}(N+13)$

The methodology presented in this paper investigates which thermal resistances and solar factors and capacitances provide the best fit between the model predicted indoor air temperatures and the measured ones, meaning that it is dealing with structural identifiability. For the model to be properly calibrated there should be no data-dependent identifiability problems. Practically this means that the measured dataset should contain enough thermal dynamics information for the system identification. Ljung [129] explains that a dataset is informative if the system is excited sufficiently by the external signals (in this case the heating outputs). Therefore, the model calibration could still struggle to succeed if the dataset contains many zones without significant heating outputs or temperature variation.

Equation (3.1) and Equation (3.2) can be written in a continuous state space form as follows, where $\mathbf{x}$ are the states $\mathbf{x} = \begin{bmatrix} T_1 & \cdots & T_N & T_{1,e} & \cdots & T_{N,e} \end{bmatrix}^T$, $\mathbf{y}$ are the outputs $\mathbf{y} = \begin{bmatrix} T_1 & \cdots & T_N \end{bmatrix}^T$ and $\mathbf{u}$ are the inputs $\mathbf{u} = \begin{bmatrix} T_a & Q_{h,1} & \cdots & Q_{h,N} & Q_{i,1} & \cdots & Q_{i,N} & G_t \end{bmatrix}^T$.

$$\dot{\mathbf{x}} = \mathbf{A}\mathbf{x} + \mathbf{B}\mathbf{u} \tag{3.3}$$

$$\mathbf{y} = \mathbf{C}\mathbf{x} \tag{3.4}$$

$$\mathbf{A} = \begin{bmatrix}
-\frac{\sum_m^N U_{1,m} + U_{1,e}}{C_1} & \cdots & \frac{U_{1,n}}{C_1} & \cdots & \frac{U_{1,N}}{C_1} & \frac{U_{1,e}}{C_1} & \cdots & 0 & \cdots & 0 \\
\vdots & \ddots & \vdots & & \vdots & \vdots & \ddots & \vdots & & \vdots \\
\frac{U_{1,n}}{C_n} & \cdots & -\frac{\sum_m^N U_{n,m} + U_{n,e}}{C_n} & \cdots & \frac{U_{n,N}}{C_n} & 0 & \cdots & \frac{U_{n,e}}{C_n} & \cdots & 0 \\
\vdots & & \vdots & \ddots & \vdots & \vdots & & \vdots & \ddots & \vdots \\
\frac{U_{1,N}}{C_N} & \cdots & \frac{U_{n,N}}{C_N} & \cdots & -\frac{\sum_m^N U_{N,m} + U_{N,e}}{C_N} & 0 & \cdots & 0 & \cdots & \frac{U_{N,e}}{C_N} \\
\frac{U_{1,e}}{C_{1,e}} & \cdots & 0 & \cdots & 0 & -\frac{U_{1,e} + U_{1,1,e}}{C_{1,3}} & \cdots & 0 & \cdots & 0 \\
\vdots & \ddots & \vdots & & \vdots & \vdots & \ddots & \vdots & & \vdots \\
0 & \cdots & \frac{U_{n,e}}{C_{n,e}} & \cdots & 0 & 0 & \cdots & -\frac{U_{n,e} + U_{n,n,e}}{C_{n,e}} & \cdots & 0 \\
\vdots & & \vdots & \ddots & \vdots & \vdots & & \vdots & \ddots & \vdots \\
0 & \cdots & 0 & \cdots & \frac{U_{N,e}}{C_{N,e}} & 0 & \cdots & 0 & \cdots & -\frac{U_{N,e} + U_{N,N,e}}{C_{N,e}}
\end{bmatrix}$$

$$\mathbf{B} = \begin{bmatrix}
\frac{U_{1,1}}{C_1} & \frac{1}{C_1} & \cdots & 0 & \cdots & 0 & \frac{1}{C_1} & \cdots & 0 & \cdots & 0 & \frac{\alpha_1}{C_1} \\
\vdots & \vdots & \ddots & \vdots & & \vdots & \vdots & \ddots & \vdots & & \vdots & \vdots \\
\frac{U_{n,n}}{C_n} & 0 & \cdots & \frac{1}{C_n} & \cdots & 0 & 0 & \cdots & \frac{1}{C_n} & \cdots & 0 & \frac{\alpha_n}{C_n} \\
\vdots & \vdots & & \vdots & \ddots & \vdots & \vdots & & \vdots & \ddots & \vdots & \vdots \\
\frac{U_{N,N}}{C_N} & 0 & \cdots & 0 & \cdots & \frac{1}{C_N} & 0 & \cdots & 0 & \cdots & \frac{1}{C_N} & \frac{\alpha_N}{C_N} \\
\frac{U_{1,1,e}}{C_{1,e}} & 0 & \cdots & 0 & \cdots & 0 & 0 & \cdots & 0 & \cdots & 0 & \frac{\alpha_{1,e}}{C_{1,e}} \\
\vdots & \vdots & \ddots & \vdots & & \vdots & \vdots & \ddots & \vdots & & \vdots & \vdots \\
\frac{U_{n,n,e}}{C_{n,e}} & 0 & \cdots & 0 & \cdots & 0 & 0 & \cdots & 0 & \cdots & 0 & \frac{\alpha_{n,e}}{C_{n,e}} \\
\vdots & \vdots & & \vdots & \ddots & \vdots & \vdots & & \vdots & \ddots & \vdots & \vdots \\
\frac{U_{N,N,e}}{C_{N,e}} & 0 & \cdots & 0 & \cdots & 0 & 0 & \cdots & 0 & \cdots & 0 & \frac{\alpha_{N,e}}{C_{N,e}}
\end{bmatrix}$$

$$\mathbf{C} = \begin{bmatrix} \underbrace{1 \cdots 1}_{N} & \underbrace{0 \cdots 0}_{N} \end{bmatrix}$$

The continuous state-space representation is converted to a discrete state-space form by assuming zero-order hold.

An additional challenge arises with the inclusion of envelope nodes, as they are not measured by typical thermostats. To address this challenge, the initial temperature of an envelope node is chosen to be the average of the equivalent initial air zone temperature and the outdoors and a warm-up period is used in the beginning of the simulation to ensure steady-periodic conditions.

Including all the thermal conductances, solar factors and envelope nodes in the model will make it over-parametrized. The automatic generation of RC models presented in this study selects which of these parameters are more likely to exist.

3.3.2 Model calibration

The set of optimal model parameters θ^* can be identified by minimizing the error between the measured and the predicted zone temperatures [41]:

$$J_{MRI} = \sum_{k=0}^{Nd-CH} \sum_{j=1}^{CH} \left(T^{k+j} - \hat{T}^{k+j|k} \right)^2 \tag{3.5}$$

where T^{k+j} is the measured temperature and $\hat{T}^{k+j|k}$ is the predicted temperature using available information up to timestep *t*, *Nd* is the total number of datapoints and *CH* is the prediction horizon during the identification, which in the rest of the text will be called *calibration horizon*.

When the calibration horizon *CH* is one timestep, the error can be referred to as one-step ahead prediction error. When the calibration horizon *CH* is greater than 1, the model is using its own predictions to predict multiple timesteps ahead. When a model is used in an MPC framework it can be beneficial to calibrate the model using multistep ahead prediction errors. When the calibration horizon is the same as the prediction horizon used in MPC the method is called MPC Relevant Identification (MRI). Many studies have shown that MRI yields models with better accuracy in the prediction horizon, although at the cost of significantly increasing the computational resources needed [120], [134]–[138]. It has been reported that MRI may not be beneficial when the model order is correct, but the data noisy [139]. Since the calibration horizon affects the parameter estimation, Wang and Chen [87] suggest that it is selected based on the purpose of the model itself.

During the MRI at timestep *k* the model uses the temperatures of timestep *k* and inputs (heating

outputs, internal gains and weather conditions) of timestep *k* to predict the temperatures of timestep *k+1*. The temperatures for the timesteps after *k+1* are not available at timestep *k*, therefore the model is using its own predicted temperature for timestep *k+1* to estimate temperature *k+2*, etc.

Building models are often non-linear in the parameter space, especially if they are of a higher order. A significant challenge of the calibration is ensuring that the optimization does not get stuck in a local minimum, but the optimal parameters correspond to the global minimum instead. This is affected by the optimization technique and the initial guess of the calibrated values required by many of these techniques. As an answer to this problem, some studies are using global optimization techniques, often in combination with local optimizers [123], [157]–[159]. On the positive side, these methods are less sensitive to initial guesses. On the negative side, they are significantly more computationally demanding and a global minimum is not guaranteed, especially when the parameter space is large. A compromise between the two methods is running a local optimization multiple times with different initial conditions. This study uses Latin Hypercube sampling (similar to [133]) to sample 10 initial guesses for each step of the model selection procedure.

This study explores the effect of the prediction horizon during identification in Section 3.5. All zone temperatures are weighted the same in the optimization procedure. The estimated parameters are bound into a certain range in order to constraint the values to have a (somewhat) physical meaning ($C_n \in (1, 10^9)$ J/K, $C_{n,e} \in (10^3, 10^9)$ J/K, $U_{nm} \in (1, 10^7)$ W/K and $\alpha_n \in (10^{-5}, 10^3)$). It should be noted that the lumped nature of the parameters may make them lose their strict physical meaning and instead represent the physics of the system more loosely.

Model performance evaluation

There are multiple metrics for the performance evaluation of building energy models [41], [93]. The most commonly used metrics include the Root Mean Squared Error (RMSE), shown in Equation (3.6), the coefficient of determination R^2, shown in Equation (3.7) and the goodness of fit FIT, shown in Equation (3.8). FIT is equal to $1 - NRMSE$, where NRMSE is the Normalized Root Squared Error.

$$RMSE = \sqrt{\frac{1}{Nd}\sum_{i=1}^{Nd}\left(T_i - \hat{T}_i\right)^2} \tag{3.6}$$

$$R^2 = 1 - \frac{var\left(T_i - \hat{T}_i\right)}{var\left(T_i - \bar{T}\right)} \tag{3.7}$$

$$FIT = 1 - NRMSE = \left(1 - \frac{\sqrt{\sum_{i=1}^{N}\left(T_i - \hat{T}_i\right)^2}}{\sqrt{\sum_{i=1}^{N}\left(T_i - \bar{T}\right)^2}}\right) \cdot 100\% \tag{3.8}$$

To evaluate and compare models during the model selection procedure, the aforementioned metrics would have to be estimated and compared by performing cross-validation. A cross-validation technique would ensure that the model selection procedure is not prone to overfitting. However, such an approach would significantly increase the computational resources needed, as the optimization procedure of the calibration process would have to run multiple times (e.g., 10 times in the case of a 10-fold cross-validation).

Another way to compare models to each other is through the Akaike Information Criterion (AIC) [143] and the Bayesian Information Criterion (BIC) [144]. They are both founded on information theory and they penalize both overfitting and underfitting [145]. They do not provide any insight as to how good the prediction of a model is. Both criteria do not have a physical meaning or a meaning by themselves; they are only meaningful as a comparison between different models that were calibrated using the same dataset [146]. The model with the lower AIC or BIC predicts the model better. The very nature of BIC and AIC does not allow for comparison of a model with one-step ahead predictions with one with multiple-step ahead predictions.

The BIC and AIC do not need to be used in a cross-validation manner, reducing the computational time significantly. The BIC inherently penalizes complex structures more than AIC. Because of that, the BIC will be used in the following model selection. It is given by Equation (3.9), where Nd is the number of datapoints, p is the number of calibrated parameters and $\mathcal{L}^*$ is the maximized likelihood function of the model with parameters θ^* given observed data T.

$$BIC = -2\ln\left(\mathcal{L}^*\left(\theta^*|T\right)\right) + p\ln\left(Nd\right) \tag{3.9}$$

Assuming that the model errors are independent and sampled by a gaussian distribution, the BIC can be written as shown in Equation (3.10) [147].

$$BIC = Nd\ln\left(\frac{\sum_{i=1}^{Nd}\left(T_i - \hat{T}_i\right)^2}{Nd}\right) + p\ln\left(Nd\right) \tag{3.10}$$

The evaluation metrics of different zones need to be aggregated in order to evaluate a single metric for each model. For that reason the RMSE and the BIC are evaluated over the residuals of all zones, while the R^2 and FIT are weighted over the variance of the data of each zone.

Residual analysis can also be used to evaluate a model. One such way is using the periodogram of the residuals, which is the discrete Fourier transformation of their autocovariance function. The cumulative periodogram can be used to test how close the residuals of the final model are to white noise. If the normalized cumulative periodogram differs significantly from the one of white noise, then the null hypothesis that the residuals are white noise can be rejected. In that case the residuals show signs of periodic patters and indicates that there are thermal dynamics that the model fails to capture. More information can be in [41], [87], [115], [116].

3.3.3 Model selection

This study proposes an algorithm for automated model selection by iteratively adding and removing parameters in the model. Table 3.2 outlines the steps of the algorithm.

At first the set of all possible parameters is defined. For N number of zones that means $\frac{N}{2}(N+13)$ parameters (see Table 3.1). The initial model consists of only the thermal capacitances representing the air nodes of the zones (total of N parameters) and the heating load inserted into each zone. This is set as the best model.

Lines 7-15 iteratively increase the parameter space of the model. One parameter at a time is added to the best model from a set of all possible parameters that are not already included in the best model. For example, during the first iteration the best model consists only of thermal capac-

Table 3.2: Algorithm for automated model selection

1 :	Define set P of all possible parameters with cardinality $\|P\| = \frac{N}{2}(N+13)$
2 :	Calibrate model only with C (C_e, U, α=0). Set as best model (ϑ, BIC)
3 :	Initialize final model (BIC*=∞)
4 :	**while** BIC < BIC* **do**:
5 :	final model ←best model (ϑ*←ϑ, BIC*←BIC)
6 :	Initialize best candidate model (BIC_c←BIC-1)
7 :	**while** BIC_c < BIC **do**:
8 :	best model ←best candidate model (ϑ←ϑ_c, BIC←BIC_c)
9 :	Define set *S* of *unused parameters* with cardinality $\|P\| - \|\theta\|$
10:	**for** *parameter* in *S* **do**:
11:	Add *parameter* to best model
12:	**for** ϑ_0 in Latin Hypercube samples **do**:
13:	Calibrate new model (ϑ_z, BIC_z)
14:	**if** BIC_z < BIC_c:
15:	best candidate model ←new model (ϑ_c←ϑ_z, BIC_c←BIC_z)
16:	Initialize best candidate model (BIC_c←BIC-1)
17:	**while** BIC_c < BIC **do**:
18:	best model ←best candidate model (ϑ←ϑ_c, BIC←BIC_c)
19:	Define set *S* of *used parameters* with cardinality $\|\theta\|$
20:	**for** *parameter* in *S* **do**:
21:	Add *parameter* to best model
22:	**for** ϑ_0 in Latin Hypercube samples **do**:
23:	Calibrate new model (ϑ_z, BIC_z)
24:	**if** BIC_z < BIC_c:
25:	best candidate model ←new model (ϑ_c←ϑ_z, BIC_c←BIC_z)

itances of air nodes, leaving $\frac{N}{2}(N+13) - N = \frac{N}{2}(N+11)$ available parameters. $\frac{N}{2}(N+11)$ models are calibrated, each having a total of N+1 parameters. The new models are calibrated 10 times with different initial conditions using Latin Hypercube sampling. The calibration minimizes Equation (3.5) over the chosen calibration prediction horizon. The BIC for one-day predictions is calculated for each model and the best candidate model is selected as the one with the smallest BIC. If the BIC of the best candidate model is smaller than the BIC of the current best model, the best candidate model replaces the best model and the algorithm repeats to step 8. If the BIC of the best candidate model is not smaller than the BIC of the best model, adding any one parameter cannot increase the quality of the model further and the algorithm continues to step 16. These steps repeat until adding another parameter does not decrease the BIC any further.

Lines 17-25 iteratively decrease the parameter space of the model. The algorithm works exactly like when increasing the parameter space, with the difference that now one parameter at a time is removed from the parameter set of the model parameters. This step is necessary because increasing the parameters one by one can lead to a final parameter set that still includes redundant parameters — parameters that did increase the quality of the model in the early iterations but became redundant in the late iterations with the addition of other parameters. It should be noted that the parameters that are removed from the model include the thermal capacitances of the air nodes themselves. When a capacitance is removed Equation (3.1) and Equation (3.2) are adjusted accordingly to represent the new heat balance equation on that node.

When neither adding nor removing any one parameter increases the quality of the model the algorithm terminates and produces the final model.

3.4 Case study

As a case study, the methodology is applied on data from an experimental facility: the Experimental House for Building Energetics (EHBE). It is an unoccupied research house of Hydro Québec, located in Shawinigan, Québec, Canada. It is a two-storey detached home with an excavated basement and a 60m^2 footprint. The wall assemblies of the building represent a typical light-weight wood framed house in Québec. The total fenestration area is 19m^2 consisting of vinyl-framed

double-glazed windows with an air gap. The orientation of the house is 35° west of south and it is heated with baseboard heaters in each room located under the window of each room and controlled by individual programmable thermostats. More information about the house and its construction can be found in [160] and [122].

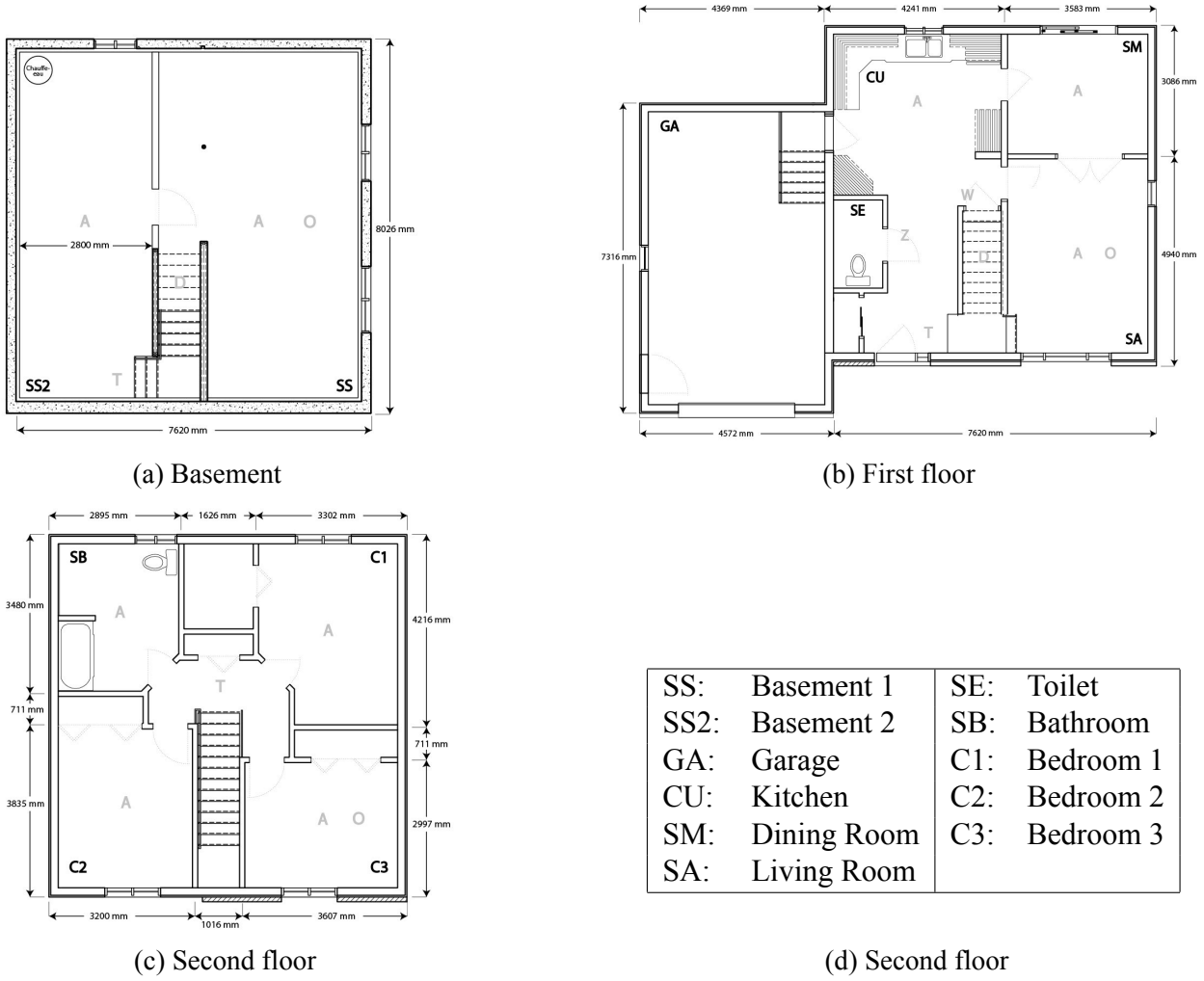

(a) Basement

(b) First floor

(c) Second floor

(d) Second floor

Figure 3.2: The layout of EHBE

The house is equipped with more than 150 sensors. The available dataset spans from March 30th 2019 to April 15th 2019, and includes air temperature (°C) and heating load (Wh) for each baseboard heater, horizontal solar irradiance (W/m^2) and outdoor ambient air temperature (°C). The layout of the house is shown in figure Figure 3.2 and the available dataset in Figure A.1 and Figure A.2 in Appendix A. The 16 days of available data are split into a training set of 14 days used in model calibration and a test set of 2 days used to evaluate the accuracy and robustness of

the final model.

The experimental house is not occupied, however, there are some internal gains related to lights that switch on/off based on schedules and plug loads used by the data acquisition system, as well as the hot water tank located in the basement. These internal gains are considered negligible. The data has a temporal resolution of 1 hour.

3.5 Results and discussion

The methodology presented in Section 3.3 was applied on the EHBE and different models were calibrated by minimizing different step ahead prediction errors: 1-step (1-hour), 6-steps (6-hours) and 24-steps (24-hours) predictions. Table 3.3 shows the RMSE, R^2 and FIT for the three cases. The model with calibration horizon of 1 hour has good 1-hour prediction accuracy (RMSE of 0.39°C and FIT of 69.2%), but the accuracy decreases significantly as it predicts further into the future. On the other hand, the model calibrated for 24-hour predictions has worse 1-hour prediction accuracy, but performs the best for 24-hour predictions, having an RMSE of 0.44°C and a FIT of 64.9%.

Table 3.3: Evaluation metrics on the training set for the different models for 1-hour, 6-hour and 24-hour ahead predictions.

	RMSE (°C)			R^2			FIT (%)		
	1-hour	6-hour	24-hour	1-hour	6-hour	24-hour	1-hour	6-hour	24-hour
Calibration horizon: 1 hour	0.39	0.44	0.52	0.903	0.874	0.821	69.2	65.5	59.0
Calibration horizon: 6 hours	0.49	0.46	0.49	0.851	0.862	0.854	61.1	62.8	61.8
Calibration horizon: 24 hours	0.44	0.42	0.44	0.878	0.887	0.876	65.4	66.4	64.9

Figure 3.3 shows the normalized cumulative periodograms for the three models. For the model with calibration horizon of 24 hours the residuals of all zones are white noise sequences. For the model with calibration horizon of 1 hour has most of the zones in the white noise deadband, with the dining room, bathroom and first bedroom deviating slightly. Out of the three models the one with calibration horizon of 6 hours performs the worst, as is shown by both its quantitative statistics and its cumulative periodogram. The model with calibration horizon of 24 hours is identified as the best candidate for applications of MPC requiring accurate day-ahead predictions.

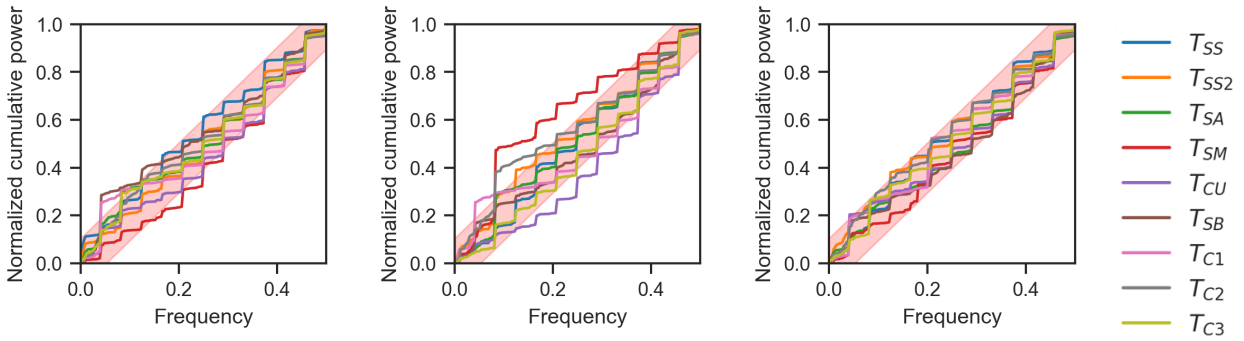

(a) 1-hour ahead (b) 6-hours ahead (c) 24-hour ahead

Figure 3.3: Cumulative periodograms of 1-step prediction errors of each zone of the models calibrated by minimizing 1-hour (a), 6-hour (b), and 24-hour (c) prediction errors. The shaded area corresponds to 5% confidence level.

3.5.1 Analysis of final model

This section investigates the results of the model with a 24 hour calibration horizon.

The progression of RMSE, R^2 and FIT throughout the automated model selection procedure is shown in Figure 3.4. The metrics show a high increase in model quality during the initial iterations, while towards the end the model metrics increase only slightly while the model is being refined, before reaching the final structure after 57 iterations. The incremental increase in quality in the final iterations indicates the possibility of stopping the procedure early, slightly sacrificing model accuracy for computational time. Choosing a threshold of the metrics that needs to be met at every iteration could stop the procedure early when time is of the essence, as is often the case in online control applications, while at the same time yielding a model with satisfactory accuracy.

Figure 3.5 shows the predicted temperatures of the model with calibration horizon of 24 hours for both the training set and the test set (the latter is denoted by the shaded area). The orange line shows the 1-hour predictions of the model and the green line shows the 24-hour predictions. For visual clarity the 24-hour predictions were not shown for every timestep, but every 24 hours. Both predictions show good agreement with the measured data.

Figure 3.6 shows the thermal network of the final model and its parameter estimates are shown in Table 3.4. The values of all estimated parameters are within logical physical bounds. Some observations and interpretations of the parameter estimates are discussed here:

- The thermal capacitance of the first basement zone (SS) is 0, but its thermal conductance with

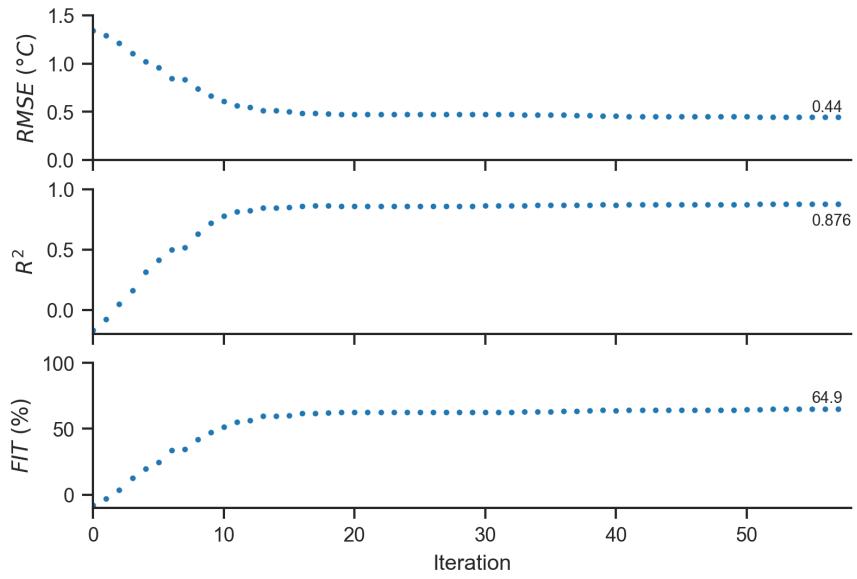

Figure 3.4: Progression of RMSE, R^2 and FIT during the proposed methodology

the second basement zone (SS2) is very high, indicating that any change in temperature of one of the zones will be immediately detected at the other. This effect is a form of aggregation of the two zones.

- A very similar effect is observed for the first floor, where the living room (SA) and the kitchen (CU) have no thermal capacitance, whereas the dining room (SM) one is high, with the thermal conductances between the three zones being high.
- An envelope node is identified for the basement and the second floor, likely a result of the high-mass concrete basement and the roof respectively.
- The heat exchange between the first floor and second floor happens mainly with the bathroom (SB) and the first bedroom (C1), which are facing the stairway.
- The solar radiation factors are present in zones facing south (since the house is oriented 35° of south).

In conclusion, the temperature predictions of the model seem to be close to the measured ones and the estimated parameters of the final model seem to reflect the layout of the house, validating the proposed methodology.

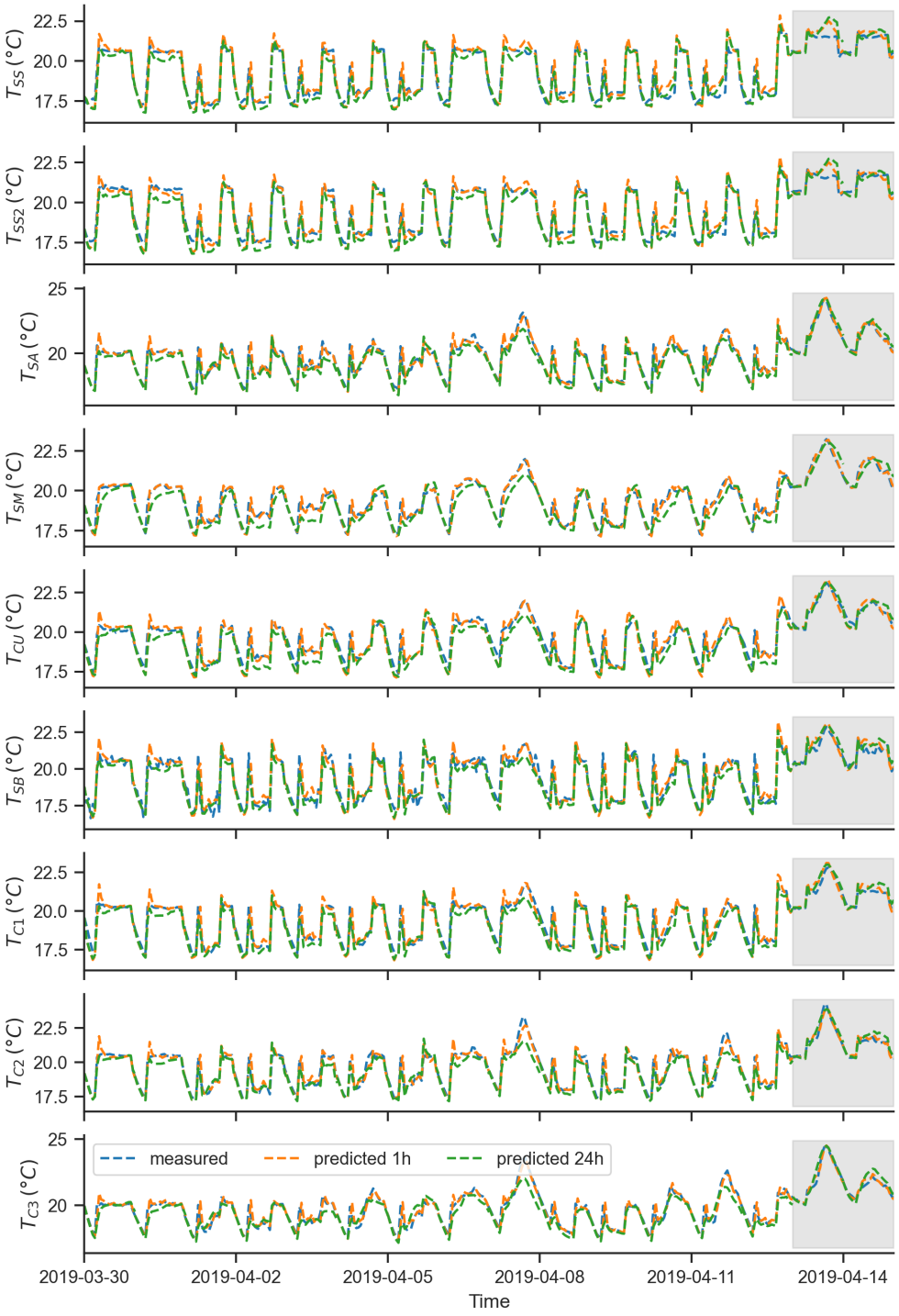

Figure 3.5: Measured and predicted zone temperatures of the EHBE. The 24-hour step predictions are shown every 24 hours for visual clarity. The shaded area denotes the two days of the test set

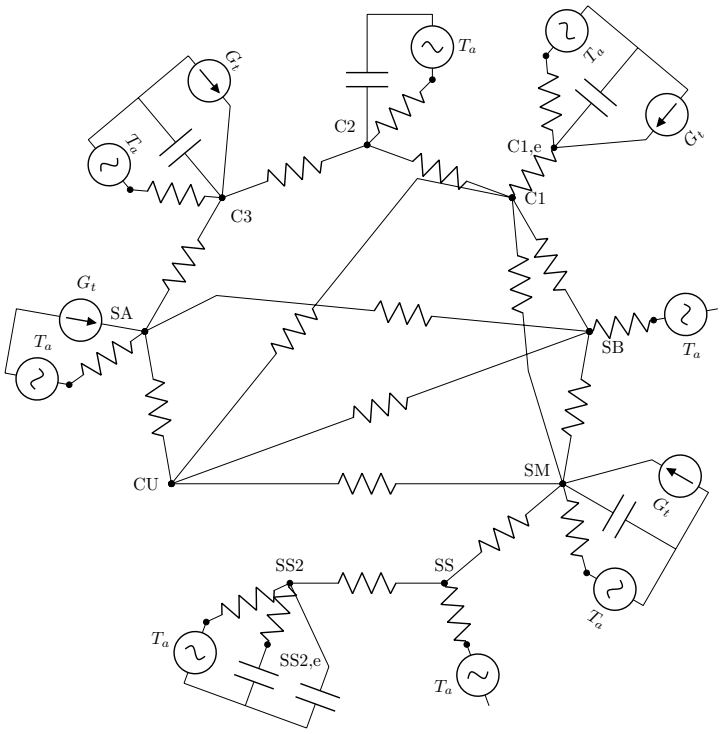

SS:	Basement 1
SS2:	Basement 2
CU:	Kitchen
SM:	Dining Room
SA:	Living Room
SB:	Bathroom
C1:	Bedroom 1
C2:	Bedroom 2
C3:	Bedroom 3

Figure 3.6: The thermal network of the final model. Its parameters are shown in Table 3.4. **Each air zone node also has a heating source from its respective baseboard heater, but these sources are omitted for visual clarity**

Table 3.4: Calibrated parameters for EHBE, corresponding to the thermal network of the final model shown in Figure 3.6

Zone n:	SS	SS2	SA	SM	CU	SB	C1	C2	C3
$U_{SS,n}$ (kW/K)	1.50e-2	8.43e+3	-	7.66e-1	-	-	-	-	-
$U_{SS2,n}$ (kW/K)	8.43e+3	1.11e-3	-	-	-	-	-	-	-
$U_{SA,n}$ (kW/K)	-	-	7.45-3	-	1.79e-1	2.51e-2	-	-	2.62e-1
$U_{SM,n}$ (kW/K)	7.66e-1	-	-	2.47e-2	1.22	9.68e-2	1.89e-1	-	-
$U_{CU,n}$ (kW/K)	-	-	1.79e-1	1.22	-	1.04e-1	2.84e-1	-	-
$U_{SB,n}$ (kW/K)	-	-	2.51e-2	9.68e-2	1.04e-1	7.05e-3	1.43e-1	-	-
$U_{C1,n}$ (kW/K)	-	-	-	1.89e-1	2.84e-1	1.43e-1	-	2.10e-1	-
$U_{C2,n}$ (kW/K)	-	-	-	-	-	-	2.10e-1	6.06e-3	3.83e-1
$U_{C3,n}$ (kW/K)	-	-	2.62e-1	-	-	-	-	3.83e-1	4.06e-3
$U_{n,e}$ (kW/K)	-	1.39e-1	-	-	-	-	1.50e-2	-	-
$U_{n,n,e}$ (kW/K)	-	-	-	-	-	-	9.19e+1	-	-
C_n (MJ/K)	-	1.53	-	1.47e+1	-	-	-	1.58e-2	3.42
$C_{n,e}$ (MJ/K)	-	4.72e+2	-	-	-	-	2.61e+3	-	-
α_n (-)	-	-	4.58e-1	2.00	-	-	-	-	8.73e-1
$\alpha_{n,e}$ (-)	-	-	-	-	-	-	1.21	-	-

3.5.2 Future work

The methodology presented is not restricted to the specific model structure, but can work by adding any kind of parameters. The final objective is an automated multi-zone model selection algorithm that will work on data from smart thermostats. Some ways that the presented algorithm can be improved are to:

- Improve the solar gains estimation. This study used a constant solar factor for each zone and its envelope node. However, the different orientation of each zone would also affect the profile of solar gains throughout the day. There are various modeling approaches proposed in the literature, such as using B-splines [161].
- Introduce a term for unmeasured disturbances. The lack of measured internal heat gains can prove to be a challenge when modeling occupied buildings. There are various approaches to modeling unmeasured idsturbances proposed in the literature, such as using the lumped disturbance method [162].

3.5.3 Conclusion

The paper proposed a methodology for automatic generation of building models using data from smart thermostats. It aims to create RC models with accurate predictions up to 24 hours in the future. Each zone with a smart thermostat of the house is modeled with one equivalent air thermal capacitance and up to one equivalent thermal capacitance for the envelope. The methodology investigates which model structure (i.e., which thermal resistances and solar factors) provide the best fit between the measured indoor air temperatures and the predicted ones.

The methodology starts with a simple model consisting only of one air thermal capacitance for each zone. Then it iteratively increases the complexity of the model by adding one parameter at a time — the parameter that increases the quality of the model the most. When adding any parameter does not further increase the quality of the model, the same procedure is followed, but reversed, removing redundant parameters. When neither adding nor removing a parameter to the model increases the quality of the model, the procedure has generated the final model and stops. The Bayesian Information Criterion was used to evaluate the quality of the models.

The methodology was applied on an experimental residential building in Québec, Canada. The models were calibrated using only information from smart thermostats and historical weather data. No additional information was used, like the layout of the house or the lighting loads.

The methodology was applied with 3 different calibration techniques; the models were calibrated by minimizing the prediction error of 1-hour, 6-hour and 24-hour predictions. The analysis of the residuals showed that both 1-hour and 24-hour calibration horizons produce models that capture the thermal dynamics of the house, but the latter has a better accuracy for 24-hour predictions, confirming the available literature. The model with 24-hour calibration horizon predicted very well the temperature of all 9 zones 24 hours in advance, with an overall RMSE of 0.44°C and FIT of 64.9%.

Investigating the estimated parameters showed that the algorithm performs a form of zone aggregation for the basement and the first floor, by allocating a high thermal capacitance to one of the zones and high conductance between that zone and the rest of the zones on that floor. Additionally, the solar gain factors are present only in 4 south-facing zones, where the effect of solar irradiance is expected to be the highest.

4 Online model-based predictive control with smart thermostats: Application to an experimental house in Québec[1]

4.1 Abstract

This paper tests the impact of model resolution and structure on the performance of Model Predictive Control (MPC) implementation in an unoccupied research house in Québec equipped with smart thermostats. Two low-order models and a high-order multi-zone model were calibrated with measured data, with the structure of the multi-zone model being generated automatically during the calibration procedure. The three models were used to apply real-time MPC to an experimental house in Québec using the established dynamic tariffs for morning and evening peaks. MPC with any of the three models successfully preheated the house before the demand-response events, outperforming the reference reactive controller, reducing cost and thermal discomfort. The high-order multi-zone model performed the best, reducing average cost of electricity by 55% and high-price energy consumption by 71%, compared to the low-order models, which achieved cost reductions of 40% and 44% and energy consumption reductions of 48% and 54% respectively.

[1] C. Vallianos, M. Abtahi, A. Athienitis, *et al.*, "Online model-based predictive control with smart thermostats: Application to an experimental house in Québec," *Journal of Building Performance Simulation*, pp. 1–17, 2023. DOI: 10.1080/19401493.2023.2243602.

4.2 Introduction

Advanced control strategies of heating and cooling systems, and specifically Model Predictive Control (MPC), can reduce energy consumption while ensuring occupant thermal comfort [34], [153], [154]. MPC uses a building model and the forecast of weather and other disturbances to predict the future behaviour of a building and produce optimal control actions [37]. MPC has also been identified as a good candidate for Demand-Response (DR) applications, because it can take advantage of the electrical and thermal storage of a building and increase its energy flexibility [23], [164] and also interact with the grid in a transactive way [21]. DR measures are becoming increasingly common due to the challenges introduced to the utility grid from heating electrification with the widespread adoption of heat pumps [15] and the growing popularity of electric vehicles [165].

Building energy flexibility has been defined by International Energy Agency's Energy in Buildings and Communities (IEA-EBC) Annex 67 "Energy Flexible Buildings" [24] as "the ability to manage the demand and generation according to climate conditions, user needs, and energy network requirements". Athienitis, Dumont, Morovat, *et al.* [25] have defined a Building Energy Flexibility Index (BEFI), which measures and compares the flexible power demand over a specific period to a reference power demand for the business-as-usual case.

Both the estimation of BEFI and MPC require and rely on a building model that can accurately predict building energy consumption and thermal comfort conditions over a prediction horizon. Building thermal models can be categorized into three main categories: white-box, black-box, and grey-box [86]. White-box models are based on fundamental physical principles, mainly conservation of mass and energy. Their parameters are often identified from the geometry and materials of the building and its equipment. Most Building Performance Simulation tools, like EnergyPlus and TRNSYS, use detailed white-box models and therefore require expertise to create, are time-consuming to calibrate [53] and require a great deal of knowledge about the building, which is often not available but assumed [49]. For these reasons they are not ideal candidates for control applications.

Black-box models rely on statistics and machine learning methods. They are trained with measured data, they can be highly accurate and do not require the expertise of a building engineer [60]. However, black-box models often lack the ability to extrapolate to situations not "seen" in the train-

ing set or from building to building [68]. This can pose a challenge when using black-box models to improve or optimize building operation, since they are trained on data from sub-optimal control strategies or for specific seasons or operating modes [30].

Grey-box models are a combination of white-box and black-box models; they are based on physics like white-box models, but they have a simplified structure, and their parameters are calibrated with measured data like black-box models. A very common representation of grey-box models is the resistance-capacitance (RC) model, or thermal network [77]. RC models have been identified by multiple studies as the best candidates for control and district-level applications [53], [83], [87]. They have fewer parameters than white-box models, making them much faster to calibrate and at the same time they have a better extrapolation ability than black-box models [78] and require less data for calibration [85].

Although grey-box models are the preferred choice for MPC, choosing its structure and order (i.e., the thermal capacitances and resistances) is not a straightforward task. Having a very low or very high model order affects its structural identifiability [128]. An over-simplified model may be unable to properly capture building thermal dynamics and indoor thermal conditions in different zones, whereas a model of a very high order may be over-parameterized and suffer from parameter redundancy, meaning that there are multiple sets of parameter values that yield the same model [125].

Many studies have listed the lack of an automated and practical methodology for the calibration of building thermal models as one of the main challenges for wide-spread adoption of MPC [37], [83], [84]. Bacher and Madsen [116] automatically selected the structure of a model with a forward selection procedure that iteratively compares more complex models to a base model and tested it on an experimental setup.Prívara, Váňa, Žáčeková, *et al.* [41] proposed a two-stage building modelling procedure for MPC applications. It first chooses the inputs to the model and then it identifies the model order. They validated it using a TRNSYS model. Wang, Chen, and Li [123] proposed a model development methodology for RC models that starts with a very complex model and iteratively deletes parameters based on the asymptotic confidence intervals of their estimates. They validated their procedure using measured data from a low-energy house. Arroyo, Spiessens, and Helsen [133] presented a methodology for the identification of multi-zone models, which selected the best structure of each zone from a number of pre-set model structures. They used BOPTEST [150],

an open-source initiative for simulated-based benchmarking of advanced control strategies, to simulate the building response. Leprince, Madsen, Miller, *et al.* [115] presented a methodology that automatically chooses the best model from a set of given models. They applied the methodology to 247 Dutch residential buildings. Vallianos, Saeed Hosseini, Athienitis, *et al.* [166] presented a methodology for multi-zone model generation that chooses the best model structure by iteratively adding or removing model parameters. They applied the methodology to measured data from an experimental house.

Studies [41], [115], [116] used a single-zone model, while [123] assumed one zone for each of the basement, first floor and second floor. Generally, a building should be modelled with enough thermal zones so that each zone representing a region of the building with distinct boundary or operating conditions [119]. Representing a building with only a few zones — or even just one — is common when using simplified or reduced-order grey-box models for control applications [80], [110], [120]–[122]. Representing a large space with one thermal node may estimate correctly the overall energy consumption, but not necessarily thermal comfort in different zones [167], nor building energy flexibility [124].

Another factor necessary for successful MPC implementation is disturbance forecasts, i.e., the forecast of any non-controllable input to the building system. The most common disturbances are the weather conditions (exterior temperature and solar radiation) and internal heat gains (occupancy schedules, equipment etc.). Carlucci, De Simone, Firth, *et al.* [140] presented a systematic review of occupant behavior models. They concluded that most studies use data-driven methods to predict either occupant presence, occupant interaction with building devices, or both. Weather forecasts can be included in the form of a data-driven linear model [32], with stochastic [141] or adaptive [142] mechanisms to increase their accuracy. However, it is easier to use an online weather forecast service, which usually uses advanced climate models [37].

MPC implementation in smart thermostats is a very promising topic in the province of Québec, Canada specifically, where electric space heating is already widely adopted in the residential sector. According to the 2023 “State of Energy in Québec” report [94], electricity accounts for 77% of the total energy consumption of the residential building sector. When examining the distribution of energy consumption by category, space heating emerges as the primary factor, accounting for 61%. Most houses are equipped with decentralized electric baseboards, which can potentially provide

high energy flexibility potential, since they allow for individual control of each room according to its purpose and need. Therefore, space heating in the residential sector is detrimental in shaping the whole province's demand profile in the winter, putting the grid under stress on very cold weekday mornings and evenings (before and after a typical work schedule).

Hydro-Québec, who is the public utility that manages the generation, transmission, and distribution of electricity in Québec, has introduced a dynamic tariff (Rate Flex-D) [95], and a smart home service with tailored instructions for energy efficiency through their subsidiary Hilo. These services provide an opportunity for homeowners to reduce their cost of electricity by shifting their load to off-peak periods and, as a result, relieve some of the pressure on the grid. Vallianos, Candanedo, and Athienitis [168] used measured data from thousands of houses in Ontario and Québec to calibrate low-order models and then used these models to estimate the benefits of MPC. Based on a sample of 138 houses in Québec, the study showed that using Rate Flex-D during a winter day with average ambient temperature lower than -15 °C can reduce the cost of electricity by 43 ¢/kW installed on average, or $ 5.6 for a house with 13 kW total installed heating capacity.

In light of the above, this study aims to:

- Compare the effect of different model resolutions and structures on the practical implementation and performance of day-ahead MPC in residential buildings, contributing to the mass development of MPC using smart thermostats.

- Test and facilitate an automated way to develop building models, calibrate them using measured data from smart thermostats, and use them in real-time MPC frameworks, directly addressing the lack of an automated and practical methodology for the calibration of building thermal models, which is stated as one of the main challenges for wide-spread adoption of MPC.

- Quantify the effects of equipping houses with smart thermostats that can perform MPC during demand response events in Québec both in terms of cost reduction for the homeowner and energy consumption and peak power reduction for the utility grid, showcasing the pertinent role that smart thermostats can play in dynamic electricity pricing.

The rest of the document is organized as follows: Section 4.3 describes the experimental house and the available dataset, Section 4.4 explains the methods used for model calibration and MPC

implementation, Section 4.5 presents and discusses the results, and Section 4.6 concludes the article.

4.3 Description of case study and available data

The study uses an unoccupied research house of Hydro-Québec located in Shawinigan, Québec, the Experimental House for Building Energetics (EHBE). It is a two-storey house with an excavated basement and an attached garage. The house is 7.6 m by 7.9 m (its footprint is 60 m^2) with a fully uninsulated basement. The first floor consists of the living room, dining room, kitchen and a small powder room, while the second floor has 3 bedrooms and a full bathroom. It is a typical Québec residence, with R-20 insulation for the walls, R-30 insulation for the roof, and a total of 19 m^2 of fenestration consisting of double-glass windows with an air gap. The building walls are representative of the typical lightweight wood-framed house in Québec, while the basement is more thermally massive and includes an exposed concrete floor.

The house is oriented 35 ° west of south and is heated with an electric baseboard in each room controlled with an individual thermostat. The convective nature of the electric baseboards may lead to thermal stratification, especially in the zones connected to the open stairway. The layout of the house is shown in Figure 4.1, while Table 4.1 shows the location and installed heating capacity for each electric baseboard.

Table 4.1: Location and installed power of each electric baseboard

Abbreviation	Room	Location	Orientation	Installed heating capacity (kW)
SS	Basement 1	Basement	Basement	2
SS2	Basement 2	Basement	Basement	2
CU	Kitchen	First Floor	North	1.5
SM	Dining Room	First Floor	North	1.25
SA	Living Room	First Floor	South	1.5
SE	Powder Room	First Floor	South	-
C1	Bedroom 1	Second Floor	North	1.25
C2	Bedroom 2	Second Floor	South	1.25
C3	Bedroom 3	Second Floor	South	1.25
SB	Bathroom	Second Floor	North	1
Total	-	-	-	13

There are two separate datasets included in this study. One came from a previous experiment

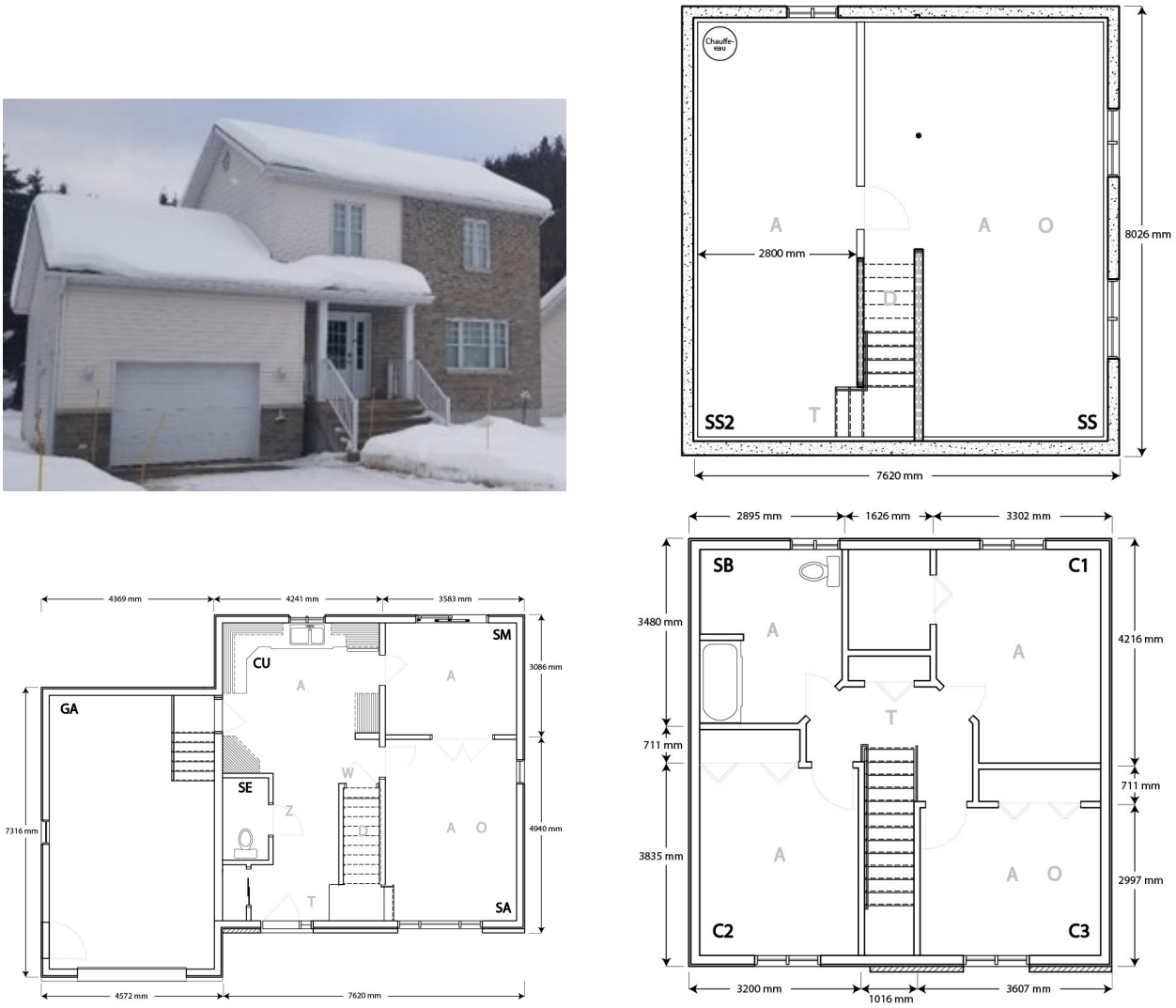

Figure 4.1: Hydro-Québec's Experimental House of Building Energetics (EHBE) and its floor plans for the basement (top right), the first floor (bottom left), and the second floor (bottom right)

(March 30th to April 14th 2019 inclusive) and was used to calibrate the models used in the MPC, and the other (March 1st to March 30th 2023 inclusive) resulted from the application of MPC on the house. Both provide zone-by-zone values for the indoor air temperature value, temperature setpoint and heating percentage. The temporal resolution of the data is 15 minutes. Historical weather information for both periods were retrieved from SIMEB (in French, SIMulation Energétique des Bâtiments) website [169], which provides (among others) outdoor temperature and global horizontal irradiance in hourly intervals from several weather stations in Québec. The data were obtained for the location of Trois-Rivières, which is the closest weather station location with less than 35-km distance, and the data were interpolated to 15 minutes using linear interpolation for the

outdoor temperature and backfilling for the solar irradiance. Weather forecast in real time was also necessary for the MPC application, which was retrieved from Solcast using their API [170].

The house is equipped with a Raspberry Pi, which is connected to the internet and serves as an access point. The smart thermostats (as well as any other sensors) communicate directly with the Raspberry Pi, which collects the data and saves them in a local database, before transferring them to an offline server. The Raspberry Pi module could possibly be used as the computation node; however, in this experiment, another local computer served as a computation tele-node.

4.4 Method

This study examines how the structure and order of the model affect the accuracy of the model and the performance of MPC. Three approaches are considered:

1. Defining the model structure based on the number of floors, i.e., discretizing by floor. Each floor is assumed to be a separate thermal zone represented by a lumped thermal capacitance. The main assumption is that the air of each floor is uniform and there is not much zone-to-zone air mixing.

2. Defining the model structure based on the orientation of each room, i.e., discretizing by orientation. The southern and northern parts of the house are assumed to be separate thermal zones represented by a lumped thermal capacitance. This discretization could prove particularly helpful in buildings like typical Québec houses, where the solar heat gains have a significant effect and may even overheat the air temperature during the day.

3. Defining the model structure based on the number of rooms, i.e., discretizing by room. Each room is assumed to be a separate thermal zone represented by a lumped thermal capacitance for the air and another one for the structural elements. This approach allows the estimation of each zone separately and could be particularly helpful when thermal comfort or energy flexibility is of the utmost importance.

For both the floor model and the orientation model a third-order model is developed, shown in Figure 4.2.

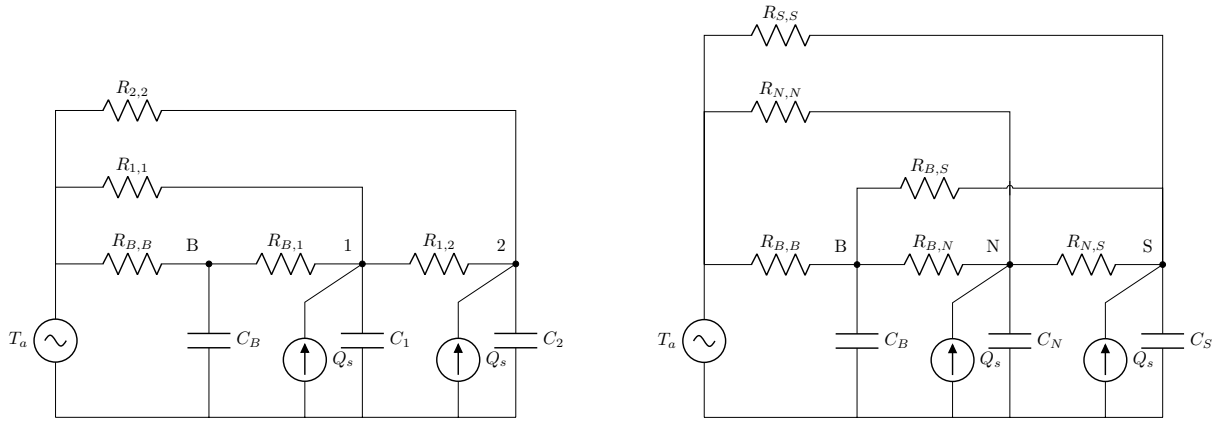

Figure 4.2: Structure of thermal networks for floor model (left) and orientation model (right). Node B represents the basement, node 1 the first floor, 2 the second floor, N the north side and S the south side of the house. Each air zone node also has a heating source from its respective electric baseboard heater, which is omitted for visual clarity

The heat transfer differential equation for air node n is shown in Equation (4.1):

$$C_n \frac{dT_n}{dt} = \sum_{m \neq n} U_{n,m} \left(T_m - T_n\right) + U_{n,n} \left(T_a - T_n\right) + Q_n \tag{4.1}$$

where C represents thermal capacitance (J/K), U represents thermal conductance (K/W) between node *n* and any other node *m*, T represents temperature (°C), Q represents the sum of heat generated or received (W), t represents time (s), and subscript *a* represents the outdoor air. The total heating load Q_n of node *n* can be further divided into the load of the heating system $Q_{h,n}$ and the solar heat gains $Q_{s,n}$ (since the house is unoccupied the rest of the internal gains are considered negligible): $Q_n = Q_{h,n} + Q_{s,n} = Q_{h,n} + \alpha_n G_t$. α is the solar factor of node *n* (which includes its solar aperture) and *Gt* is the global horizontal irradiance (W/m^2).

Using an explicit finite difference scheme to discretize Equation (4.1) temporally results in Equation (4.2), where *k* and *k+1* denote the current and the next time step respectively, and Δt denotes the time interval of the simulation.

$$T_n^{k+1} = \frac{\Delta t}{C_n} \left(\sum_{m \neq n} U_{n,m} \left(T_m - T_n\right) + U_{n,n} \left(T_a - T_n\right) + Q_n \right) + T_n^k \tag{4.2}$$

The floor and the orientation models are calibrated by minimizing the error between the pre-

dicted and the measured temperatures.

$$J = \sum_{k=0}^{N} \left(T^k - \hat{T}^k \right)^2 \tag{4.3}$$

where N is the total number of datapoints, T^k is the measured temperature, and $\hat{T}^k$ is the predicted temperature of timestep k. The temperatures of the two models are estimated as an area-weighted average of the individual zones they encompass.

Deciding the structure of the multi-zone model is not as straightforward as with the low-order models. Not all zones exchange heat or interact with each other, nor are all of them affected by solar radiation. On one hand, including all parameters in the calibration process would over-parameterize the model and pose identifiability problems, while, on the other hand, creating a model by identifying which zones exchange heat through studying the floor plans has to be done manually and requires the time and expertise of an engineer.

Instead, the structure of the multi-zone model is decided using the automated methodology presented in [151]. According to the methodology, each zone is modelled with one equivalent air zone capacitance and up to one node representing the building materials. The objective of the methodology is to prevent overparameterization by automatically finding the minimum number of parameters that maximizes the accuracy of the model for 24-hour predictions. In the beginning, the algorithm assumes a simple model consisting only of the air thermal capacitance of each zone. Then it iteratively adds one parameter at a time: during each iteration, it tests adding each available parameter one by one, and eventually only adds the parameter that increases model quality the most. When adding any parameter does not further increase model quality, it follows the same procedure, but this time it iteratively removes any redundant parameters. For a more detailed description of the procedure, the reader is referred to [151].

The multi-zone model is calibrated using the MPC Relevant Identification (MRI) method. MRI methods identify the set of optimal parameters by minimizing the multi-step ahead prediction error [41]:

$$J_{MRI} = \sum_{k=0}^{N} \sum_{j=1}^{PH} \left(T^{k+j} - \hat{T}^{k+j|k} \right)^2 \tag{4.4}$$

where PH is the prediction horizon of the MPC framework that the model will be used for, T^{k+j} is the measured temperature, and $\hat{T}^{k+j|k}$ is the predicted temperature using available information up to timestep k. During the MRI method, the model uses its own temperature predictions of timestep $k+1$ to predict temperatures of timestep $k+2$, etc, over the entire prediction horizon. Therefore, MRI significantly increases calibration computation runtime, but results in models with better accuracy during the prediction horizon [135]. However, Zhao, Zhu, and Patwardhan [139] reported that MRI does not increase model accuracy when the data are noisy, even if the model structure is correct.

The three models were trained on measured data of 14 days (from March 30th to April 12th 2019 inclusive) and then evaluated on April 13th and 14th, which the models had not seen at all during the training stage. All models are trained on the same dataset so that their performance can be easily compared, and their generalization ability tested. There have been no significant renovations or changes to the house since 2019, so the models are expected to adequately represent the house thermal dynamics when used to apply MPC in 2023.

4.4.1 Model Predictive Control (MPC)

The three models are used in an MPC framework, along with weather forecast, to optimally control the electric baseboards of the house during days with dynamic pricing. The main objective is to minimize the cost of electricity for the homeowner, while maintaining thermal comfort. In Québec, there is no Time-of-Use cost of electricity, but there is dynamic pricing for some residential users with certain peak demand events in the winter [95]. These events can occur from 6 a.m. to 9 a.m. and from 4 p.m. to 8 p.m. and the price of electricity increases to 51.967 ¢/kWh instead of the normal 4.449 ¢/kWh.

The daily reference setpoint profile is based on a recent study by Henao, Fournier, and Kelouwani [171], who analysed data from 300 smart thermostats located in 30 houses located near Trois-Rivières in Québec and found that the most likely time for morning setpoint set-ups was between 5 a.m. and 6 a.m., for morning set-backs 8 a.m., for evening set-ups between 4 p.m. and 5 p.m., and for evening set-backs 10 p.m. The most probable setpoint temperature was 21 °C. Therefore, Figure 4.3 shows the daily reference setpoint. The high temperature is 21 °C and the low temperature is 19 °C with a morning set-up at 5 a.m. and a set-back at 8 a.m. and an evening set-up at 5 p.m. and a set-back at 10 p.m. The grey area represents the high-price period when the cost of

electricity reaches 51.967 ¢/kWh. The days assume both a morning and an evening event to test for the worst-case scenario and to explore whether the morning event affects the evening event negatively.

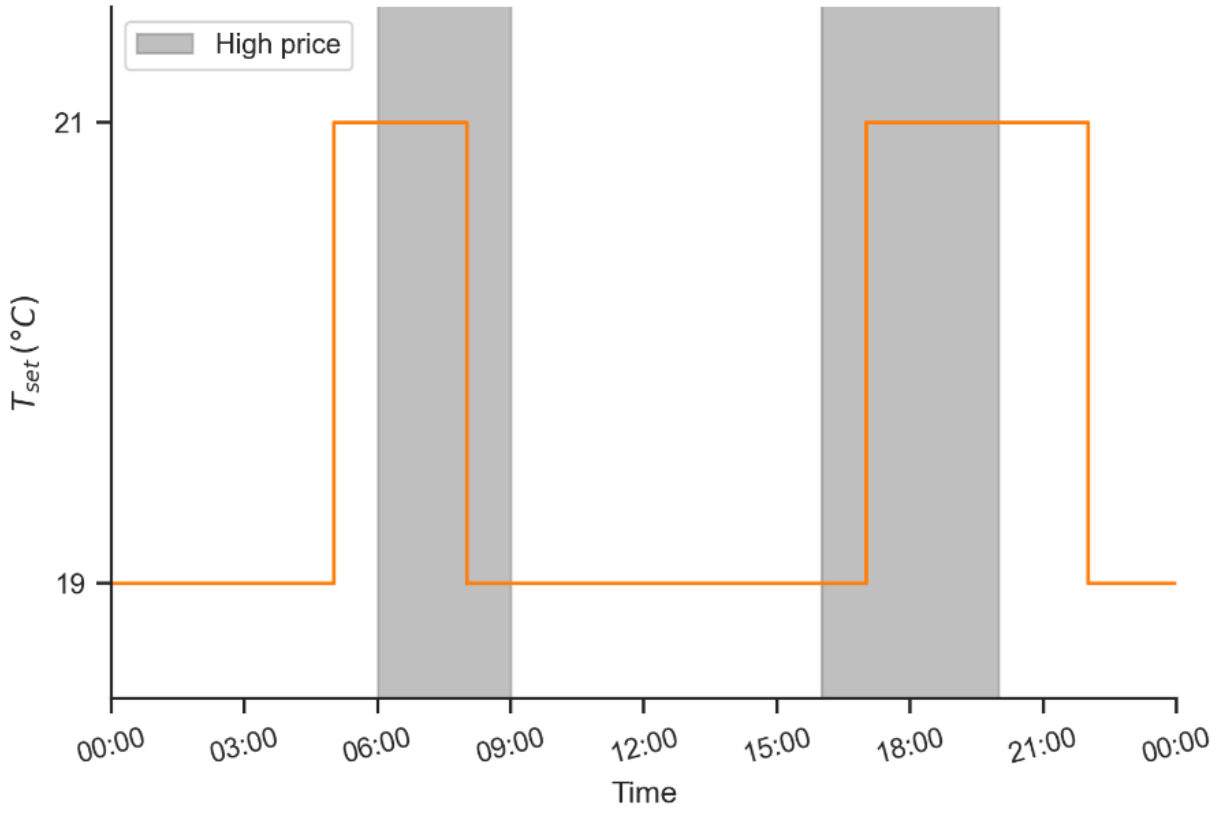

Figure 4.3: Daily temperature setpoint profile. The grey shaded area represents the high-price period when the cost of electricity is 51.967 ¢/kWh instead of 4.449 ¢/kWh

In an MPC framework, a common practice to achieve thermal comfort is to enforce indoor temperature within a certain range, which can be implemented as a soft constraint or a hard constraint. Hard constraints cannot be violated but complicate the optimization process and cannot be handled by some optimizers. On the other hand, soft constraints are penalized in the cost function and can therefore be violated but are preferable because they are more practical and do not pose any challenges to the optimization technique. A detailed overview of thermal comfort constraints in building control can be found in [37]. Both soft and hard constraints have been used extensively. For example, Cole, Powell, Hale, *et al.* [35] used a hard constraint, allowing a setpoint range of 4 °C when the house is occupied and 8 °C when it is unoccupied, while Huchuk, Sanner, and O'Brien [33] and Vallianos, Candanedo, and Athienitis [168] used a soft constraint, penalizing

thermal discomfort when the indoor temperature was below the setpoint or above it by more than 2 °C.

The MPC controller is trying to minimize the cost of electricity over a prediction horizon *PH*. The optimal actions are implemented for a period called control horizon, which as a rule of thumb is roughly 20% of *PH*, when the optimization is run again and the MPC controller updates the optimal actions [37]. The full MPC formulation is shown in Equation (4.5). C is the price of electricity (¢/kWh) and Q is the heating output (kW) of timestep k. Thermal discomfort was considered as a soft constraint, penalizing it if the indoor temperature of a zone was lower than the setpoint, or if it was greater by more than 3 °C. β is a factor that weighs the cost of energy to the "cost" of discomfort. It needs to be large enough that thermal comfort violations are penalized adequately. The value was chosen to be β=250 ¢/°C hr (in contrast to the highest cost of electricity of 51.967 ¢/kWh), penalizing 1 °Chr of discomfort roughly as much as 5 kWh of energy consumption during the high-price period or 55 kWh during the low-price period.

$$
\begin{aligned}
J &= \min\left(\sum_{k=1}^{PH} C^k Q^k \Delta t + \sum_{k=1}^{PH} \beta d^k\right) \\
&\; so\, that \\
&\mathbf{T}^{k+1} = \mathbf{A}\mathbf{T}^k + \mathbf{B}\mathbf{u}^k \\
&\mathbf{0} \le \mathbf{Q} \le \mathbf{Q}_{inst} \\
d^k &= \begin{cases} \left(T_{set}^k - T^k\right)\Delta t, & \text{if } T^k < T_{set}^k \\ 0, & \text{if } T_{set}^k \le T^k \le T_{set}^k + 3 \\ \left(T^k - T_{set}^k\right)\Delta t, & \text{if } T_{set}^k + 3 < T^k \end{cases}
\end{aligned}
\tag{4.5}
$$

The rest of the constraints force the MPC formulation to use the building model and restrict the heating output to the installed capacity of each zone as described in Table 4.2. The prediction horizon was 24 hours, and the control horizon was 6 hours. Every 6 hours, the MPC controllers fetched the measured zone temperatures and heating outputs, the actual weather conditions and the new (imperfect) weather forecast. For the floor and orientation models the measured zone temperatures of the last timestep were used as initial temperature estimates T^0. For the multi-zone

model, not all state temperatures are measured in the house since the representation of each zone can also include an effective node for the building material. Therefore, the initial temperature estimates T^0 were estimated using the moving horizon estimation method [172], a common method for state estimation, which used the calibrated model parameters, the measured heating outputs, and weather data of the last 7 days to estimate the initial temperature states. The uncertainty of the weather forecast was not considered in the deterministic MPC formulation. The optimization problem is convex and was solved using the cvxpy library in Python [173].

Table 4.2: Schedule of experiments at EHBE

Reference	Floor model	Orientation model	Multi-zone model
2023-03-01	2023-03-02	2023-03-06	2023-03-17
2023-03-04	2023-03-28	2023-03-23	2023-03-19
2023-03-05	2023-03-29	2023-03-24	2023-03-20
2023-03-16			
2023-03-18			
2023-03-21			
2023-03-25			
2023-03-30			

To evaluate the effect of the MPC strategies, the Building Energy Flexibility Index (BEFI) is estimated. As mentioned in the introduction, the BEFI represents the ability of a building to change its power demand relative to a reference profile during a specific period demanded by the grid. The average dynamic BEFI at time *t* and for duration Δt was calculated using Equation (4.6) [25], where Q_{ref} is the total power consumption under a reference energy consumption profile and Q_{flex} is the total power consumption of the flexible strategy (in this case the MPC strategy).

$$BEFI_{\Delta t}(t) = \frac{\int_t^{t+\Delta t} Q_{ref}(t)dt - \int_t^{t+\Delta t} Q_{flex}\,(t)\,dt}{\Delta t} \tag{4.6}$$

4.5 Results and discussion

The three models were trained on measured data of 14 days (from March 30th to April 12th 2019 inclusive) and then evaluated on April 13th and 14th, which the models had not seen at all during the training stage. Then they were used to implement MPC on the EHBE for days in March 2023. The results of model calibration, including a discussion on the structure of the multi-zone model, are

presented in Section 4.5.1. Section 4.5.2 presents the MPC implementation and analyzes the performance of the different models. The advantages and disadvantages of each model are presented in Section 4.5.3, while some limitations and potential future work are discussed in Section 4.5.4.

4.5.1 Model calibration

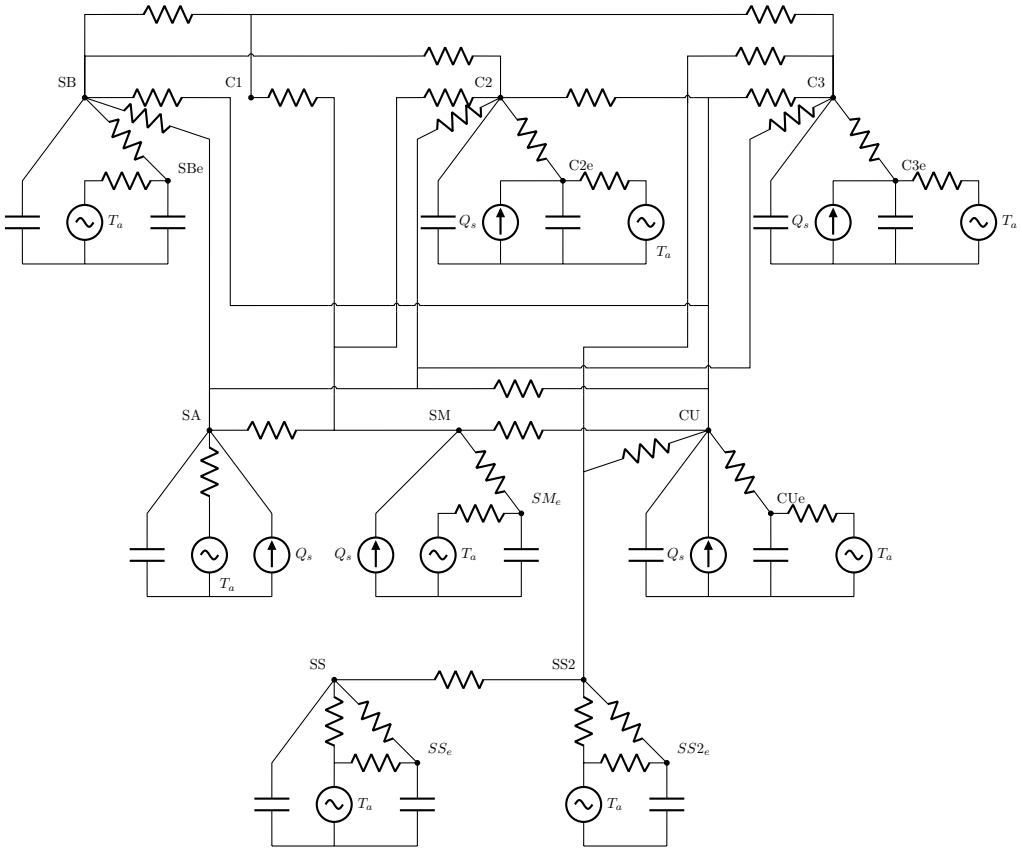

Figure 4.4: Structure of the final 13th-order multi-zone model. Each air zone node also has a heating source from its respective electric baseboard heater, which is omitted for visual clarity.

The structure of the floor and the orientation model is shown in Figure 4.2, while the structure of the multi-zone model was automatically defined during the calibration procedure and the resulting structure is shown in Figure 4.4. The final model is of 13th order with a total of 52 calibrated parameters (compared to 10 parameters for the floor model and 11 for the orientation model). The resulting model structure is complicated and includes an intricate layout of thermal resistances to capture all the mechanisms of heat exchange in the house. The model structure seems to be reflect-

ing the layout of the house accurately. The basement has no solar heat gains, while all zones of the first floor do, as do the 2 south zones of the second floor. Without prior knowledge of the layout, the methodology managed to infer the relative location of the basement zones, relatively isolating them. The basement exchanges heat only with the kitchen on the first floor, with which it is connected with a staircase, and Bedroom 3, likely because it is located at the top of the aforementioned open staircase.

Table 4.3 shows the Root Mean Square Error (RMSE) of each zone for each model for both the train and the test periods for 24-hour predictions. The multi-zone model outperforms the floor and the orientation models, having an RMSE of 0.29 °C compared to 1.01 °C and 1.27 °C respectively. The 24-hour predictions are plotted against the measured data in Figure A.3 in Appendix A. The difference in their accuracy is attributed to the order of the models and their calibration method. A model with a more detailed structure can often capture better the building thermal dynamics (when not over-parameterized). At the same time calibrating a model using the MRI method also increases its accuracy, albeit at the cost of an exponential increase in computational resources.

Table 4.3: Accuracy of the three models for each zone of the house

Zone	RMSE(°C)		
	Floor model	Orientation model	Multi-zone model
SS	1.19	1.59	0.27
SS1	1.13	1.48	0.30
SA	1.04	1.24	0.28
SM	0.79	1.14	0.25
CU	0.85	1.09	0.25
SB	1.09	1.36	0.33
C1	0.92	1.27	0.27
C2	1.03	1.15	0.34
C3	1.07	1.11	0.34
Total	1.01	1.27	0.29

4.5.2 MPC application

Each of the three models was used to perform MPC on EHBE for 3 days and their performance was compared to the reference days, during which the electric baseboards were controlled with a reactive controller. All days had similar weather conditions, being cold, with the daily average

outdoor temperature fluctuating between -4 °C and 2 °C, and cloudy or overcast, with total daily global horizontal irradiance below 4 kWh/m^2 .

Figure 4.5 shows the daily temperature profile for each day of the experiment, along with the applied setpoint. During the reference cases, the reactive controller started heating the zones as soon as the setpoints changed. The time it took for the zones to reach the setpoints resulted in some thermal discomfort and was more significant for the two basement zones, which expectedly seemed to have longer thermal inertia due to the exposed concrete slabs. Another important observation regarding the reference days is the effect of solar radiation on all zones except for the basement. The indoor temperature started increasing around midday and could eventually overheat the zones, some days even exceeding the setpoint set-up at 5 p.m.

The MPC controller followed the same "strategy" for all three models: preheating the zones before the high-price periods to minimize the cost. The preheating can also be seen in Figure 4.6, which shows the total heating output for the 4 different cases. The MPC controller using the multi-zone model started preheating much earlier than the ones using the floor and the orientation model. This effect is also noticeable in Figure 4.5, where the zone temperatures of the multi-zone model were significantly higher, and the controller preheated significantly more, especially during the morning peak. This happened mainly due to the effect of the basement. The MPC controllers with the floor and orientation model tried to preheat the basement in anticipation of the morning peak, but the preheating was not significant enough, resulting in the temperature of the two zones reaching the setpoint soon after 6 a.m., which triggered the heating between 6 a.m. and 8 a.m. as seen in Figure 4.6. This indicates that the floor and orientation models overestimated the thermal inertia of the zones and, consequently, the respective MPC controllers underestimated the required preheating. On the other hand, the multi-zone model achieved the maximum allowed temperature during the night, "charging" the building materials, which are represented with a dedicated thermal node, and it managed to preheat the basement sufficiently so that no additional heating is required during the high-price period. As a result, although the controllers with the floor and the orientation model ended up reducing the heating output considerably, the controller with the multi-zone model managed to eliminate it almost completely. The controllers with the three models performed similarly to each other in regard to the evening peak. They did preheat but with smaller intensity than during the morning peak, likely because the temperatures were already fairly high due to solar heat

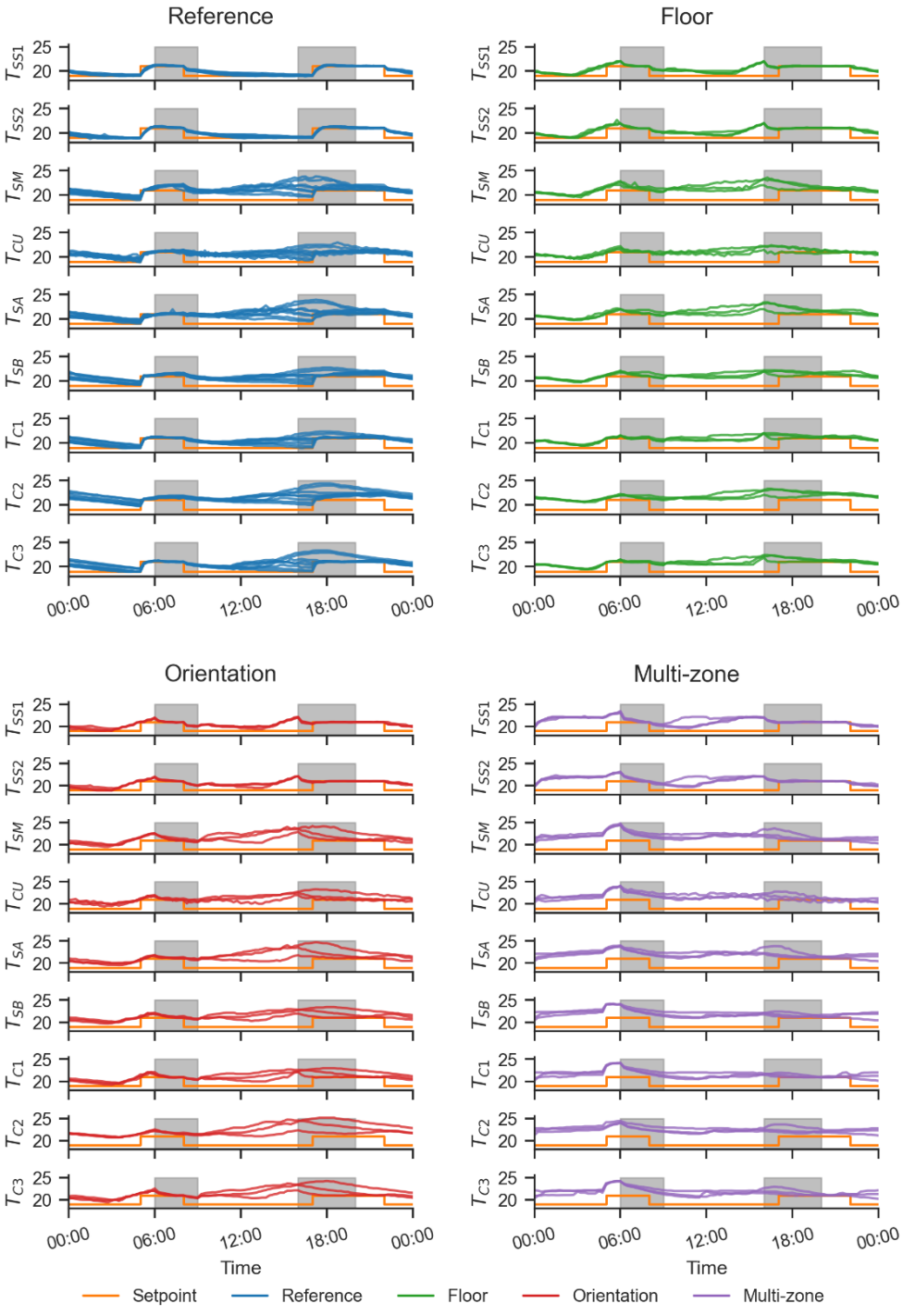

Figure 4.5: Measured zone temperature values and setpoints (in °C) for the reference days (top left) and days with MPC application with the floor model (top right), the orientation model (bottom left) and the multi-zone model (bottom right). The shaded areas correspond to high-price periods

gains. Another factor is the duration of the evening event, which is longer than the morning one.

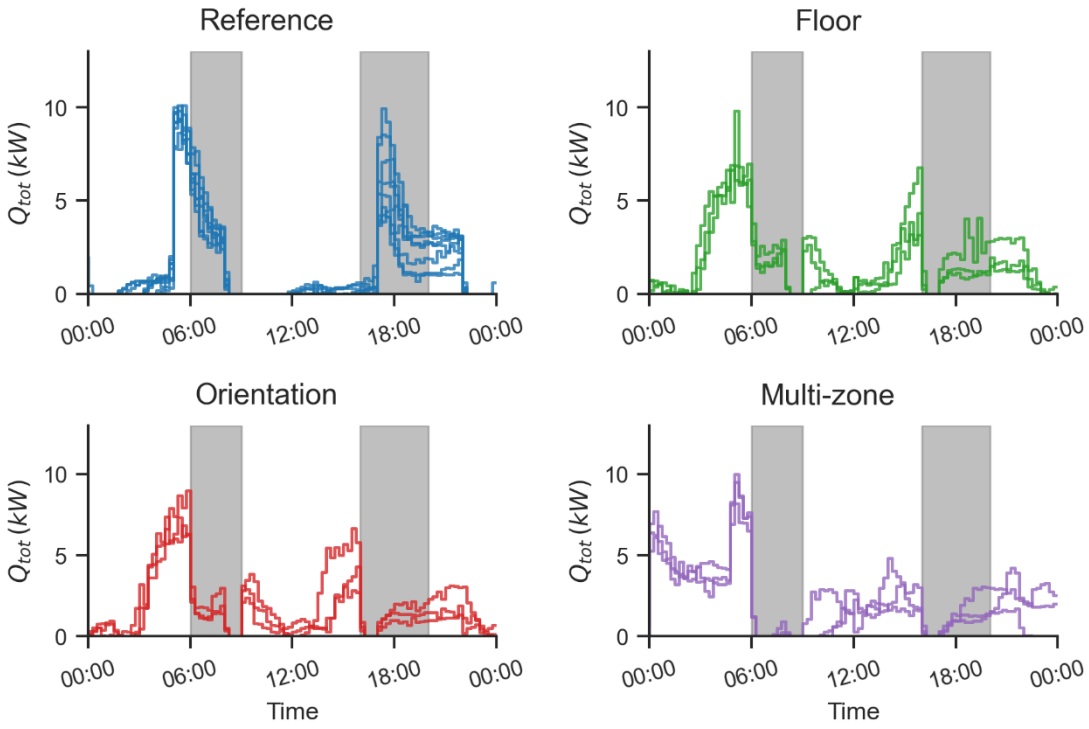

Figure 4.6: Total measured heating output for reference days (top left) and days with MPC application with the floor model (top right), orientation model (bottom left) and multi-zone model (bottom right). The shaded areas correspond to high-price periods

Figure 4.7 compares the performance of the different control strategies for the days of the experiment. The daily average outdoor temperature and the daily total solar radiation are shown as reference for the heating needs of the house for that day. The rest of the columns show the total energy consumption of the day, the energy consumption during the high-price periods, the actual cost of electricity for the homeowner and the discomfort. The solid circles denote the values measured during the experiments, while the hollow circles denote what the (respective) model predicted during the MPC process using the weather forecast.

Upon initial observation, MPC with any of the three models managed to reduce the cost of electricity and almost eliminate thermal discomfort. The daily cost of electricity for the reference case was in the range of \$7.8 to \$16.5, with an average of \$11.9. The MPC controllers reduced it to a range of \$6.1 to \$8.8 for the floor model (average of \$7.2, or 40% reduction), \$5 to \$7.5 for the orientation model (average of \$6.6 or 44% reduction) and \$4.3 to \$6.8 for the multi-zone model

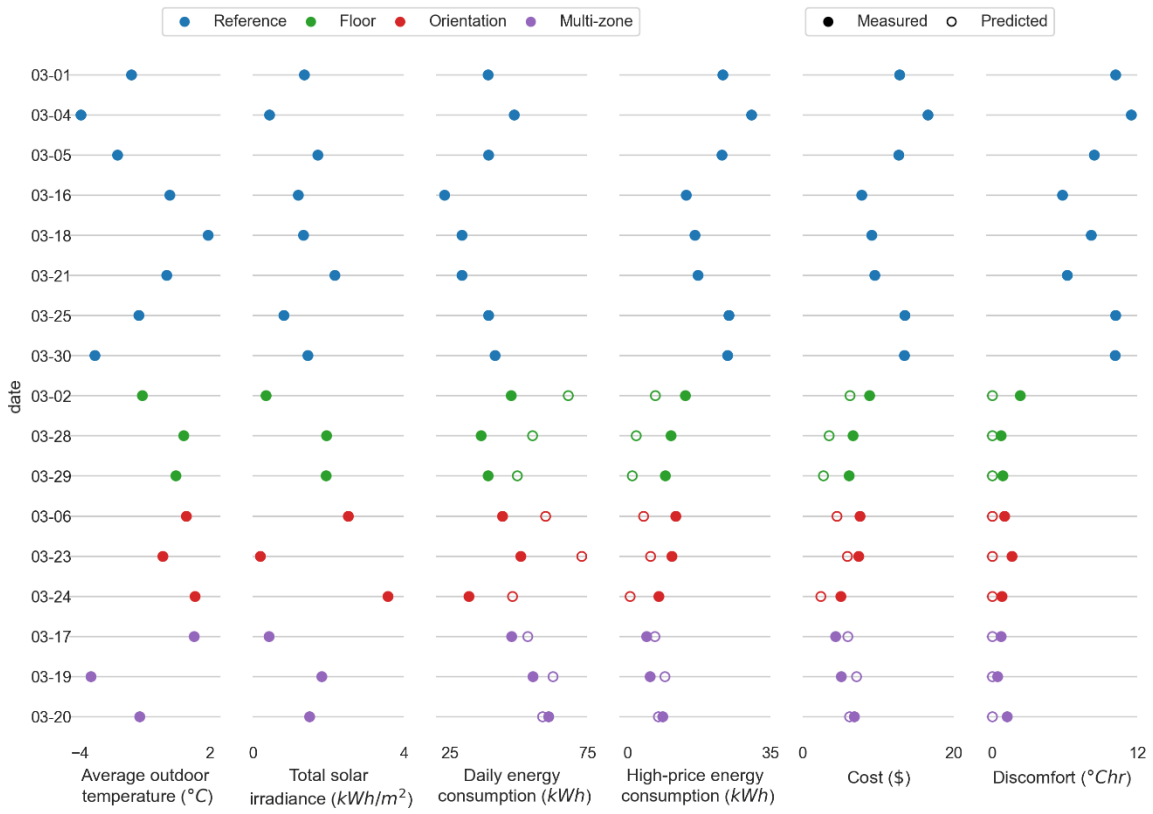

Figure 4.7: Comparison of MPC performance for the different models and days. Each line on the y-axis represents a day of experiments. The first 8 days correspond to the reference reactive control (blue markers) and each next 3 to the floor model (green markers), orientation model (red markers) and multi-zone model (purple markers). The two first columns show the average outdoor temperature and total solar irradiance as a reference for the heating needs of the day

(average of $5.4, or 55% reduction). The reduction in price was achieved by successfully shifting the load from on-peak to off-peak periods.

MPC managed to reduce significantly both the energy consumption and the peak power demand during the high-price periods. The energy consumption during high-price periods for the reference case was in the range of 14.3 kWh to 30.2 kWh, with an average of 21.7 kWh. The MPC controller reduced it to the range of 9.2 kWh to 14.1 kWh for the floor model, 7.5 kWh to 11.7 kWh for the orientation model, and 4.6 kWh to 8.5 kWh for the multi-zone model, achieving an average reduction of 48%, 54% and 71% respectively. However, the total daily consumption was actually increased, especially for the multi-zone model, which preheated more before the morning peak. This increase is justified by the very large difference in electricity price between the on- and off-peak periods. The overall peak power demand was not significantly reduced, just shifted to the off-peak periods. This shifting could potentially place a strain on the grid if enough customers implement MPC to reduce cost, highlighting the need for smart and transactive grids [174].

Another observation concerns the difference between the measured performance and the predicted performance of the MPC controller, which is attributed to both the inaccuracy of the model and the weather forecast. In general, the predictions of the MPC controller with the multi-zone model were much closer to the measured values than in the case of the floor and orientation model, indicating the positive effect of model accuracy on MPC. The floor and orientation models consistently underpredicted the high-price energy consumption, and therefore the price, while the multi-zone model provided more consistent results.

Figure 4.8 shows the BEFI for a duration of 3 hours for the days of the experiment. The reference profile was established as the average measured heating consumption of the reference days. During the reference days the BEFI variates slightly in the morning because of the different outdoor temperatures, but the largest variation can be seen during the evening set-up, when the effect of solar radiation is more significant. During the MPC days the profiles are similar regardless of the model used, because of the similar preheating strategies followed by the MPC controllers. The BEFI is negative in the early morning and afternoon when the house is preheating in anticipation of the morning peak. This effect is more intense in the case of the MPC controller with the multi-zone models, which preheats significantly more and earlier than the MPC controllers with the floor and orientation model. The BEFI reached its highest peak exactly before the respective set-up. During

the morning peak the multi-zone model reaches a maximum BEFI of 3.24 kW, compared to 2.3 kW for the floor model and 2.7 kW for the orientation model, while all strategies reach a maximum of approximately 2.9 kW during the evening peak.

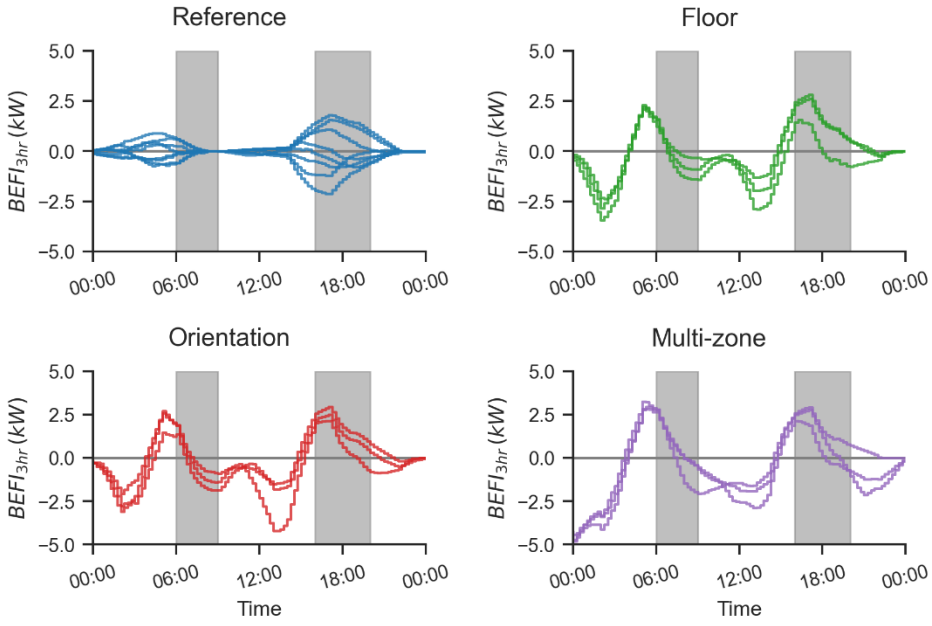

Figure 4.8: Building Energy Flexibility Index for a duration of 3 hours for reference days (top left) and days with MPC application with the floor model (top right), orientation model (bottom left) and multi-zone model (bottom right). The shaded areas correspond to high-price periods

Overall, MPC with any of the three models outperforms the reactive controller, with the multi-zone model yielding the best results. Implementing MPC with both morning and evening demand-response events for two consecutive days showed no difference between the performance on the first and the second day. This indicates that the first day is not preconditioning the house negatively, at least not in the specific weather conditions. Further analysis should be conducted for extreme weather days, with outdoor temperatures closer to -20 °C.

4.5.3 Model comparison

After applying MPC with the three different models and analysing their performance, the following observations can be noted:

- Although low-order models, like the floor and the orientation model, are much faster to create and calibrate, they still require information about the layout of the house and an engineer

to pre-process the data and aggregate them appropriately. On the other hand, the multi-zone model is fully automatic and can be calibrated from data from smart thermostats directly, but requires significantly more computational resources to calibrate, which increase exponentially as the timestep of the model decreases.

- MPC using any of the three models outperformed reactive control, reducing electricity consumption during the high-price periods by 48% and 54% for the low-order models and 71% for the multi-zone model. Although the accuracy of the model defines the accuracy of the MPC, even the less accurate low-order models were accurate enough to reduce the cost of electricity.

- The multi-zone model was more accurate than low-order models for 24-hour predictions, and the increased accuracy made MPC more consistent and reliable. That becomes increasingly important as the uncertainty concerning disturbances (weather forecast, occupancy forecast, etc.) increases.

- MPC with the multi-zone model resulted in slightly less thermal discomfort than the floor and orientation model, but that is in part contributed to the identical setpoints applied on all zones. If the setpoints were different, then aggregating them would not be as simple and respecting them would become a tedious task.

4.5.4 Limitations and future work

As part of the future work, the MPC framework that was established using a local computer as a computational node can be integrated into the local Raspberry Pi, creating an autonomous and independent local system. With the full framework in place, it becomes possible to study the effect of various parameters on practical MPC. For example, part of the future work is to study:

- The performance of models of different resolutions under different occupancy scenarios. A main limitation of this study is the lack of occupancy and internal gains. They can be studied using artificial gains on typical occupancy schedules. The occupancy schedule can be stochastic to simulate the uncertain nature of occupancy.

- The performance of models of different resolutions under different weather conditions and seasons, including extreme cold weather.
- The frequency of model recalibration, or adjustment, required to maintain performance.
- The effect of a variable control horizon, where the model updates its predictions only when they become inaccurate.
- The performance and robustness of the MPC controllers in the case of very inaccurate weather forecasts.

4.6 Conclusions

The paper presented the practical real-time implementation of MPC using smart thermostats in an unoccupied residential house in Québec, Canada for optimal heating load management and load shifting. Three different models were developed and calibrated to be compared and used in the MPC framework: a low-order model grouping zones by floor, a low-order model grouping zones by orientation and a higher-order multi-zone model that assumes one zone per room. The three models were calibrated using measured data from previous experiments conducted in the house in 2019, with the floor and the orientation models having a root mean squared error over 24-hour predictions of 1 °C or more, and the multi-zone model being the most accurate with 0.3 °C. The structure of the multi-zone model was decided in an automated way using smart thermostats data as part of the calibration process and the resulting model was of 13^{th} order.

The three models were applied in an MPC framework for day-ahead optimization, with the objective of minimizing the cost of electricity during days with morning and evening demand-response events. They were also compared to a regular reactive controller, established as the reference case.

Overall, all three models preheated the house successfully before the high-price periods, reducing the overall cost of electricity for the homeowners and eliminating thermal discomfort. The higher accuracy of the multi-zone model made it the best candidate with its MPC application being more consistent and reliable. The multi-zone model reduced the cost of electricity by 55% (compared to 40% and 44% for the floor and orientation model), and the energy consumption during

high-price periods by 71% (compared to 48% and 54% for the floor and orientation model).

Although the peak power demand and the energy consumption during the high-price periods were reduced, the total daily consumption was increased due to the preheating, and the daily peak power demand was not reduced – it was just shifted, highlighting the need for smart or transactive grids.

4.7 Data availability statement

The data that support the findings of this study are openly available in Zenodo at [175].

5 Application of a large smart thermostat dataset for model calibration and Model Predictive Control implementation in the residential sector[1]

5.1 Abstract

Electrification of space heating combined with electricity generation through renewable resources has a significant potential to reduce greenhouse gas emissions, especially when coupled with advanced control strategies that utilize building energy flexibility. This study analyses data from approximately 7,800 houses in Ontario and Québec, Canada to investigate the most suitable data length, data interval and calibration horizon of building models for assessment of Model Predictive Control strategies on a large scale. Overall, models with calibration horizon of 24 hours, data length of 7 days and time interval of 15 minutes provided the best balance between accuracy and computational resources. The calibrated models were used to compare a simple deadband controller to a Model Predictive Controller that minimizes the cost of electricity for a cold day in January. The results showed that the Model Predictive Controller can systematically reduce the high-price energy consumption, while improving thermal comfort, by successfully preheating before the high-price periods. Preheating shifts the peak power consumption, reducing it by 15 % for Ontario and 30 % for Québec. If just 1,000 houses adopt optimal strategies, the grid could see an average reduction in energy consumption of up to 15 MWh and 11 MWh during high-price periods in Ontario and Quebec respectively.

[1] C. Vallianos, J. Candanedo, and A. Athienitis, "Application of a large smart thermostat dataset for model calibration and Model Predictive Control implementation in the residential sector," *Energy*, vol. 278, p. 127 839, 2023. DOI: 10.1016/j.energy.2023.127839.

5.2 Introduction

Reducing electricity consumption is an established research topic in the building engineering field, gaining more popularity in recent years as the measures against climate change increase [176]. Its importance is emphasized as renewable energy sources are substituting polluting fossil fuel power plants. The price of photovoltaic (PV) solar panels has decreased exponentially since 1980 and continues to drop; this is mainly due to manufacturing advances and governmental financial incentives [7]. As a result, PV panels have become a familiar feature of building design and are now often found in residential areas [8]. However, one of the barriers to the large-scale integration of PV is the challenge it presents to the electricity grid, due to a mid-day drop of electricity demand followed by a high evening peak, when the sun sets [10].

At the same time, the electrification of space and water heating, the widespread adoption of heat pumps, as well as the increasing adoption of electric vehicles are becoming progressively popular as means to reduce Greenhouse Gas (GHG) emissions [13]. Heating electrification in particular can reduce GHG emissions up to 30% and energy consumption up to 20% [15]. However, the electrification of space heating poses similar challenges to the grid as the adoption of PV technologies because it increases building electricity demand, especially in cold climates in the morning and evening when the occupancy is higher [16].

Advanced or "smart" controllers have been identified as a potential way to mitigate both problems by utilizing concepts that leverage energy flexibility, such as electrical [20] and thermal [23] storage of a building, or by interacting with the grid in a transactive way [17].

Building Energy Flexibility (BEF) is defined as "the ability to manage the demand and generation according to climate conditions, user needs, and energy network requirements" [24]. The need to quantify the BEF in respect to a reference profile has led to the definition of the Building Energy Flexibility Index (BEFI), which quantifies the change in power demand over a certain period relative to a reference power demand profile [25].

The estimation of the BEFI requires a building energy model that can accurately predict the thermal response of the building. Building energy models are often categorized into white-box, black-box and grey-box. White-box models are based on the conservation of mass, energy and momentum, while black-box models are purely statistical correlations between inputs and outputs [155].

Grey-box models combine the two methods; they are simpler than white-box models, but still rely on physics. Instead of using basic assumptions to estimate their parameters, they are calibrated with measured data.

There are multiple review articles comparing the different kinds of building models. A full review of the literature on building models is beyond the scope of this paper. Harish and Kumar [83] presented a detailed literature review of the three modeling approaches and highlighted the need for a method to systematically develop simplified building models and the need for full integration into advanced control systems. Drgoňa, Arroyo, Cupeiro Figueroa, *et al.* [37] conducted a literature review on the three modeling approaches and concluded that grey-box models are more likely to be suitable for Model Predictive Control (MPC), because they require less data, are less prone to overfitting, and have higher building-to-building generalizability. Wang and Chen [87] presented a literature review on data-driven models and concluded that Resistor-Capacitor (RC) grey-box models are mode suitable for physical interpretation. Li, O'Neill, Zhang, *et al.* [86] also compared the three modeling approaches and identified RC models as the preferred choice for control and district applications. Increased building-to-building generalization can facilitate knowledge transfer in regards to both choosing the order and the structure of the model, and the bounds and initial estimation of the parameters [53].

5.2.1 Large-scale model development using smart thermostat data

With the adoption of Internet-of-Things and smart thermostats, big data sources are becoming increasingly available. Smart thermostats provide a valuable opportunity to develop building energy models on a large scale; these models can then be used to evaluate the aggregated impact of their control strategies on the grid. Although there are a lot of individual studies that use smart thermostat data to model a few houses, there are not many that focus on a larger number of houses. It should be noted that most of them utilize subsets of the same dataset.

John, Vallianos, Candanedo, *et al.* [110] used smart thermostat data to identify time constant values of more than 10,000 residential buildings in North America. They used an exponential decay method based on the solution of a simple 1R1C in a steady-state condition. They used only periods during the night (no solar gains), when the HVAC systems were off, and the outdoor temperature stayed relatively constant. They found that the time constants vary seasonally, being lower in the

summer likely due to open windows.

Baasch, Wicikowski, Faure, *et al.* [111] used smart thermostat dataset of 4,646 houses in Ontario, Canada and New York, USA to compare different grey-box methods to derive building properties. They used 3 different methods to identify the time constant τ of a house: the energy signature, exponential decay, and an overall energy balance. They concluded that the first method showed the most unreliable results, and that the energy balance method systematically overpredicts the time constants τ compared to the exponential decay method.

Hossain, Zhang, and Ardakanian [112] used smart thermostat data from 8,884 in Canada to identify grey-box models with Bayesian neural networks. They use a Bayesian Neural Network (NN) based on a nRnC structure to model each house, and they show that the 2R2C model has the best performance. They also explored the idea of transfer learning across seasons for the same house and across different houses with similar characteristics and they showed that the models can achieve the same or better accuracy with much less data.

Doma, Ouf, Newsham, *et al.* [113] used smart thermostat data to investigate the thermal performance of 11,000 Canadian houses. They represented each house with a simple 1R1C model and used two methods to identify the model parameters: least-squares fitting of exponential decay curves and of the overall energy balance. The two methods resulted in time constant values with a median of 60 and 59 hours respectively. The authors identified the building age as the most influential parameter on the time constant and the number of floors the least.

Huchuk, Sanner, and O'Brien [33] used smart thermostat data to develop and evaluate data-driven models for residential buildings. They used ResStock [105] to generate 500 representative single-family houses in the United States. They modified the houses to match the metadata of the available houses and used EnergyPlus to simulate one year of operation. They tested three different types of control for each house: a simple deadband control, MPC using a ridge regression with history of 20 minutes and a Reinforcement Learning (RL) model-free control. The MPC controller managed to reduce the costs compared to the deadband controller, while the RL controller showed poor performance.

In a different study, Huchuk, Sanner, and O'Brien [114] used smart thermostat data from 1,000 houses in the United States to evaluate data-driven thermal models for multi-hour predictions. They compared simple 1R1C grey-box models and various black-box models, including Lasso and Ridge

Regression, Random Forest and Autoregressive models with exogenous variables, to a baseline model that consisted of a constant temperature (the one of the last timestep). They concluded that the best estimator was the ridge regression model.

Leprince, Madsen, Miller, *et al.* [115] proposed an automated method for stochastic single-zone model generation. The algorithm iteratively increases the complexity of the model until the increased complexity does not statistically increase the quality of the model. They applied the algorithm on smart thermostat data of 247 Dutch houses, out of which 93 were identified as good fits. They used the identified parameters from the resulting models to benchmark the building envelope insulation performance.

Doma and Ouf [118] used smart thermostat data from 60,000 houses in North America to target buildings for retrofits. They calibrated a 1R1C model for each house using two methods: least-squares fitting of exponential decay curves and of the energy balance. The resulting models had time constant values with a median of 52 hours. Then they clustered the model parameters and ranked each cluster to indicate the need for retrofit.

5.2.2 Contributions

The present work uses smart thermostat data to model approximately 7,500 houses located in Ontario and Québec, Canada. The vast majority of Québec houses use electric baseboards for space heating, creating an average winter morning peak power demand of 38,000 MW, mainly because of residential space heating, highlighting the need for peak shifting measures [177]. Using MPC to participate in Demand-Response (DR) events or to assess the energy flexibility of a house requires accurate predictions up to 24 hours in advance.

Taking the above points into account, the objectives of this work are to:

- Rapidly and efficiently develop control-oriented models suitable for the large-scale application of optimal heating load management of residential buildings. The models need to have adequate accuracy for 24-hour predictions.
- Investigate the effect of training data length, calibration horizon, and data interval on model calibration and model accuracy.

- Apply the developed models in an MPC one-day-ahead framework for each house, targeting the reduction of electricity costs for the homeowners based on current DR events and pricing structures.
- Explore the potential aggregated effect for the population of homes.

5.3 Methods

This section outlines the methods used in the study. More specifically, Section 5.3.1 provides a description of the available dataset, while the structure of the proposed building model along with its discretization is presented in Section 5.3.2. Detailed information about the different model calibrations for each house is provided in Section 5.3.3 and about the model evaluation in Section 5.3.4. Section 5.3.5 explains the pricing structures of the DR events and the MPC formulation applied on each house.

5.3.1 Data description

Ecobee provides researchers with user-inputted metadata, which, among other information, include a unique identifier for each house, the country, province/state and city that the house is located in, the floor area and age of house, the number of occupants and floors, the style of the house, whether it has a heat pump or not and what the auxiliary fuel type is.

For every house, the Ecobee thermostats collect 5-minute interval measurements which contain the information about the indoor temperature, the cooling and heating setpoint, the outdoor temperature, relative humidity value and upper and lower setpoint and the runtime of the heating and cooling systems equipment in seconds.

The 7,800 houses considered in this study include houses heated with natural gas and electricity and some that are equipped with heat pumps. Considering that space heating electrification is becoming popular, in order to assess its potential effect on the grid, all houses are assumed to use electricity-powered systems with an equivalent installed capacity. A key feature missing from the dataset is solar radiation, which is often necessary for models to have accurate predictions since solar heat gains are a major disturbance to a building energy model [53]. The location of each ther-

mostat (with the city, province/state and country entries as inputs) was used to find the latitude and longitude through python's library `geopy` [178] using the Nominatim Application Programming Interface (API) [179]. As mentioned, this information is user-supplied and therefore is bound to have inaccuracies and mistakes, rendering some entries unusable.

The historical solar radiation data were fetched from the National Solar Radiation Database of the National Renewable Energy Laboratory of the U.S. Department of Energy, using their API [180] and the latitude and longitude of each location. The solar radiation has units of W/m^2 and is available in 5-minute intervals for some years and locations and in 30-minute intervals for some others. In the latter case the values were interpolated to 5 minutes.

5.3.2 Model description

Each house is represented by a second-order thermal network, as shown in Figure 5.1. The whole house is represented with one effective interior node and one effective envelope node. Equation (5.1) shows the differential equations that correspond to the thermal network.

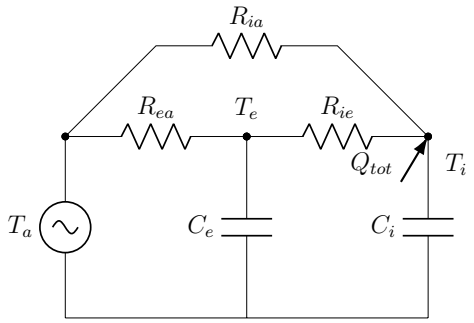

Figure 5.1: A 3R2C thermal network is used to model each house

$$\begin{aligned} C_i \frac{dT_i}{dt} &= \frac{T_a - T_i}{R_{ia}} + \frac{T_e - T_i}{R_{ie}} + Q_h + Q_c + Q_{i,sol} \\ C_e \frac{dT_e}{dt} &= \frac{T_a - T_e}{R_{ea}} + \frac{T_i - T_e}{R_{ie}} + Q_{e,sol} \end{aligned} \tag{5.1}$$

Where t (s) denotes time, R (°C/W) thermal resistance, C (J/°C) thermal capacitance, T temperature (°C), Q (W) power inserted into the space, and subscript i the interior, a the ambient air, e the

envelope, *h* heating, *c* cooling, and *sol* solar gains. The indoor loads from the occupants as well as from potential equipment and appliances are assumed to be negligible.

Discretizing Equation (5.1) using a forward time finite difference scheme and rearranging it leads to Equation (5.2):

$$\begin{aligned} T_i^{k+1} &= \left(1 - \frac{\Delta t}{R_{ie}C_i} - \frac{\Delta t}{R_{ia}C_i}\right) T_i^k + \frac{\Delta t}{R_{ie}C_i} T_e^k + \frac{\Delta t}{R_{ia}C_i} T_a^k + \frac{Q_{h,inst}}{C_i}\delta_h^k + \\ &\quad + \frac{Q_{c,inst}}{C_i}\delta_c^k + \frac{\alpha_i}{C_i} G_t^k \Delta t \\ T_e^{k+1} &= \left(1 - \frac{\Delta t}{R_{ie}C_e} - \frac{\Delta t}{R_{ea}C_e}\right) T_e^k + \frac{\Delta t}{R_{ie}C_e} T_i^k + \frac{\Delta t}{R_{ea}C_e} T_a^k + \frac{\alpha_e}{C_e} G_t^k \Delta t \end{aligned} \tag{5.2}$$

Where Δt (s) is the timestep, $Q_{h,inst}$ (W) is the installed power of the heating system, $Q_{c,inst}$ (W) the installed power of the cooling system, G_t (W/m^2) the global horizontal irradiance, α an effective solar factor that includes solar aperture, δ_h (s) and δ_c (s) the runtime of the heating and cooling systems accordingly and the superscript *k* denotes the k-th timestep. Equation (5.2) can also be written in a matrix notation:

$$\mathbf{T}^{k+1} = \mathbf{A}\mathbf{T}^k + \mathbf{B}\mathbf{u}^k \tag{5.3}$$

Where $\mathbf{T} = \begin{bmatrix} T_i & T_e \end{bmatrix}^T$, $\mathbf{u} = \begin{bmatrix} T_a & \delta_h & \delta_c & G_t \end{bmatrix}^T$ and **A** and **B** are given by Equation (5.4) and Equation (5.5) respectively.

$$\mathbf{A} = \begin{bmatrix} 1 - \dfrac{\Delta t}{R_{ie}C_i} - \dfrac{\Delta t}{R_{ia}C_i} & \dfrac{\Delta t}{R_{ie}C_i} \\ \dfrac{\Delta t}{R_{ie}C_e} & 1 - \dfrac{\Delta t}{R_{ie}C_e} - \dfrac{\Delta t}{R_{ea}C_e} \end{bmatrix} \tag{5.4}$$

$$\mathbf{B} = \begin{bmatrix} \dfrac{\Delta t}{R_{ia}C_i} & \dfrac{Q_{h,inst}}{C_i} & \dfrac{Q_{c,inst}}{C_i} & \dfrac{\alpha_i \Delta t}{C_i} \\ \dfrac{\Delta t}{R_{ea}C_e} & 0 & 0 & \dfrac{\alpha_e \Delta t}{C_e} \end{bmatrix} \tag{5.5}$$

For the stability of the explicit finite difference scheme Equation (5.6) must hold [77].

$$\Delta t < min \left(\frac{1}{\dfrac{1}{R_{ie}C_i} + \dfrac{1}{R_{ia}C_i}}, \frac{1}{\dfrac{1}{R_{ie}C_e} + \dfrac{1}{R_{ea}C_e}} \right) \tag{5.6}$$

The parameters of Equation (5.2) are calibrated with measured data for each house. However, since only the runtimes of the heating and cooling systems are available and there is no information about the installed power of the systems, it is impossible to identify all the parameters, but rather their combinations: $R_{ie}C_i$, $R_{ia}C_i$, $Q_{h,inst}/C_i$, $Q_{c,inst}/C_i$, α_i/C_i, $R_{ie}C_e$, $R_{ea}C_e$ and α_e/C_e.

5.3.3 Data selection and model calibration

Although the Ecobee dataset includes data for more than 100,000 houses in North America since 2015, this study targeted only houses located in Québec and Ontario (Canada). The total number of dwellings is 7,831. Every house has different periods of missing data, so, for every house, the longest period of consecutive data between November and February (inclusive) was identified. The study aimed to test the effect of data length on the accuracy of the model. Therefore, data lengths of 3 days, 7 days and 14 days were used, resulting in 3 different models for each house and comparing their accuracy. All models also had a test set of 2 days not used in the calibration at all, in order to test the generalizability of the model.

To calibrate the models, the data points can be treated either as (a) independent observations,

resulting in an ordinary least-squares calibration, or (b) as sequential observations. In the latter case, the model uses its own predictions to predict multiple timesteps ahead during the calibration stage and the number of steps is called calibration horizon. It has been reported that models calibrated to predict as many steps ahead as the prediction horizon of the MPC yield better results [120]. This method is called MPC Relevant Identification (MRI) and in that case the calibration horizon equals to the prediction horizon.

Calibrating models with the MRI method makes the calibration process non-linear, thus significantly increasing the computational resources required. A non-linear least squares solver from python's library scipy [181] is used to calibrate the models.

The models of this study were then used to predict the response of the building over the next 24 hours. For the present dataset, where the time interval between two datapoints is 5 minutes, the model needs to look forward 288 steps. Such an approach can increase dramatically the computational time needed by the MRI calibration; because of this, this study explored the effect of temporal resolution on the final models. Three time intervals were used: 5-min (original sampling rate), 15-min and 60-min. These are the typical intervals used by most utilities when estimating the peak power and energy consumption of residential buildings [182]. To create the datasets for the 15-minute and 60-minute intervals the datasets were resampled using the summation for the HVAC runtimes, the average for the solar radiation and the instant values for the temperatures. Another reason to prefer larger time intervals is that low-order models do not have the ability to capture the small and fast thermal changes that happen in just 5 minutes [53], due to the low structural identifiability [128].

To summarize, 18 models were calibrated in total for each house: 3 models corresponding to each of the 5-minute, 15-minute and 60-minute intervals, for each one of the 3 data lengths (3 days, 7 days and 14 days), using both the ordinary least squares and MRI calibration methods.

5.3.4 Model evaluation

The models were evaluated using the Root Mean Square Error (RMSE) criterion. RMSE is a commonly used metric used to measure the difference between measured and predicted values. As a secondary metric, a baseline model was used to help assess whether the calibrated models predict the indoor temperature well. The baseline model predicted a constant temperature over the predic-

tion horizon equal to that of the initial condition. All metrics were estimated using the predictions of the models for 24 hours in the future. Moreover, the models were also used on the test set to check their generalizability and avoid overfitting.

In order to assess whether the resulting models and their parameters encompassed building physics the time constants of each house were evaluated. The time constants of each model can be found by estimating the poles of the transfer function of Equation (5.3). For a real and positive pole *pole*, the time constant τ is given by Equation (5.7) [183].

$$\tau = -\frac{1}{ln(pole)} \tag{5.7}$$

The transfer function for Equation (5.3) has two poles, therefore there are two time constants. These two time constants characterize the main ways that heat flows from the indoors to the outdoors. The shorter time constant might be associated with the heat transfer between the indoor air an the thermal mass of the house, whereas the longer one can be associated to the heat transfer between the indoor and outdoor air [184].

5.3.5 Model Predictive Control (MPC)

The calibrated models were used to assess the aggregated impact of an MPC controller that optimally adjusts to the Time-of-Use (TOU) tariffs or DR events issued by the grid. The DR potential was assessed during January 20, 2020, which is a cold day in Ontario and Québec, with an average outdoor temperature in the studied locations fluctuating between -20 °C and -10 °C and an average solar radiation reaching a maximum of 420 W/m^2. The indoor air temperature setpoint was assumed to be at 21 °C with a night setback of 19 °C between 9 p.m. and 6 a.m. The weather conditions along with the temperature setpoint and the price of electricity during the day are shown in Figure 5.2.

The current TOU price of electricity in Ontario during the winter weekdays is 7.4 ¢/kWh from 7 p.m. to 7 a.m., 10.2 ¢/kWh from 11 a.m. to 5 p.m. and 15.1 ¢/kWh from 7 a.m. to 11 a.m. and 5 p.m. to 7 p.m [185]. On the other hand, in Québec there is no TOU cost of electricity, but there is dynamic pricing for some of the residential users with certain peak demand events during the winter [95]. During these events, which can occur from 6 a.m. to 9 a.m. and from 4 p.m. to 8 p.m.,

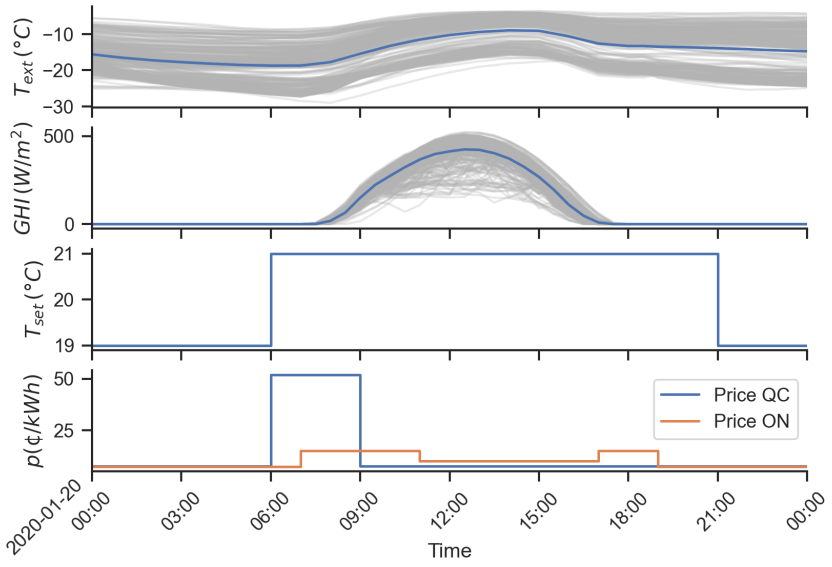

Figure 5.2: Exterior temperature, solar radiation, indoor air temperature setpoint and cost of electricity for the MPC formulation. Each grey line represents the outdoor temperature and solar radiation of one location and the blue line is the average

the electricity is billed at 51.967 ¢/kWh instead of the normal 7.65 ¢/kWh.

The standard way to achieve thermal comfort is to keep the indoor temperature within a certain range, which during MPC can be implemented as a hard constraint or a soft constraint. Hard constraints cannot be violated, while soft constraints can, but are included in the cost function and therefore penalized. They are often multiplied by a large factor in the cost function to ensure that they are not violated often. Generally, soft constraints are preferable, because they are more practical and do not hinder optimization convergence. An in-depth discussion on thermal comfort constraints used in building control can be found in [37]. Both hard and soft constraint approaches have been used by many studies. For example, Huchuk, Sanner, and O'Brien [33] and Seal, Boulet, and Dehkordi [34] included thermal comfort as a soft constraint, with the former penalizing it when the indoor temperature deviated from the (heating or cooling) setpoint by more than 2 °C and the latter using a temperature setpoint range of 1 °C when the house was occupied and 5.5 °C when the house was unoccupied. On the other hand, Cole, Powell, Hale, *et al.* [35] and Bianchini, Casini, Vicino, *et al.* [36] used a hard constraint, with the former having a setpoint range of 4 °C when the house was occupied and 8 °C when the house was unoccupied and the latter a range of 2 °C (occupied) and 6 °C (unoccupied).

Because the installed power of the heating system in each house is not available, it is impossible to quantify the power demand, the energy consumption, and the cost in absolute terms. However, a relative calculation is possible: to quantify the difference of the reference case to the MPC case, these quantities are formulated per unit of installed heating power of the system $Q_{h,inst}$. Therefore, Equation (5.8) shows Q_h, which is the heating power consumption formulated per kW installed (kW/kW_{inst}), Equation (5.9) shows q_h, which is the heating energy consumption formulated per kW installed (kWh/kW_{inst}), Equation (5.10) shows c, which is the total cost for heating per kW installed ($¢/kW_{inst}$)

$$Q_h = \frac{Q_{h,inst}\frac{\delta_h}{\Delta t}}{Q_{h,inst}} = \frac{\delta_h}{\Delta t} \left[\frac{kW}{kW_{inst}}\right] \tag{5.8}$$

$$q_h = \frac{Q_{h,inst}\delta_h}{Q_{h,inst}} = \frac{\delta_h}{3600} \left[\frac{kWh}{kW_{inst}}\right] \tag{5.9}$$

$$c = q_h p = \frac{\delta_h p}{3600} \left[\frac{¢}{kW_{inst}}\right] \tag{5.10}$$

Equation (5.11a) shows the MPC controller formulation, which is trying to minimize the price of electricity, as seen in Figure 5.2, over a prediction horizon *PH*. Equation (5.11b) forces the formulation to use the building model of the house shown in Equation (5.3). Equation (5.11c) constrains the heating equipment runtime to be at most as large as the timestep itself. Thermal comfort was considered as a soft constraint, which does not allow the temperature to fall below the setpoint nor exceed the setpoint by more than 2 °C. β is a factor that weights the cost of energy to the "cost" of discomfort. It needs to be large enough that thermal comfort violations do not happen often, and is chosen to be $\beta = 100 \left[\frac{¢}{°Chr \cdot kW_{inst}}\right]$. In comparison, the cost of electricity c ranges from 1.85 to 13 $\frac{¢}{kW_{inst}}$ depending on the time of day. The prediction and control horizons of the MPC formulation were 24 hours, and the initial temperature was assumed to be 20 °C. The optimization problem is convex and was solved using the cvxpy library in python [173].

$$J = min\left(\sum_{k=1}^{PH} c^k + \sum_{k=1}^{PH} \beta d^k\right) \tag{5.11a}$$

$$s.t.\ \mathbf{T}^{k+1} = \mathbf{A}\mathbf{T}^k + \mathbf{B}\mathbf{u}^k \tag{5.11b}$$

$$0 \leq \delta_h^k \leq \Delta t \tag{5.11c}$$

$$d^k = \begin{cases} \left(T_{set}^k - T_i^k\right)\Delta t, & \text{if } T_i^k < T_{set}^k \\ 0, & \text{if } T_{set}^k \leq T_i^k \leq T_{set}^k + 2 \\ \left(T_i^k - T_{set}^k\right)\Delta t, & \text{if } T_{set}^k + 2 < T_i^k \end{cases} \tag{5.11d}$$

As mentioned in the introduction, the BEFI represents the ability of a building to change its power demand during a specific period demanded by the grid. The average dynamic BEFI at time t and for duration Dt (per kW installed) was calculated with Equation (5.12) [25], where Q_{ref} is the power consumption under a reference energy consumption profile, Q_{flex} is the power consumption of the flexible strategy. The reference case was established by using a deadband controller with on/off cycling and a single-sided deadband of 0.5 °C (1 °F). This is similar to the strategy found both in the Ecobee dataset and in [33].

$$\begin{aligned} \overline{befi}\,(t, Dt) &= \frac{\int_t^{t+Dt} Q_{ref}dt - \int_t^{t+Dt} Q_{flex}}{Q_{h,inst}Dt} = \\ &= \frac{\int_t^{t+Dt} q_{ref}dt - \int_t^{t+Dt} q_{flex}}{Dt} \left[\frac{kW}{kW_{inst}}\right] \end{aligned} \tag{5.12}$$

5.4 Results and discussion

Out of the 7,831 houses, 527 did not have data for at least 5 consecutive days (at least 3 days for the training set and 2 days for the test set) in any winter between the years 2015 and 2021, reducing the available houses to 7,304. Most of the houses are located in Ontario; only 624 houses are located in Québec.

Figure 5.3 shows the distribution of the RMSE of the 7,304 houses for the 3 different lengths of

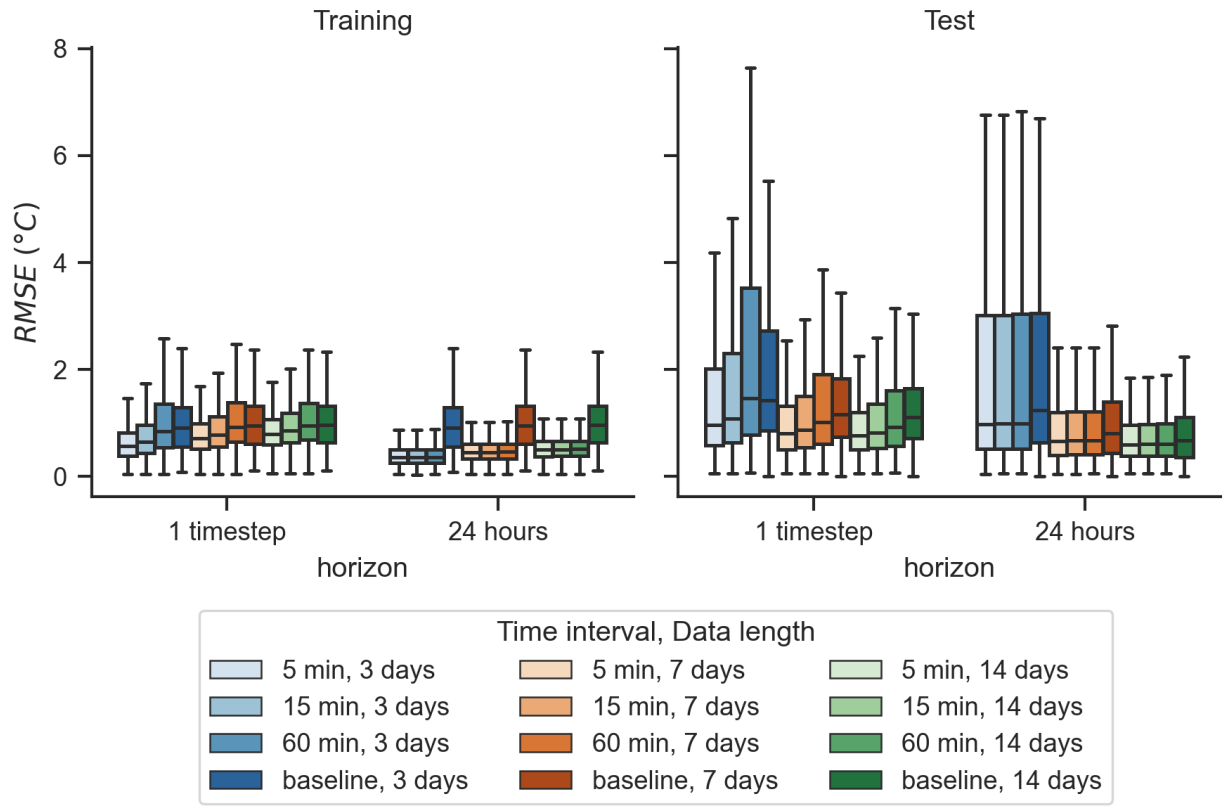

Figure 5.3: Distribution of RMSE of the 7,304 houses for the training sets (left) and the 2 days of the test set (right) for different time intervals, data lengths and calibration horizons

the training set and the 2 days of the test set. The first observation is that models with a calibration horizon of 24 hours have a much lower RMSE on the training set than the ones with calibration horizon of 1 timestep, but that difference in accuracy seems to be small in the test set. Overall, models with calibration horizon of 24 hours and higher training data lengths performed better on average. Models with calibration horizon of 1 timestep performed better when calibrated with smaller timesteps, while models with calibration horizon of 24 hours had similar performance for different timesteps. Finally, models calibrated with data length of 3 days performed well on the dataset they had already "seen" during the calibration, but their accuracy was reduced significantly on the test set.

5.4.1 Evaluation and filtering of the models

Naturally, not all 7,304 models captured the thermal dynamics of the respective house adequately, but at the same time it is impossible to plot the response of every single one of them. Instead, an automated rule is necessary to filter out models that may not be accurate enough for the MPC formulation. The models were filtered based on how much better their predictions were compared to the baseline; more specifically, any model that did not achieve an RMSE decrease of at least 0.5 °C for the training and any RMSE decrease for test set was discarded.

Calibration horizon	1 timestep									24 hours								
Data length (days)	3			7			14			3			7			14		
Time interval (min)	5	15	60	5	15	60	5	15	60	5	15	60	5	15	60	5	15	60
Number of models	1878	1568	982	1652	1400	949	1394	1189	861	2436	2403	2302	2245	2229	2131	2039	2007	1893

Table 5.1: Number of house models which performed at least marginally better than the baseline for the test set and with at least a 0.5 °C RMSE decrease compared to the baseline for the training set

Table 5.1 shows the number of models satisfying these criteria and Figure 5.4 shows the updated distributions of RMSE based on the filtered models. Models with 24-hour calibration horizon produced more models that perform significantly better than the baseline and they performed on average better than the models with 1-timestep calibration horizon. Although having 3 days for training and calibration horizon of 24 hours produced the most models, they suffered from overfitting, indicated by their significantly larger RMSE on the test set. On the other hand, 7 and 14 days of training data performed slightly worse on the training set, sacrificing training accuracy for generalizability,

having a much better performance on the test set. When it comes to the time interval of the data, models with 1-timestep calibration horizon performed better as the time interval decreased, but the ones with 24-hour calibration horizon seemed to be less affected. Models with 24-hour calibration horizon showed similar performance for 5-minute and 15-minute data intervals, but there was a small increase of RMSE for 60-minute intervals in the test set. Although this increase was small, it could indicate that 60-minute intervals are large enough to not allow the capture of some shorter building thermal dynamics.

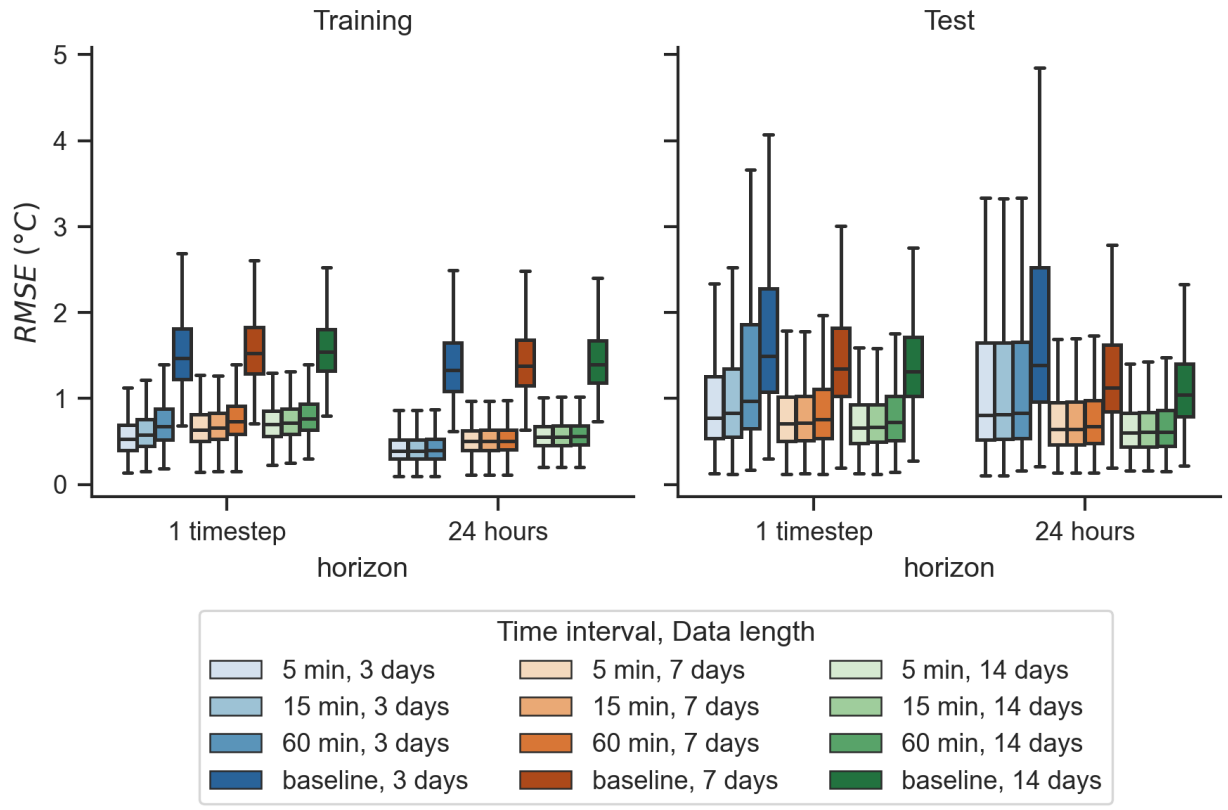

Figure 5.4: Distribution of RMSE of the filtered houses. Each distribution includes the number of houses shown in Table 1

Figure 5.5 shows the distribution of time constants τ_1 (in minutes) and τ_2 (in hours) of the filtered houses for different data lengths and time intervals and calibration horizons. Time constants of models with 24-hour calibration horizon were very similar for different data intervals and were slightly larger than the ones with 1-timestep calibration horizon, which concentrated towards smaller values of τ_1. As data length increases the distributions become less spread for all cases. All distributions of models with 24-hour calibration horizon have a median τ_1 of approximately

200 minutes, and τ_2 of 100 hours. Overall all distributions seem to roughly follow expert knowledge [184].

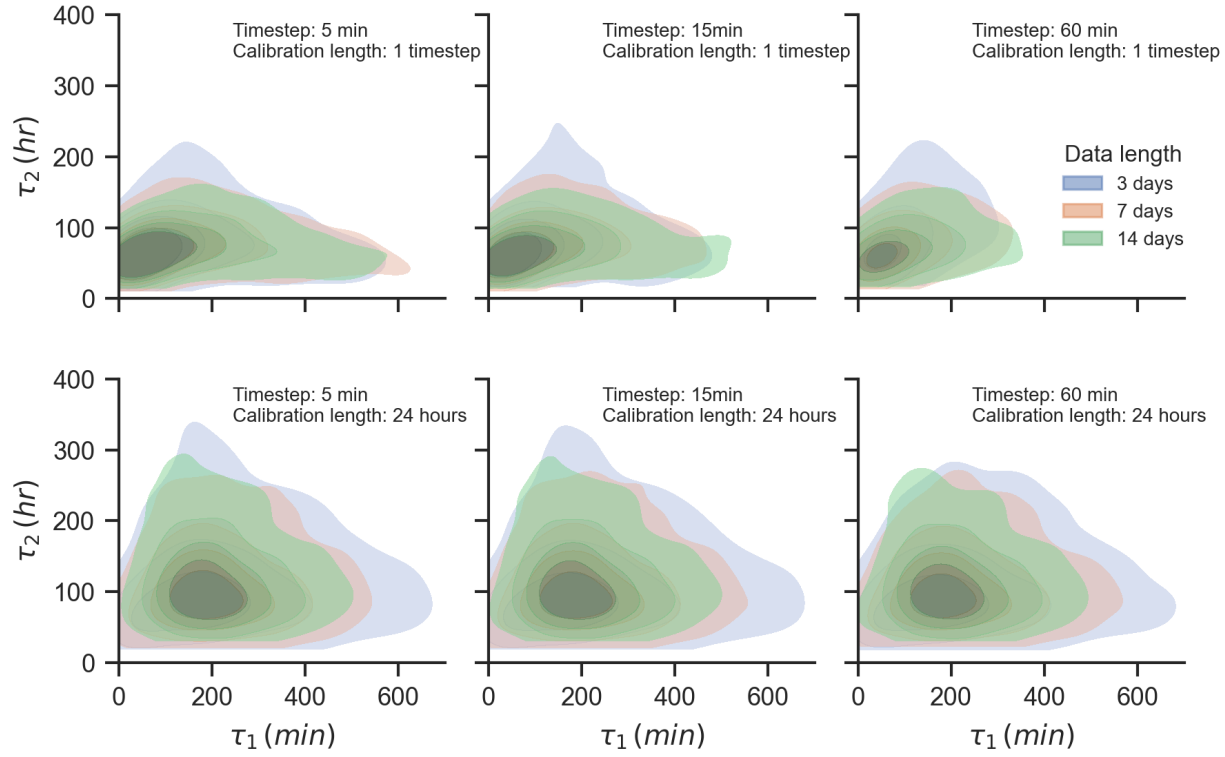

Figure 5.5: Distributions of time constants τ_1 (in minutes) and τ_2 (in hours) of the filtered houses for different data lengths and time intervals and calibration horizons. Each distribution includes the number of houses shown in Table 5.1

The models with 15-minute interval data and calibration horizon of 24 hours were used to assess the DR potential using MPC, because they provided a good balance between accuracy, resolution and computational resources. The final dataset included 2,229 houses, out of which 2,091 were located in Ontario and 138 in Québec. The models had a mean RMSE of 0.5 °C, median RMSE of 0.5 °C and standard deviation of 0.24 °C on the training set and mean RMSE of 0.74 °C, median RMSE of 0.62 °C and standard deviation of 0.44 °C on the test set for 24-hour predictions.

5.4.2 MPC application on the population of houses

Figure 5.6 shows the distributions of the results for the reference case and the MPC strategy that tries to reduce the cost of electricity based on the TOU rate in Ontario (top row) and the DR event in Québec (bottom row).

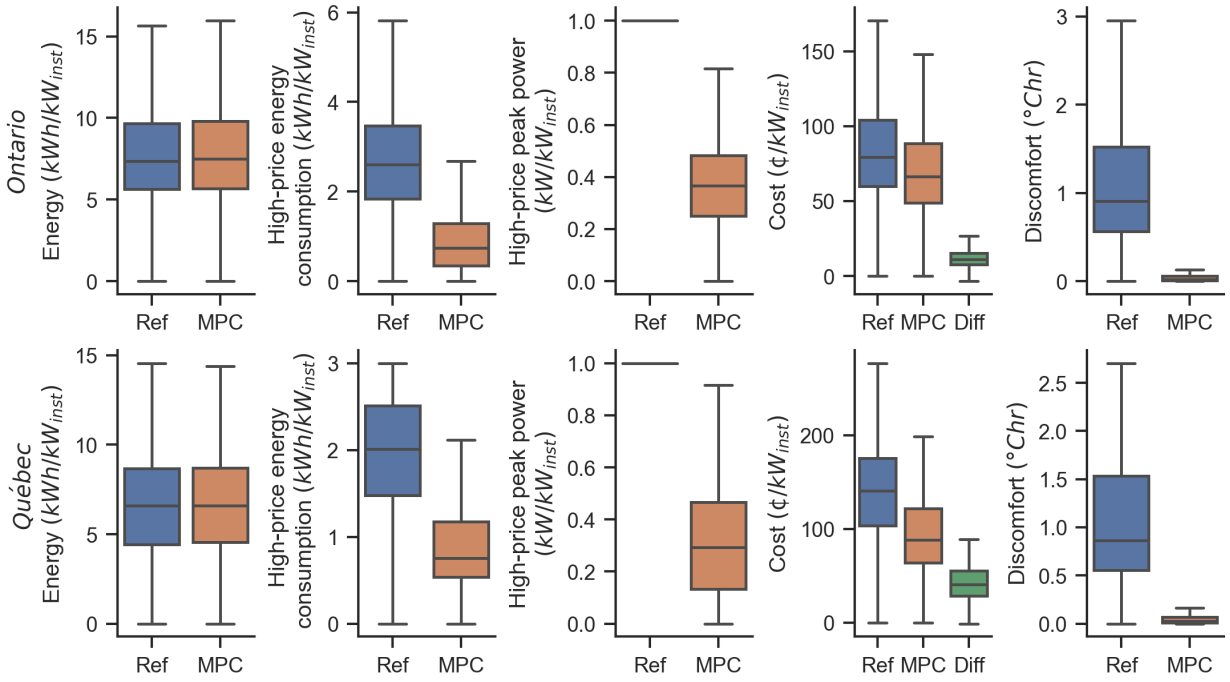

Figure 5.6: Distributions of total heating energy consumption, peak power during the high-price period, total cost and thermal discomfort for the reference and MPC case. All quantities are presented per kW installed. The top row shows results for the province of Ontario (2,091 houses) and the bottom for Québec (138 houses)

Examining the results for the province of Ontario, at first glance the distribution of the total heating energy consumption of the MPC seems to be slightly higher than the reference, with the median consumption of the reference case being 7.40 kWh/kW_{inst} and the one for the MPC case 7.54 kWh/kW_{inst}. However, the MPC performed well during the high-price periods (7 a.m. to 11 a.m. and 5 p.m. to 7 p.m.). The MPC strategy reduced the peak power consumption from being always at the maximum (which is the total installed power) to a median of 0.4 kW/kW_{inst} and the energy consumption from a median of 2.6 kWh/kW_{inst} to a median of 0.77 kWh/kW_{inst}. Because the optimization algorithm was trying to reduce the cost of electricity while maintaining thermal comfort, the strongest effect of the MPC strategy is reflected in the total cost of electricity and thermal discomfort for the occupant. The MPC strategy managed to reduce cost in all cases, with a median reduction of 12 $¢/kW_{inst}$, or 16 %, while completely eliminating thermal discomfort.

Because there are only 138 houses in Québec, the results are less likely to accurately reflect the average home than in the Ontario case. The patterns of the total heating energy consumption and the energy and peak power consumption during high-price periods are very similar to the Ontario ones. However, MPC managed to achieve much greater cost savings of an average 43 $¢/kW_{inst}$, or 31 %.

Assuming a typical residential building with 10 kW of installed power, the median homeowner could achieve a reduction of $1.07 in Ontario and $4.07 in Québec in one day. Similarly, each house could reduce the energy consumption during high-price periods by 15 kWh in Ontario and 11 kWh in Québec. From the grid's perspective, during the high-price periods, Ontario and Québec could see a reduction in energy consumption of 15 MWh and 11 MWh per 1000 houses that adopt optimal strategies respectively.

The difference in the magnitude of the results between Ontario and Québec can be explained by the very large difference between the off- and on-peak cost of electricity in Québec, and is attributed to the different strategies the provinces have adopted to reduce power demand. In Ontario, the TOU rate is in effect every day giving modest savings to homeowners who lower their peak consumption daily, whereas in Québec the DR events can only happen up to 33 times in one year.

Figure 5.7 shows the distribution of BEFI for a duration of 3 hours during the whole day. For both Ontario and Québec, the BEFI was on average negative in the morning hours because the house was trying to preheat in anticipation of the morning peak when the setpoint increased from

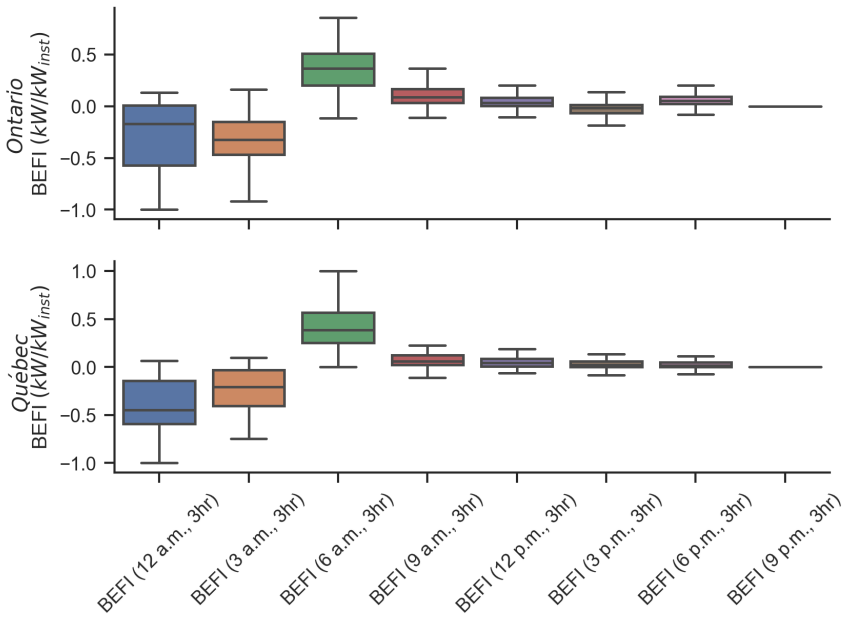

Figure 5.7: Distribution of Building Energy Flexibility Index (BEFI) with optimized control for a duration of 3 hours every 3 hours. All quantities are presented per kW installed. The top row shows results for the province of Ontario (2,091 houses) and the bottom for Québec (138 houses)

19 °C to 21 °C. In both cases the BEFI increased a lot during the high-price periods; on average a house in Ontario achieved a BEFI of 0.37 kW/kW$_{inst}$ and in Québec 0.39 kW/kW$_{inst}$ from 6 a.m. to 9 a.m. In the case of Ontario, the same effect —– but of a smaller magnitude —– was observed during the evening peak, when the average BEFI increased from -0.02 kW/kW$_{inst}$ during 3 p.m. to 6 p.m. to 0.06 kW/kW$_{inst}$ during 6 p.m. to 9 p.m.

Figure 5.8 shows the power consumption throughout the day for each house for the reference case and the MPC case. The average power consumption of all the houses is shown in blue. The comparison between the reference case and MPC highlights the preheating that happened before the high-price periods, especially in the morning.

The MPC potential of a house and its cost reduction are defined by its ability to preheat and maintain comfortable temperatures for as long as possible. That means that houses with larger time constants (as shown in Figure 5.5) have a higher MPC potential. The time constant of a house is affected by its thermal mass, i.e., its construction materials, as well as its overall building envelope insulation properties, which mainly include building envelope elements, thermal bridges, ventilation, and infiltration. In consequence, buildings with better thermal insulation properties

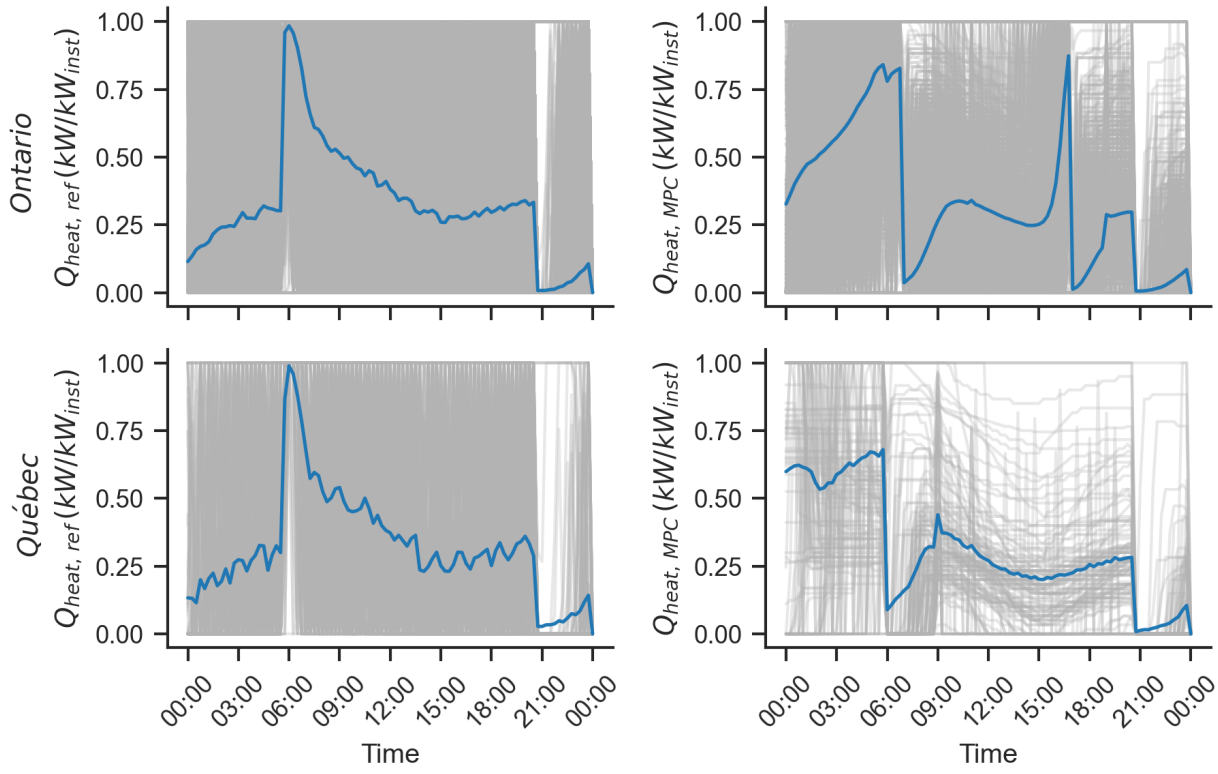

Figure 5.8: Power consumption of the houses for the reference (left) and the MPC case (right) for Ontario (top) and Québec (bottom). Each grey line represents the power consumption of one house and the blue line is the average

have overall a higher potential for energy flexibility and demand response applications.

In general, the larger the time constants of the house, the earlier the house can preheat, and the earlier it can harvest its energy flexibility potential. The different times that the houses started to preheat resulted into the relatively large interquartile range of the BEFI during night hours in Figure 5.7. The new average heating profile shown in Figure 5.8 had a slightly smaller peak, around 85 % of the reference one in Ontario and 70 % in Québec (or a power peak reduction of 0.15 kW/kW_{inst} in Ontario and 0.3 kW/kW_{inst} in Québec), due to the different preheating start times. However, there was still a peak that essentially just shifted to the hours exactly before the original one. If enough customers implement optimal controls, then that shifting effect could potentially prove to be a challenge for the grid, highlighting the need for dynamic pricing and smart and transactive grids [174].

5.5 Conclusion

As smart thermostats become increasingly available in residential buildings, there is an opportunity to study the effect of data resolution, length, and calibration on control-oriented building models and the effect of advanced control strategies. To do that, this study used smart thermostat data from 7,800 houses in Ontario and Québec, Canada.

Each house was modeled with a second-order model and calibrated with different data intervals, training data lengths and calibration horizons. Models calibrated with calibration horizon of 24 hours performed significantly better than models with calibration horizon of 1 timestep. Data length of 3 days led to model overfitting, whereas data with 60-minute time intervals led to a small loss of information. Overall the models with calibration horizon of 24 hours, data length of 7 days and time interval of 15 minutes provided the best balance between accuracy and computational resources.

These models were then used to perform MPC on a cold day of January using the TOU rates of Ontario and the dynamic pricing of Québec. The MPC performance was compared to the performance of a reference deadband controller with a single-sided deadband. The analysis showed that the MPC controller can systematically reduce the high-price energy consumption, reducing the cost for homeowners by 16 % in Ontario and 31 % in Québec, while at the same time eliminating thermal discomfort usually introduced by setpoint setback. MPC achieves that by preheating the

houses, successfully harvesting the energy flexibility of the houses. The preheating shifts power peak consumption, reducing it by 0.15 kW/kW_{inst} in Ontario and 0.3 kW/kW_{inst} in Québec.

6 Thermal modeling for control applications of 60,000 homes in North America using smart thermostat data[1]

6.1 Abstract

As smart thermostats become increasingly available in residential buildings, there is an opportunity to use measured building data to calibrate models for community and district applications, instead of relying on high-fidelity simulations. This study used smart thermostat data from 60,000 houses in North America to create single-zone models. The model structure was defined with an automated forward selection procedure. 61% of the final models were classified as good fits and the structure of 80% of them was of 5th-order (5 thermal capacitances). An investigation of the 24-hour prediction error of the models showed that the ones classified as good fits are accurate enough for day-ahead predictions and Model Predictive Control (MPC) applications. An analysis of the model parameters suggested no strong correlation between them and the available metadata. The time constants of the houses were estimated, providing valuable information about the houses thermal inertia. Building models that can accurately capture and leverage building thermal inertia are ideal candidates for MPC and energy flexibility applications.

[1] C. Vallianos, J. Candanedo, and A. Athienitis, "Thermal modeling for control applications of 60,000 homes in north america using smart thermostat data," *Energy and Buildings*, p. 113 811, 2023. DOI: 10.1016/j.enbuild.2023.113811.

6.2 Introduction

The increasing implementation of intermittent renewable energy resources [187], the widespread adoption of heat pumps for space electrification [16], as well as the growing uptake of electric vehicles [188] have underlined the need to balance energy consumption and generation at a building and grid level. Advanced building control strategies, such as Model Predictive Control (MPC), have been identified as suitable candidates for this challenge because they can leverage energy flexible technologies, such as thermal [23] and electrical [20] energy storage, and facilitate the transactive interaction of buildings with the utility grid [98].

The International Energy Agency's Energy in Buildings and Communities (IEA-EBC) Annex 67 "Energy Flexible Buildings" defined energy flexibility as "the ability to manage the demand and generation according to climate conditions, user needs, and energy network requirements" [24]. Dozens of Key Performance Indicators (KPIs) can be used to characterize energy flexibility. In most cases, this quantification takes place in comparison with a baseline or benchmark [43]. For example, Athienitis, Dumont, Morovat, *et al.* [25] defined the average dynamic Building Energy Flexibility Index (BEFI) for time t and duration Δt as shown in Equation (6.1), where Q_{ref} is the total power consumption under a reference energy consumption profile and Q_{flex} is the total power consumption of the flexible strategy (e.g., an MPC strategy).

$$BEFI_{\Delta t}(t) = \frac{\int_t^{t+\Delta t} Q_{ref}(t)dt - \int_t^{t+\Delta t} Q_{flex}\,(t)\,dt}{\Delta t} \tag{6.1}$$

Energy and demand flexibility are tightly connected to Demand Side Management (DSM), an encompassing name given to techniques that aim to modify customer load patterns, and more specifically to its Demand Response (DR) aspect, which offers incentives to the customers to encourage change in their consumption patterns [44].

6.2.1 Literature Review

Both MPC strategies and energy flexibility applications rely on building models. In the former case, the building model is necessary to obtain the optimal control; in the latter, the model is used to estimate the reference and flexible power profiles needed to quantify energy flexibility [45] (e.g.,

Q_{ref} and Q_{flex} in Equation (6.1)).

Building modeling methods

Building thermal models are traditionally categorized in the scientific literature as white-box, black-box and grey-box models [86]. White-box models use mathematical equations based on fundamental physical principles to model the energy response of a building. The parameters of these models are user-defined based on information (either available or assumed) about the building, such as geometry, construction materials, equipment, etc. Most Building Performance Simulation tools, like EnergyPlus and TRNSYS, use high-fidelity, detailed white-box models. White-box models can be extremely accurate, but they are time-consuming to calibrate and require the expertise of an engineer, which often involves high costs [53]. Moreover, necessary information for their calibration is frequently not available, leading to assumptions that can compromise the model accuracy [49].

On the other hand, black-box models are purely data-driven relationships between inputs and outputs, ranging from simple statistical regressions to complex machine learning algorithms [155]. Black-box models are trained on measured data, can be greatly accurate, and they do not need engineering expertise during their training [60]. The growing availability of machine learning methods has also contributed to the popularity of black-box models. However, black-box models lack interpretability and do not guarantee the ability to extrapolate to situations not captured in the training dataset or from building to building [68]. During the last few years, there has been significant effort to constrain the parameters of a black-box models to "physical" bounds and improve their interpretability, but such research is still at the early stages [37], [76].

Grey-box models are a compromise between white-box and black-box models. They have a simplified structure that has physical meaning (like white-box models), but their parameters are calibrated with measured data (like black-box models). Grey-box models are often represented using a resistance-capacitance (RC) analogy, or "thermal network" [77]. Their simplified structure makes them much easier and faster to calibrate than white-box models, while at the same time, they have a better extrapolation ability than black-box models [78].

Grey-box models are arguably better candidates than both white- and black-box models for MPC and flexibility assessment. Compared to white-box models, they require less computational power to calibrate and are easier to integrate into an MPC framework, while compared to black-

box models, grey-box models require fewer data and have the significant advantage of providing insight into the thermal behaviour of the building [82].

A critical challenge when modeling buildings at a district or community level is the characterization of the dynamic response of buildings on a large scale. In this case the models are called Urban Building Energy Models (UBEM), and they are bottom-up, physics-based models that simulate the thermal performance usually on a building-to-building basis [96]. UBEMs rely on the development of architectural building archetypes, which are physics-based representations (usually a high-fidelity white-box models) that simulate single buildings as generalizable typical samples of an entire building stock [97]. Such a building archetype is often generated by sampling building parameters from available distributions or databases [98]. For example, several studies (e.g., [99]–[101]) have used the TABULA database [102], which clusters residential buildings based on size and age and includes typical building material values for various European countries. Similar studies in North America (e.g., [103], [104]) use ResStock [105], a building stock energy model based on millions of EnergyPlus simulations. The high computational cost often associated with these large-scale simulations has also created a need for surrogate models, i.e., fast statistical models that emulate high-fidelity simulations and have been trained on their inputs and outputs [106]. More information on archetype buildings can be found in [107] and a detailed literature review on existing residential high-fidelity building stock classification studies can be found in [108].

Even with archetypes, however, building model parameters often rely on a certain amount of guesswork, e.g., the wall materials and insulation are estimated based on the location and the year of the house. However, with the development of novel technologies, such as the Internet of Things and smart thermostats in particular, a substantial amount of operational data has recently become available. These data can be used to develop and calibrate fast, reduced-order models for control applications (also known as control-oriented models) or UBEM for district-level applications. Using real data to calibrate UBEMs has been proposed as a means to ensure that archetype buildings are in fact representative of a district and to estimate the actual simulation error [109]. Moreover, the lack of control-oriented models has been identified as a significant hurdle for the widespread adoption of MPC solutions at a building level [37].

Some methods for automated model development using smart thermostat data have been published, both for single-zone and multi-zone models. Bacher and Madsen [116] proposed a stochastic

model identification and selection procedure for single-zone RC models. They suggested a forward selection procedure using likelihood ratio tests and applied it to an experimental setup. Prívara, Váňa, Žáčeková, *et al.* [41] suggested a two-stage forward RC model selection method for MPC applications. They first selected the inputs and then the states of the model, and then validated the procedure on a two-zone TRNSYS model simulation. Wang and Chen [87] proposed a backward RC model selection based on the ratio of parameter standard error over the identified parameter estimate. They applied the methodology to measured data from a low-energy house using one zone per floor. Arroyo, Spiessens, and Helsen [133] presented a forward selection method for multi-zone RC models. They applied their method on an emulator building model implemented in BOPTEST and showed that the multi-zone model can outperform the single-zone model for MPC because it creates less thermal discomfort. Vallianos, Athienitis, and Delcroix [151] proposed an automated method for multi-zone RC models for MPC applications that uses both forward and backward selection to ensure proper parameter identification. The Bayesian Information Criterion was used as the evaluation metric and applied the method on measured data from an experimental house.

As the number of houses increases, methods that generate models with "varying" structures require significant computational resources. As a result, most studies that have endeavoured to model houses on a large scale have used a fixed model structure. For instance, multiple studies have calibrated first-order models using large smart thermostat datasets [110], [111], [113], [114], [118]. All these studies employed the same dataset of North American houses. However, these studies focused mostly on time constant estimation, most of them neglecting the effect of solar radiation in the process ([110], [111], [113], [118]). John, Vallianos, Candanedo, *et al.* [110] showed that the time constants vary seasonally, probably as a result of opening and closing windows in response to weather. Doma, Ouf, Newsham, *et al.* [113] found the building age to be the most influential factor on time constants, and the number of floors the least influential. Huchuk, Sanner, and O'Brien [114] calibrated control-oriented first-order models for multi-hour predictions and compared it with other data-driven models. They showed that first-order models were outperformed by other models, the order and structure of the model was suggested as the most likely explanation.

Hossain, Zhang, and Ardakanian [112] used Bayesian Neural Networks based on the nRnC structure of grey-box models to model 8,884 houses in Canada. They used 3 months of data and showed that the 2R2C model performs the best. They also used transfer learning (both across

buildings and across seasons), which resulted in models with the same or better accuracy with much fewer data.

Leprince, Madsen, Miller, *et al.* [115] used data from 247 Dutch houses to calibrate stochastic single-zone models. They used the method presented in [116] and they proposed a new evaluation metric, the normalized Cumulative Periodogram Boundary Excess Sum (nCPBES), which indicates the residual auto-correlation. Based on nCPBES they classified their models as good (38%), close (38%), and poor (24%). They used the identified parameters to benchmark the building envelope insulation performance. They also published the calibrated model parameters [117].

Vallianos, Candanedo, and Athienitis [168] calibrated models for 7,800 houses in Québec and Ontario, Canada for 24-hour predictions and assessed MPC on a large scale. They used second-order models, and tested the effect of training length and calibration horizon on the 24-hour prediction accuracy of the models. They used the existing dynamic pricing and Time-of-Use tariffs to show that MPC shifts the peak power consumption, reducing it by 15% in the case of Ontario and 30% in Québec. If just 1,000 houses adopt MPC the grid could see an average reduction in high-price energy consumption of up to 15 MWh in Ontario and 11 MWh in Québec.

Doma and Ouf [118] used data from 60,000 houses in North America to calibrate first-order RC models and estimate their thermal constant. They used only periods during the night, where there are no solar heat gains, and the occupancy gains would be minimal. Then, they clustered the estimated thermal constants into four groups representing the building's need for retrofit. They reported approximately 22,000 reliable models with a median time constant of 51 hours and 90% of the values in the range of 11 to 110 hours.

6.2.2 Motivation

The increasing adoption of smart thermostats facilitates the development of control-oriented thermal models in the residential sector. At the building level, data-driven models can be used for assessment of energy flexibility, DR measures, MPC or other advanced control strategies, fault detection and diagnosis [189], [190] or retrofit evaluation [191], [192]. At the district level, data-driven models can be used for energy policymaking, assessment of renewable energy penetration potential [193], or assessment energy aggregator performance [194].

The absence of publicly available datasets of control-oriented models was identified as a chal-

lenge for large-scale studies. The issue arises from both the lack of an automated method for developing building models using smart thermostat data and the scarcity of measured data itself. This article uses smart thermostat data from 60,000 houses in North America to create single-zone models with an automated forward selection procedure and makes the resulting models publicly available to be used in community and district applications. The models are control-oriented, focusing on scalability, practicality, and simplicity. They only use information available to a smart thermostat, and, although they are physics-based, they focus on accurate predictions and not the evaluation of physical meaning of every single model component.

The work adapts the automated model selection and evaluation procedure for stochastic building model identification presented in [115] and applies it on a large dataset of 60,000 houses in North America. The calibrated models are analyzed and the most likely model structures are identified. The ability of the models to be used in MPC applications is evaluated by investigating the 24-hour multi-step prediction error and calculating the time constants of the houses. The full dataset of the resulting models is available at `https://doi.org/10.5281/zenodo.8347091` [195], allowing studies on large building stocks to gain access to and sample from building models calibrated from measured data.

Section 6.2 reviewed the literature and presented the motivation behind this work. Section 6.3 describes the dataset and provides details about the model generation and selection procedure, as well as the evaluation metrics. Section 6.4 investigates the calibrated models, their accuracy, model parameters and time constants. Lastly, the article concludes with Section 6.5.

6.3 Methods

This section describes the methods used to develop stochastic RC models from smart thermostat data. In general, this method modifies the work of Bacher and Madsen [116] for model generation and Leprince, Madsen, Miller, *et al.* [115] for automatic model selection. Section 6.3.1 describes the available data, the preprocessing procedure and the final dataset. Section 6.3.2 outlines the RC model used to represent each house, its components and the equations defining the heat transfer. Finally, section 6.3.3 presents the forward selection procedure and the evaluation metrics.

6.3.1 Data description and selection

This study uses data from thousands of houses in North America, provided by Ecobee, a smart thermostats company based in Toronto, Canada. Ecobee offers the Donate Your Data (DYD) [196] program to their customers, allowing them to donate an anonymized dataset of the data logged by their thermostats. The dataset is the same one used in [110]–[114], [118], [168].

Each house is equipped with one or more thermostats. Each Ecobee thermostat collects measurements of indoor temperature value and upper and lower setpoint, relative humidity value and upper and lower setpoint, runtime of the heating and cooling systems equipment (in seconds) and motion. The data are sampled every 5 minutes. The dataset also includes a "control" temperature, which is an aggregated temperature from all the available thermostats used to compare against the setpoints, and the outdoor temperature of the closest weather station. The control temperature is often the average of the individual zone temperatures, but it can also be a weighted average based on user input.

The dataset also comes with metadata provided by the user, which includes information about the country, province/state, and city of the house, the floor area and age of the house, the number of occupants and floors, the style of the house, whether it has a heat pump, and whether the house uses natural gas or electricity for heating. Approximately 20% of the houses are equipped with a heat pump, while the rest 80% are heated with natural gas. A breakdown of the metadata information (after preprocessing) is shown in Figure 6.1. It is worth noticing that, since the metadata are provided by the user, they included erroneous, missing, or heterogeneous values. Approximately 500 houses were excluded as outliers for having more than 6 occupants, or more than 4 floors. The house style was homogenized (e.g., "condominium", "Condominium", and "condo" to "Condo"). House style "Other" included missing values as well as answers like "I don't know", "0", or "OFF". Additionally, two home styles, "Loft" and "Multiplex" were included in "Other", as they included less than 1% of the homes. Similarly, the "other" climate category consisted of 10 climate zones that each included less than 1% of the houses.

An important piece of information missing from the dataset is the solar radiation, a major disturbance in building energy modeling. The city, province/state, and country were used to find the approximate latitude and longitude of each location through geopy [178], using the Nominatim

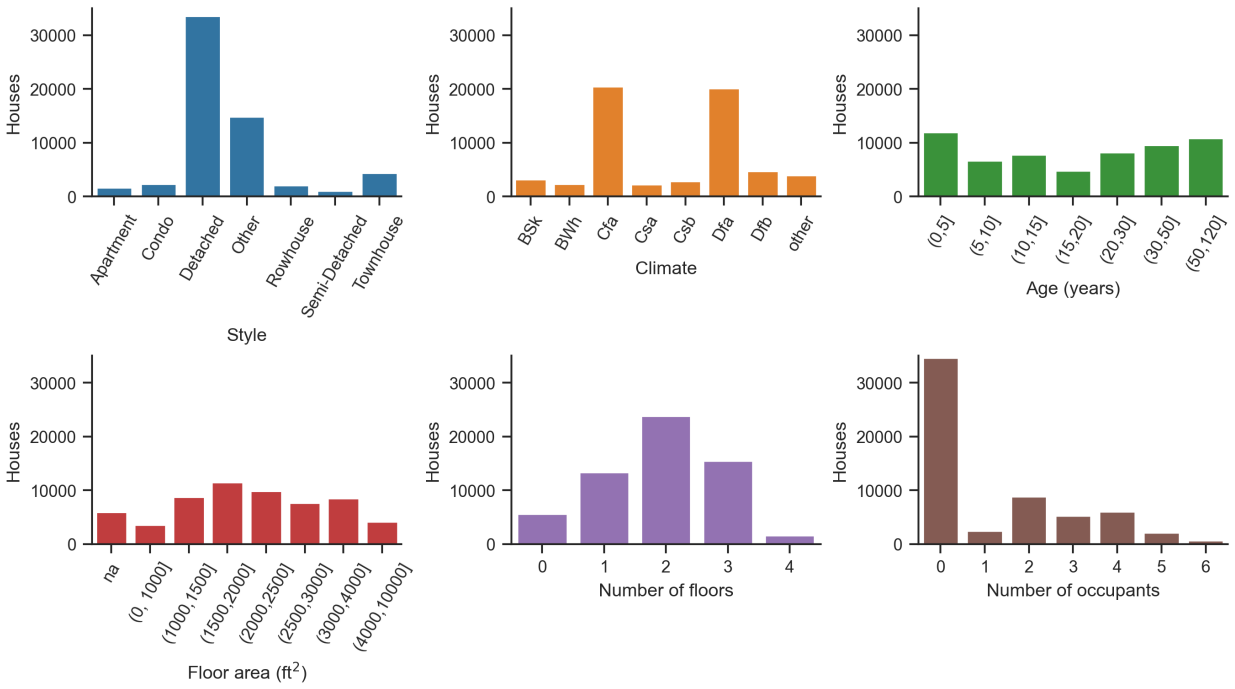

Figure 6.1: Distributions of metadata of the final dataset

Application Programming Interface (API) [179]. Then, the latitude and longitude of each location were used to fetch the historical global horizontal solar irradiance data from the National Solar Radiation Database of the National Renewable Energy Laboratory of the U.S. Department of Energy, using their API [180]. The irradiance has units of W/m^2 and its temporal resolution is either 5 minutes or 30 minutes, depending on the location and the year. The 30-minute data were interpolated to 5-minute intervals. The latitude and longitude of each location were also used to retrieve its Köppen Geiger climate zone classification [197], which was made available on arcGIS by Commission for Environmental Cooperation (CEC) [198] and was accessed using the arcGIS python API. Figure 6.2 shows the location of the used houses, along with their climate zone classification.

The available dataset includes data from approximately 100,000 houses in the United States and Canada, spanning the years from 2015 to 2021. Around 5,000 houses with typos or missing information regarding their location were excluded, since the location is necessary to retrieve historical solar irradiance data. Moreover, the nature and resolution of the dataset makes missing values unavoidable, so for each house only the periods that contain consecutive data of more than 30 days are considered. The final dataset includes approximately 60,000 houses.

Figure 6.1 and Figure 6.2 show that although there are houses all over North America, they are

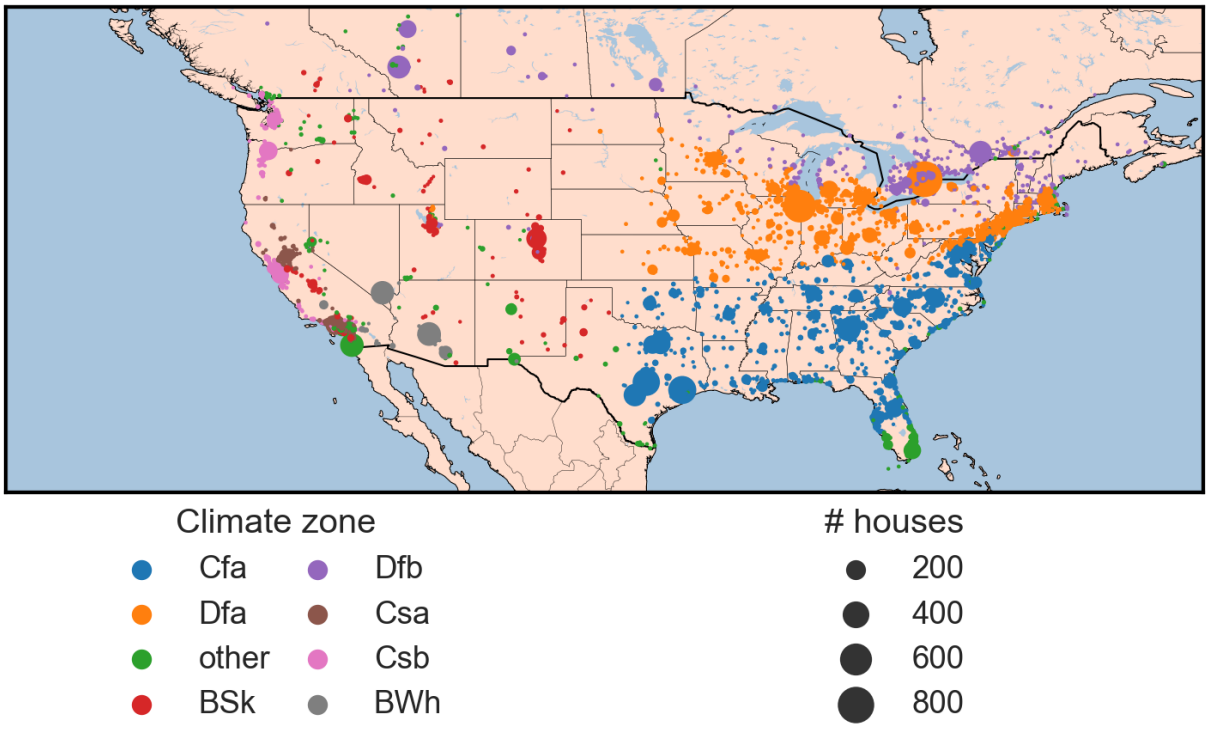

Figure 6.2: Location of houses in the final dataset

more densely distributed on the east side, where the houses are both more in quantity and better dispersed on the map. That is also reflected on the climate zone classification, where zones Cfa (temperate, without dry season, hot summer) and Dfa (cold, without dry season, hot summer) are prevalent. Observing the rest of the metadata, the house styles are also biased towards detached homes, and the prevalent number of occupants is 0, which could indicate missing information. The house age, floor area and number of floors are fairly well distributed.

6.3.2 Model structure

Each house can be modeled as single equivalent zone, using the "control" temperature T_i already calculated by the thermostats. This temperature acts as an equivalent zone temperature and is compared to the setpoints and used to define the runtime of the HVAC system. However, the actual structure and order of the single-zone model can range from a simple first-order model that only models the indoor air temperature to a more complicated fifth-order model that models the heat capacity of various elements of the house and the heat transfer between them. The model structures

and selection procedure are based on [116] and is similar to the ones used in [115].

The full model is shown in figure 6.3. The model can have up to 5 states:

- T_i (°C) is the effective indoor air temperature.
- T_m (°C) is the effective temperature of the interior thermal mass.
- T_e (°C) is the effective temperature of the building envelope mass.
- T_h (°C) is the effective temperature of the heater(s).
- T_s (°C) is the effective temperature of the sensor(s).

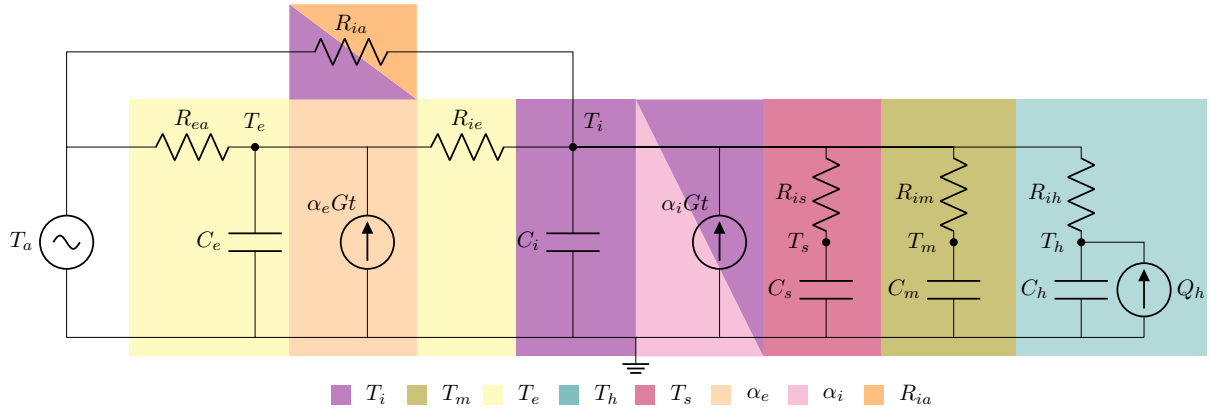

Figure 6.3: The full (most complex) model $T_iT_mT_eT_hT_s\alpha_e\alpha_iR_{ia}$. The figure is adapted from [116]. Each model contains the part of the network that corresponds to its name, e.g., T_iT_h includes the purple- and cyan-shaded areas of the network. R_{ia} is always included with T_i unless T_e is included and R_{ia} is not. α_i is always included with T_i unless α_e is included and α_i is not.

Each state is associated with an equivalent thermal capacitance C (J/°C), while R (°C/W) denotes the thermal resistance between two nodes that defines the thermal exchange between them. T_a (°C) is the ambient temperature, Q_h (W) is the total heating output, α (m^2) is a solar factor, which includes solar aperture, and G_t is the solar horizontal irradiance (W/m^2). All the available model parameters are presented and explained in Table 6.1.

The different components of the model are shown with different colors in Figure 6.3. The full model includes all the components showed and is denoted $T_iT_mT_eT_hT_s\alpha_e\alpha_iR_{ia}$. The simplest model is T_i and includes only parameters C_i, R_{ia} and α_i. The structure of the final model is decided

Table 6.1: Model parameters of the full model

C_i	Thermal capacitance of interior air (J/°C)	C_m	Thermal capacitance of interior thermal mass (J/°C)
C_e	Thermal capacitance of building envelope mass (J/°C)	C_h	Thermal capacitance of the heater(s) (J/°C)
C_s	Thermal capacitance of the sensor(s) (J/°C)	R_{ia}	Thermal resistance between interior and exterior air (°C/W)
R_{ea}	Thermal resistance between building envelope mass and exterior air (°C/W)	R_{ie}	Thermal resistance between building envelope mass and interior air (°C/W)
R_{is}	Thermal resistance between sensor(s) and interior air (°C/W)	R_{im}	Thermal resistance between interior thermal mass and interior air (°C/W)
R_{ih}	Thermal resistance between heater(s) (°C/W) and interior air	α_i	Solar factor of interior air (m^2)
		α_e	Solar factor of building envelope mass (m^2)

automatically through a forward selection procedure. A detailed explanation on the different model components and the forward selection procedure is presented in Section 6.3.3.

The heat transfer dynamics are represented by the stochastic continuous state-space equations showed in equation (6.2), where ω represents a standard Wiener process and σ represents the incremental variance of the Wiener process, which includes any thermal dynamics phenomena not captured by the rest of the model.

$$\begin{aligned}
dT_s =& \frac{T_i - T_s}{R_{is}C_s}dt + \sigma_s d\omega_s \\
dT_m =& \frac{T_i - T_m}{R_{im}C_m}dt + \sigma_m d\omega_m \\
dT_h =& \frac{T_i - T_h}{R_{ih}C_h}dt + \frac{Q}{C_h}dt + \sigma_h d\omega_h \\
dT_e =& \frac{T_i - T_e}{R_{ie}C_e}dt + \frac{T_a - T_e}{R_{ea}C_e}dt + \frac{\alpha_e}{C_e}G_t dt + \sigma_e d\omega_e \\
dT_i =& \frac{T_s - T_i}{R_{is}C_i}dt + \frac{T_m - T_i}{R_{im}C_i}dt + \frac{T_h - T_i}{R_{ih}C_i}dt + \frac{T_e - T_i}{R_{ie}C_i}dt \\
&+ \frac{T_a - T_i}{R_{ia}C_i}dt + \frac{\alpha_i}{C_i}G_t dt + \sigma_i d\omega_i
\end{aligned} \tag{6.2}$$

The physical model is connected to the observed data, i.e., the measured indoor air temperature with the discrete-time measurement equation Equation (6.3):

$$Y^k = T_s^k + e^k \tag{6.3}$$

where superscript *k* denotes the k-th timestep, *Y* the measured indoor temperature and *e* the

measurement error. *e* is assumed to be Gaussian white noise, a common assumption which enables the evaluation of the final model by testing whether the residuals are white noise, and facilitates the use of a simple Kalman filter for maximum likelihood estimation of the model parameters. The optimal parameters of the model can be identified as the parameters that maximize the joint probability density

$$\mathcal{L}\left(\theta; \mathbf{Y}^k\right) = \left(\prod_{k=1}^{N} p\left(Y^k | \mathbf{Y}^{k-1}, \theta\right)\right) p\left(Y^0 | \theta\right) \tag{6.4}$$

where $p\left(Y^0|\theta\right)$ denotes the initial conditions, $\boldsymbol{Y}^k$ represents all observations from the initial condition to timestep *k* and ϑ are the model parameters. $p\left(Y^k|\mathbf{Y}^{k-1}, \theta\right)$ represents the conditional density probability of observing Y^k given the specific parameters and all the previous observations until that timestep.

Equation (6.4) can be estimated by a Kalman filter and then maximized by an optimization function to yield the final parameter estimates θ^*. The parameter estimation was performed in programming language R [199], through the package *CTSMR* [200], a package developed by Technical University of Denmark Compute for Continuous Time Stochastic Modeling, which estimates model parameters for timeseries data. For more information on continuous stochastic modeling for buildings and *CTSMR* spcifically, the reader is referred to the work of Leprince, Madsen, Miller, *et al.* [115], Bacher and Madsen [116], Kristensen and Madsen [201], and Kristensen, Madsen, and Jørgensen [202].

The smart thermostats do not measure the heating output itself, but only the total runtime of the heating or cooling system. There is no information about the total installed capacity Q_{nom} of the systems, and including it as a parameter to be calibrated in equation (6.2) guarantees that the models are overparameterized and could pose challenges to the optimization and the effective parameter estimation. For that reason the stochastic equations are expressed in the form shown in equation (6.5), where the parameters that can be identified are not the actual values of capacitances and resistances, but their ratios and products, i.e., C_i, C_s and R_{is} cannot be identified separately, but C_i/C_s and $R_{is}C_i$ can. In this manner, the ratio Q_{nom}/C_i can be identified and used in combination with δ, which denotes the runtime of the heating or cooling system.

$$
\begin{aligned}
dT_s =& \frac{C_i}{C_s} \cdot \frac{T_i - T_s}{R_{is}C_i} dt + \sigma_s d\omega_s \\
dT_m =& \frac{C_i}{C_m} \cdot \frac{T_i - T_m}{R_{im}C_i} dt + \sigma_m d\omega_m \\
dT_h =& \frac{C_i}{C_h} \cdot \frac{T_i - T_h}{R_{ih}C_i} dt + \frac{C_i}{C_h} \cdot \frac{Q_{nom}}{C_i} \delta dt + \sigma_h d\omega_h \\
dT_e =& \frac{C_i}{C_e} \cdot \frac{T_i - T_e}{R_{ie}C_i} dt + \frac{C_i}{C_e} \cdot \frac{T_a - T_e}{R_{ea}C_e} dt + \frac{C_i}{C_i} \cdot \frac{\alpha_e}{C_i} G_t dt + \sigma_e d\omega_e \\
dT_i =& \frac{T_s - T_i}{R_{is}C_i} dt + \frac{T_m - T_i}{R_{im}C_i} dt + \frac{T_h - T_i}{R_{ih}C_i} dt + \frac{T_e - T_i}{R_{ie}C_i} dt \\
& + \frac{T_a - T_i}{R_{ia}C_i} dt + \frac{\alpha_i}{C_i} G_t dt + \sigma_i d\omega_i
\end{aligned}
\tag{6.5}
$$

The model parameters vary throughout the day due to occupant activities. For example, if the occupants open a window, the effective thermal resistance of the air zone to the outdoors will decrease. Another example is solar factors, which will vary throughout the day or even the season. The effect of global horizontal irradiance on the heat gains are influenced by the orientation of the house and its windows, as well as the position of the sun during the day. The effect of the solar radiation could be modeled in more detail by using a time-variant solar factor, or even using B-splines as described in [161]. Using time-variant model parameters may increase the model accuracy, but can increase complexity and computational resources exponentially. As in most studies in the reviewed literature, the model parameters are assumed to be time-invariant in this study, prioritizing simplicity and speed over improved accuracy.

6.3.3 Model selection

The structure of the model is decided automatically by a forward selection procedure. The procedure starts with the simplest model, T_i, and iteratively adds complexity by adding one component at a time. For every new model, a statistical test is performed; a likelihood ratio test that establishes whether the more complex model is statistically significantly better than the simpler one. The procedure is shown schematically in figure 6.4 and the components can be seen with different colors in figure 6.3. The available components include the 5 states T_i, T_e, T_m, T_s, T_h, the solar factors α_i

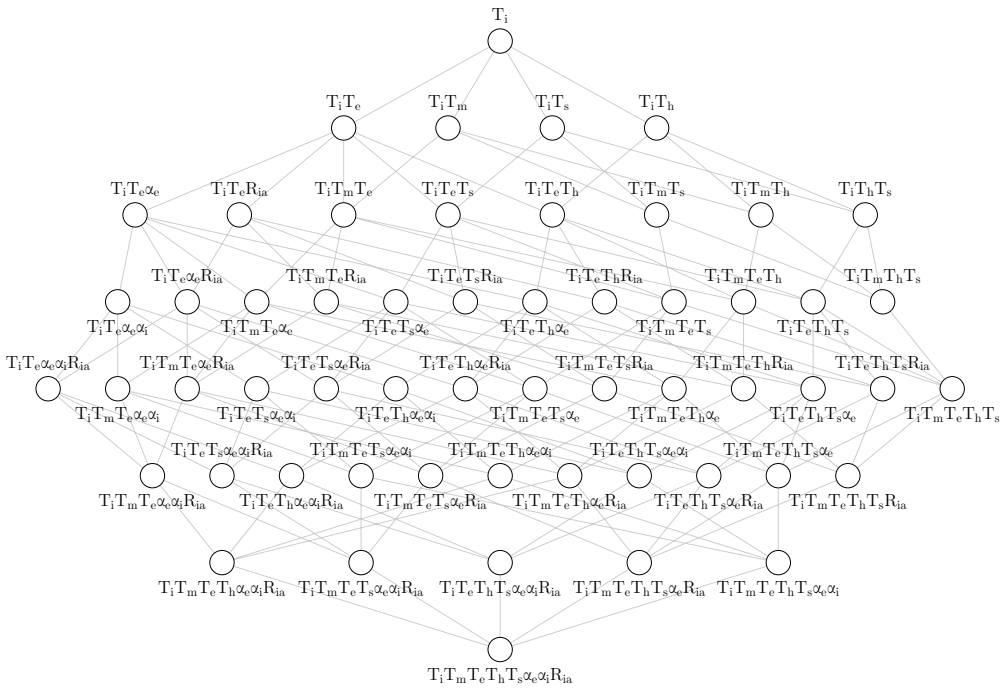

Figure 6.4: Forward selection scheme. Each row corresponds to one iteration. Adapted from [115]

and α_e, and the infiltration R_{ia}. When the state of the building envelope mass T_e is included, the parameter R_{ia} which expresses the heat exchange between indoor air and outdoor air is discarded, because it is assumed that heat transfer occurs through the envelope mass. The parameter R_{ia} is then introduced as a separate component in the following iterations to represent infiltration. Similarly, the initial inclusion of the state of the building envelope mass T_e does not include a solar factor α_e, because the solar effect is included on the interior air node. In the following iterations, a component α_e is introduced that can be included to substitute α_i. In turn, if component α_e is included, α_i is added as a component in the following iterations, allowing the effect of solar radiation on both the envelope and the interior node.

During every iteration, all models of the iteration are identified and statistically compared to the base model. The model with the lowest p-value is considered the best candidate, and the procedure moves to the next iteration. If none of the candidate models has a p-value below a 5% threshold then the procedure stops and the last model is the final model.

The accuracy of the final building model can be evaluated using root mean square error (RMSE) or the mean absolute error (MAE), the goodness of fit (FIT) and the coefficient of determination

(R^2) [37], [41]. The goodness of fit (FIT) is 1 - NRMSE, where NRMSE is the Normalized Root Mean Squared Error, and it is a percentage that expresses how good the model predictions are, with 100% meaning that the model explains even the system noise [123]. These metrics essentially evaluate how close the predicted values are to the available data. The choice of which criterion to use is often dictated by the application.

Another way to evaluate whether the model captures building thermal dynamics properly is to test the residuals for whiteness, since the model structure assumes white-noise residuals [87]. This is often done using the auto-correlation function (ACF) and cumulative periodogram (CP) of the residuals. The CP is a Fourier transformation of the autocovariance function of a stationary process. If the model residuals correspond to white noise, then the CP should be a straight line. The ACF represents the same concept as the CP, but in the time domain instead of the frequency domain.

Leprince, Madsen, Miller, *et al.* [115] extended the evaluation phase of [116] by introducing the normalized Cumulative Periodogram Boundary Excess Sum, or nCPBES, facilitating the automated evaluation of building models. The nCPBES is essentially the sum of all the instances where the CP of the residuals exceeds the boundaries where white-noise residuals would (statistically) reside. They used threshold values of 0.01 and 0.03 to classify models to three categories: "good", "close", and "poor" fits. This work uses the nCPBES with the same thresholds to check the whiteness of the residuals and differentiate between the three categories, as well as the RMSE of multi-step predictions as evaluation metrics.

6.4 Results and Discussion

This section presents and discusses the results of thermally characterizing 59,794 houses in North America. The calibrated models are presented and evaluated and their parameters are closely investigated.

6.4.1 Model evaluation

The final resulting models are shown in Figure 6.5. By far, the most likely model structure was $T_i T_m T_e T_h T_s \alpha_e$, which accounted for almost 50% of the final models. Overall, 80% of the final models were of 5th order and an additional 15% are of 4th order. The fact that models of higher

order were much more prevalent highlights that more detailed models are more likely to capture house thermal dynamics of single-zone houses better, but does not necessarily mean that models of lower order would not have adequate accuracy. Traditionally, lower-order models are preferred due to their simplicity in the calibration process, but an automated model selection process such as the one proposed mitigates the challenge.

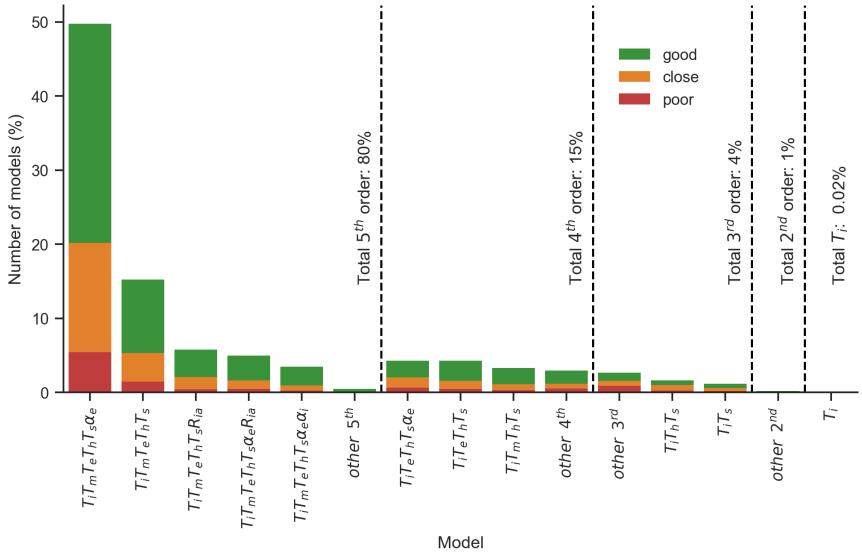

Figure 6.5: Percentage of each model structure of the final identifier models. Only model structures with at least 1% are shown, the rest are grouped together in the "other" category of the respective order. According to the nCPBES criterion, approximately 61% houses have a good fit, 28% have a close fit and 11% have a poor fit

The nCPBES was used to classify models into good, close, or poor, as explained in Section 6.3.3. An nCPBES that is not 0 suggests that there are still some thermal dynamics that are not being captured by the model. That is expected since the models do not include any information regarding occupancy or use of appliances and internal loads, which would not typically be accessible on such a large scale. As seen in Figure 6.5, from the total of 60,000 models, 61% were classified as good fits, 28% were classified as close fits and 11% were classified as poor fits.

The equivalent multi-step prediction RMSE is shown in Figure 6.6 in the form of letter-value plots. Letter-value plots are an alternative to boxplots, which is more suitable for large-scale data [203]. The widest box represents 50% of the datapoints, and every box width after that contains half of the rest of the data. Figure 6.6 shows that the RMSEs followed on average the classification of the models based on nCPBES, with good models being consistently more accurate than close

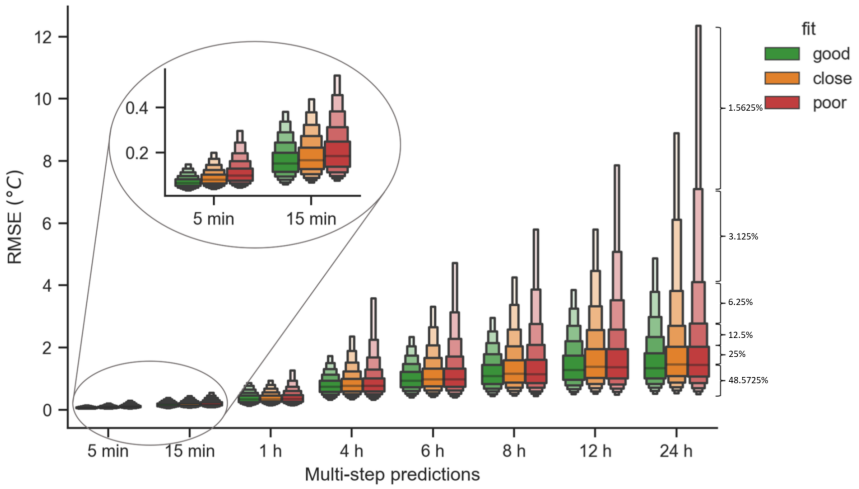

Figure 6.6: Letter-value plots of the multi-step RMSE for good, close, and poor fits. Letter-value plots are an alternative to boxplots, which is more suitable for large-scale data [203]. The plot starts with the median and a wide box containing 50% of the data, exactly like boxplots. Every box width after that contains half of the rest of the data. Therefore, the widest box contains 50%, of the data, the second widest 25%, the third 12.5%, etc.

models, which in turn were more accurate than poor models. Moreover, the figure shows that 50% of the produced good models had a 24-hour RMSE of less than 1.35 °C and 80% of them less than 2 °C, proving that the models were accurate enough and suitable for day-ahead MPC applications.

The forward model selection procedure for all houses is shown in Figure 6.7. During the first iterations, the selection procedure preferred models that include states T_s and T_h, with model $T_iT_mT_eT_hT_s$ being the most likely by the 4th iteration. After the model reached the 5th order it was fine-tuned with the addition of infiltration or solar factors on the envelope instead of the air node, or on both. Very few models (only 0.4%) reached the full configuration.

6.4.2 Parameter investigation of 5th-order models

The 5th-order models accounted for 80% of all the final models. This section investigates their model parameters in an effort to evaluate the models, find patterns, or correlate them with the available metadata. Figure 6.8 shows histograms of the calibrated parameters of the 29,500 5th-order models that were classified as good fits.

At first glance, the thermal capacitance ratios seem to make physical sense, with the thermal capacitance of the building materials C_e being 1 to 4 orders of magnitude higher than C_i, the capac-

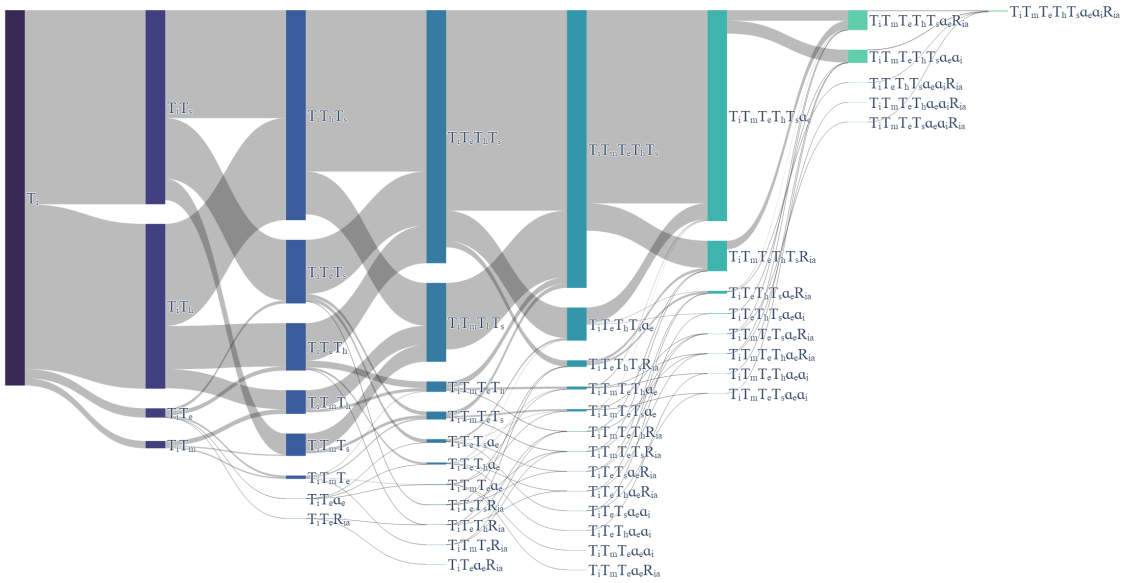

Figure 6.7: Forward model selection paths for the 60,000 houses

itance of the interior thermal mass C_m is 1 to 2 orders of magnitude higher, while the capacitance of the heater C_h and the sensor C_s are 1 to 2 orders of magnitude lower than C_i.

The envelope node parameters seemed to gravitate towards two distinct local minima areas. One is close to the lower bound of C_i/C_e, which corresponds to the smaller peak of $R_{ea}C_i$ and the values at the upper limit of α_e/C_i. The second is close to 0.1 C_i/C_e and corresponds to the larger peak of $R_{ea}C_i$ and the middle values of α_e/C_i.

Parameters $R_{is}C_i$, $R_{ih}C_i$, and $R_{ia}C_i$ were concentrated at their upper bounds at 3, 6, and 24 hours respectively, while parameter α_i/C_i was stuck at the lower bound. Running the calibration procedure with higher upper bounds had minimal effect on the model accuracy or T_i, but it did make the parameters stick to the new upper bound, also affecting parameters C_i/C_h and C_i/C_s. It seems that the many degrees of freedom in the parameter space can lead the calibration to fine tune the parameters to non-physical values, stressing the importance and need for proper parameter bounds.

It is not expected that all parameters of all 29,500 models will strictly follow physics. A single-zone representation of a large and diverse space such as a house can make parameter identification challenging. Moreover, missing essential information such as the total heating output, or occupancy and appliance loads can incline the parameter identification towards non-physical values, which can be affected with the careful selection of parameter bounds.

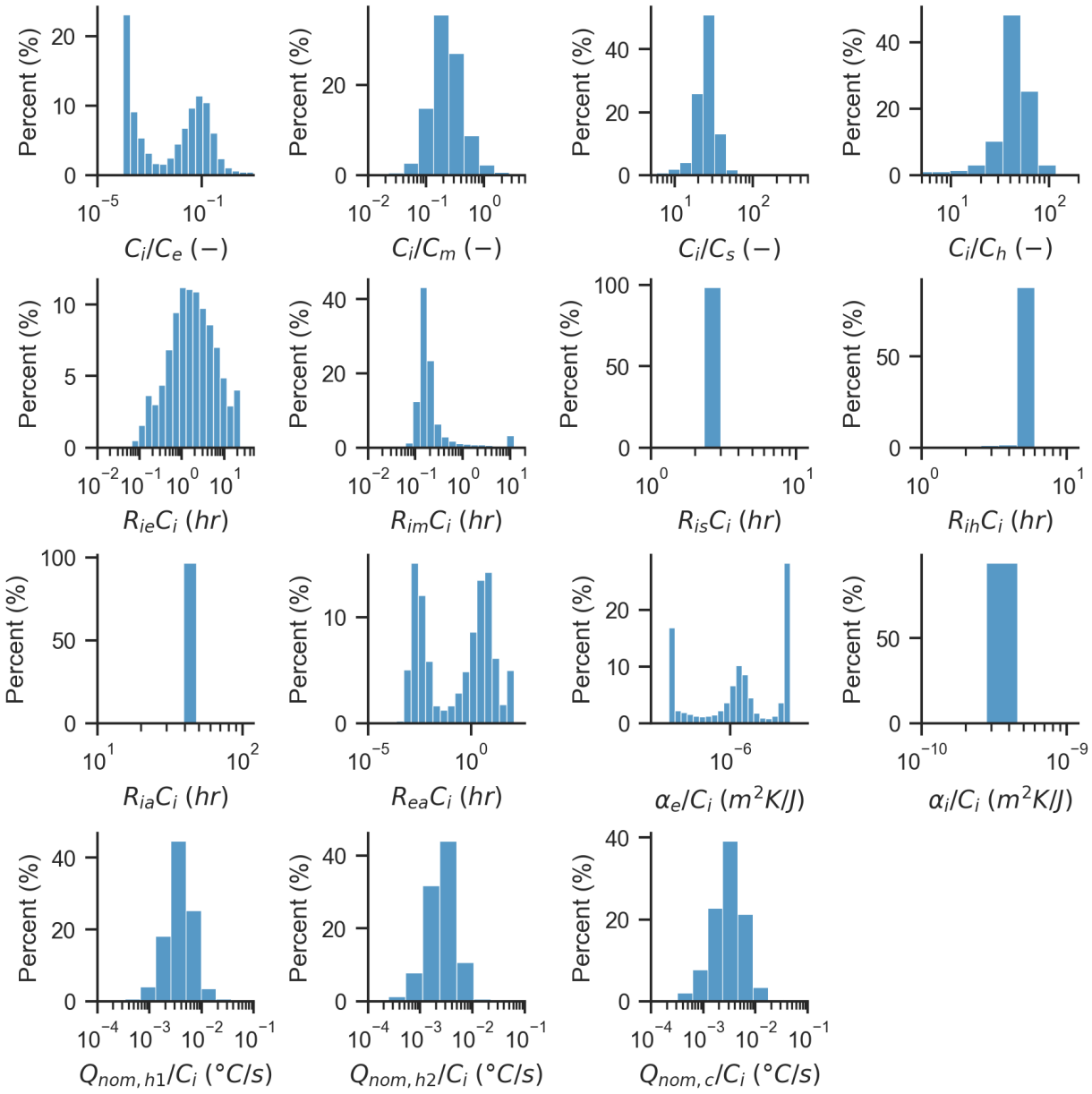

Figure 6.8: Histograms of calibrated parameters for the 29,500 5th-order models that were classified as good fits. The x-axis is in logarithmic scale.

The effect of metadata on model parameters was investigated and it is shown in Appendix B. Figures B.1 and B.3 to B.6 showed absolutely no effect of the style of house, its age, area number of floors or number of occupants on the parameter distributions. Figure B.2 shows a rather small influence of the climate on some of the model parameters, most notably on the parameters related to the envelope node T_e.

6.4.3 Time constant investigation

The time constants of each house can be identified by estimating the poles of the transfer functions of the system of equations in Equation (6.5), or, equivalently the eigenvalues of the state matrix in the state-space representation. For a real and positive pole, the time constant τ is given by Equation (6.6) [183]:

$$\tau = -\frac{1}{ln(pole)} \tag{6.6}$$

Each house has one time constant per state, i.e., per capacitance. The poles of the system were calculated in *R* using the Package "control" [204]. Therefore, the 5th-order models have 5 time constants:

- **Building material time constant** τ_e: This time constant reflects how quickly the building envelope materials respond to fluctuations in the outdoor temperature and solar radiation. A shorter time constant suggests that the building mass adjusts quickly to changes in outdoor conditions, affecting heat transfer between indoor and outdoor conditions.

- **Interior mass time constant** τ_m: This time constant characterizes the rate that the interior mass (e.g., the floor furniture etc.) of the building adjusts to fluctuations in the temperature of the indoor air, and consequently to heating and cooling. The interior thermal mass behaves like a dedicated thermal battery for the indoor air and its time constant reflects how effectively the building can store heat in its interior and how quickly it can "charge" or "discharge".

- **Indoor air time constant** τ_i: This time constant indicates how fast the indoor air temperature responds to any change in the system, such as outdoor weather conditions or changes in heating and cooling. A shorter time constant means that the indoor air temperature adjusts

faster to these changes, which is detrimental to building thermal comfort and its ability to maintain a desired indoor temperature.

- **Heater time constant** τ_h: This time constant reflects how quickly the building heating (or cooling) system reaches its steady-state condition in response to changes in heating (or cooling control). A shorter time constant implies that the heater temperature responds rapidly to changes in heating demands.

- **Sensor time constant** τ_s: This time constant indicates how rapidly the sensor temperature responds to changes in the indoor air temperature. Sensors with shorter time constants may provide quicker feedback about temperature variations.

The building material time constant τ_e is expected to be the largest, since the envelope materials are usually the most thermally massive part of a house, followed by the interior thermal mass time constant τ_m. The heater time constant τ_h and the sensor time constant τ_s are expected to be the smallest and have a magnitude of just a few minutes. The most important time constants are τ_e and τ_m, which quantify the ability of a house to store thermal energy and can be very important in studies about energy flexibility potential of a house, and τ_i, which is associated closely with occupant thermal comfort.

Figure 6.9 shows the distributions of the time constants for the 29,500 5th-order models considered a good fit. The building material time constant τ_e has a median of 52 hr, with 80% of the points being in the range of 17 to 297 hr. These values are consistent with the overall literature [184]. More specifically, John, Vallianos, Candanedo, *et al.* [110] used a first-order RC model to model 10,000 houses in Canada and found time-constants in the range of 15 to 55 hours, while Doma and Ouf [118] used the same model on 60,000 houses in North America and found time constants in the range of 11 to 110 hours with a median of 51 hours. Vallianos, Candanedo, and Athienitis [168] used a second-order model on 7,800 houses in Ontario and Québec and found time constants in the range of 15 to 280 hours, with a median of 100 hours.

About 5% of the models have a τ_e larger than 1000 hr, indicating that their parameters may not accurately reflect physics. The interior mass time constant τ_m is the next largest one with a median of 6 hr, while the indoor air time constant τ_i, heater time constant τ_h, and sensor time constant τ_s all have a median of 10 minutes or less. It should be noted that the sensor time constant τ_s

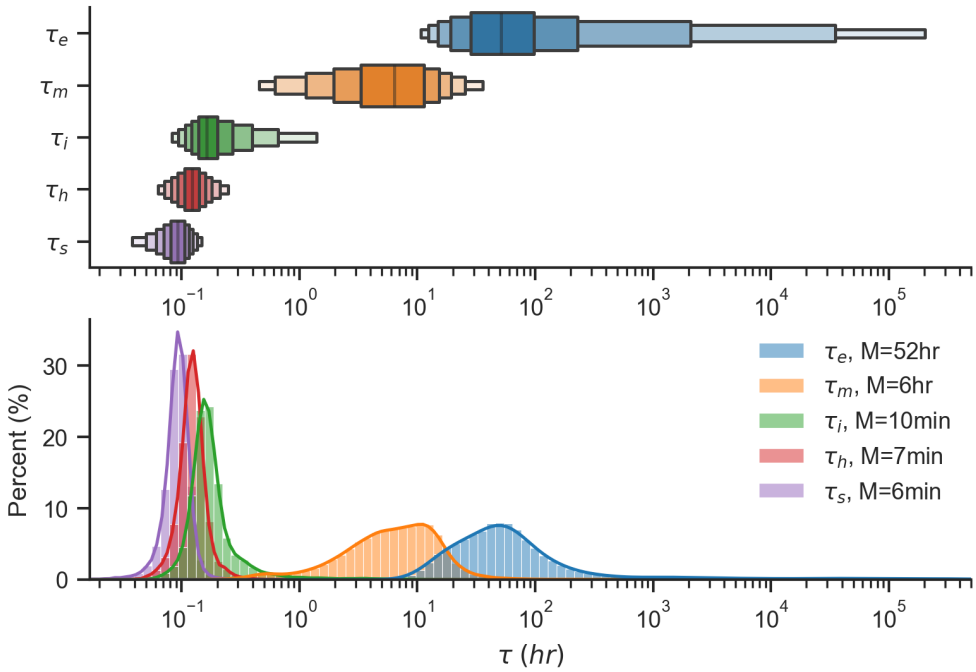

Figure 6.9: Histograms of the time constants for the 5 nodes of the model. *M* denotes the median

is comparable to the sampling time of the smart thermostats (which is 5 minutes), indicating that the sampling time is too short and the data could be resampled to 15-minutes in the modeling and calibration stage.

6.4.4 Limitations and a note on bias

Although the Ecobee dataset is a great source of insight and analysis into building models and characteristics, there are still limitations to this study. The dataset itself is potentially biased towards homeowners and a wealthier subset of population, or even occupants that are more environmentally conscious than the average North American. All houses are equipped with thermostats from the same company, meaning that there could be a form of systematic error on the sensor measurements. Another major limitation of this study is the lack of information about the installed heating and cooling capacity. Had that information been available, all the model parameters would have been identifiable, and not just their products and ratios.

6.5 Conclusion

As smart thermostats become increasingly available in residential buildings, there is an opportunity to use measured building data to calibrate models for community and district applications. To do that, this study used smart thermostat data from 60,000 houses in North America.

Each house was modeled as a single-zone. Instead of using a predefined model structure, this work uses an automated forward procedure that increases the complexity of the model structure until its quality cannot increase anymore. The heat transfer dynamics of the house were represented by stochastic continuous state-space equations.

The fit of the final models was evaluated, with 61% of the models being classified as good fits. Higher-order models were dominant in the final models, and 80% of the calibrated models were of 5^{th} order. An investigation of the 24-hour multi-step prediction of the models showed that the ones classified as good fits are accurate enough for MPC applications, with 50% of them having a 24-hour RMSE of less than 1.3°C and 80% of them less than 2°C. Insight into the model parameters showed that they are not correlated to the available metadata. The time constants of the houses were estimated and their values agree with expert knowledge. The time constant of the building materials and of internal mass had a median of 52 hours and 6 hours respectively, showcasing the ability of the model to capture the thermal inertia of the house, and therefore to leverage it for advanced control applications.

The resulting dataset is publicly available at `https://doi.org/10.5281/zenodo.8347091`.

7 Conclusion and future work

This thesis investigated the role that measured data from smart thermostats can play in the automated development and calibration of residential building models for Model Predictive Control. In Section 2.10 certain research gaps and questions were identified that this thesis attempted to address. More specifically:

1. *Is there an automated way to develop and calibrate multi-zone residential models? Are they accurate for 24-hour predictions for MPC applications?*

   A novel methodology for automatic generation of building models using data from smart thermostats was presented. It created RC models with accurate predictions up to 24 hours in advance. Each zone with a smart thermostat of the house was modeled with one equivalent air thermal capacitance and up to one equivalent thermal capacitance for the building mass. The methodology investigated which model structure (i.e., which thermal resistances and solar factors) provided the best fit between the measured indoor air temperatures and the predicted ones. The methodology was applied on an experimental residential building in Québec, Canada. The model was calibrated using only information from smart thermostats and historical weather data. No additional information was used, like the layout of the house or the lighting loads. The resulting model predicted the temperature very well for all 9 zones 24 hours in advance, with an overall RMSE of 0.44 °C. Investigating the estimated parameters showed that the algorithm performs a form of zone aggregation for the basement and the first floor, by allocating a high thermal capacitance to one of the zones and high conductances between that zone and the rest of the zones on that floor. Additionally, the solar gain factors are present only in 4 south-facing zones, where the effect of solar radiation is expected to be the highest.

2. *How can smart thermostats assist the practical implementation of MPC? Are low-order models sufficient for MPC? How do they compare in practice to detailed multi-zone models?*

   Practical real-time MPC was implemented using smart thermostats in an unoccupied residential house in Québec, Canada for optimal heating load management and load shifting. Three different models were developed and calibrated to be compared and used in the MPC framework: a low-order model grouping zones by floor, a low-order model grouping zones by orientation and a higher-order multi-zone model that assumes one zone per room, developed with the aforementioned automated methodology. The three models were applied in an MPC framework for day-ahead optimization, with the objective of minimizing the cost of electricity during days with morning and evening demand-response events. They were also compared to a regular reactive controller, established as the reference case. Overall, all three models preheated the house successfully before the high-price periods, reducing the overall cost of electricity for the homeowners and eliminating thermal discomfort. The higher accuracy of the multi-zone model made it the best candidate with its MPC application being more consistent and reliable. The multi-zone model reduced the cost of electricity by 55% (compared to 40% and 44% for the floor and orientation model), and the energy consumption during high-price periods by 71% (compared to 48% and 54% for the floor and orientation model). Although the peak power demand and the energy consumption during the high-price periods were reduced, the total daily consumption was increased due to the preheating, and the daily peak power demand was not reduced – it was just shifted, highlighting the need for smart or transactive grids.

3. *Do single-zone control-oriented models need a different calibration approach? How much data do they need and at what temporal resolution to produce accurate 24-hour predictions?*

   Smart thermostat data from 7,800 houses in Ontario and Québec, Canada, were used to develop second-order models and calibrate them with different data intervals, training data lengths and calibration horizons. Models calibrated with calibration horizon of 24 hours performed significantly better than models with calibration horizon of 1 timestep. Data length of 3 days led to model overfitting, whereas data with 60-minute time intervals led to a small loss of information. Overall the models with calibration horizon of 24 hours, data length

of 7 days and time interval of 15 minutes provided the best balance between accuracy and computational resources.

4. *What is the aggregated impact of MPC if it was widely adopted by residential buildings? How much can a homeowner benefit from MPC?*

   These models were then used to perform MPC on a cold day in January using the TOU rates of Ontario and the dynamic pricing of Québec. The MPC performance was compared to the performance of a reference deadband controller with a single-sided deadband. The analysis showed that the MPC controller can systematically reduce the high-price energy consumption, reducing the cost for homeowners by 16 % in Ontario and 31 % in Québec, while simultaneously eliminating thermal discomfort usually introduced by setpoint setback. MPC achieves this by preheating the houses, successfully harvesting their energy flexibility of the houses. The preheating shifts power peak consumption, reducing it by 0.15 kW/kW_{inst} in Ontario and 0.3 kW/kW_{inst} in Québec. However, there was still a peak that essentially shifted to the hours exactly before the original one. If enough customers implement optimal controls, this shifting effect could potentially prove to be a challenge for the grid, highlighting the need for dynamic pricing and smart and transactive grids. The estimated cost of electricity and high-price energy consumption reduction were consistent with the results from the real-time MPC implementation presented for research question 2.

5. *Urban Building Energy Modeling relies on detailed white-box models of architectural building archetypes. Is it possible to create a database of fast control-oriented models? Can the models be clustered based on their metadata (e.g., age or size of home)?*

   Smart thermostat data from 60,000 houses in North America were used to develop and calibrate building thermal models. Each house was modeled as a single-zone. Instead of using a predefined model structure, this work uses an automated forward procedure that increases the complexity of the model structure until its quality cannot increase anymore. The heat transfer dynamics of the house were represented by stochastic continuous state-space equations. 61% of the models were classified as good fits, and higher-order models being dominant, with 80% of the final models being of 5^{th} order. An investigation of the 24-hour multi-step prediction of the models showed that the ones classified as good fits are accurate enough

for MPC applications, with 80% of them having a 24-hour RMSE of less than 2 °C and 50% less than 1.35 °C. The model parameters showed no strong correlation to the available metadata. Moreover, the building time constants were computed as a means to assess building thermal storage ability. The resulting dataset has been made publicly available at `https://doi.org/10.5281/zenodo.8347091`.

7.1 Contributions

The major contributions resulting from this thesis stem directly from the thesis objectives presented in Section 1.2:

- A novel methodology for automated generation and calibration of multi-zone residential models using smart thermostat data.
- Guidelines for RC model development and order selection in practical MPC implementations.
- Data resolution, length and calibration horizon guidelines for MPC-oriented RC model development and calibration.
- Effect of large-scale application of MPC for both the utility grid and homeowners for Québec and Ontario, Canada.
- A public database of North American control-oriented models for sampling control-oriented building models.

7.2 Publications

The published or submitted journal articles, as well as the presented conference papers and other non-refereed work are presented below.

7.2.1 Journal publications

[1] **C. Vallianos**, J. Candanedo, and A. Athienitis, "Thermal modeling for control applications of 60,000 homes in north america using smart thermostat data," *Energy and Buildings*, p. 113 811, 2023. DOI: 10.1016/j.enbuild.2023.113811.

[2] **C. Vallianos**, M. Abtahi, A. Athienitis, B. Delcroix, and L. Rueda, "Online model-based predictive control with smart thermostats: Application to an experimental house in Québec," *Journal of Building Performance Simulation*, pp. 1–17, 2023. DOI: 10.1080/19401493.2023.2243602.

[3] **C. Vallianos**, J. Candanedo, and A. Athienitis, "Application of a large smart thermostat dataset for model calibration and Model Predictive Control implementation in the residential sector," *Energy*, vol. 278, p. 127 839, 2023. DOI: 10.1016/j.energy.2023.127839.

[4] A.-M. Sigounis, **C. Vallianos**, and A. Athienitis, "Model predictive control of air-based building integrated PV/T systems for optimal HVAC integration," *Renewable Energy*, vol. 212, pp. 655–668, 2023. DOI: 10.1016/j.renene.2023.05.059.

[5] A. Maturo, **C. Vallianos**, A. Buonomano, and A. Athienitis, "A novel multi-level predictive management strategy to optimize phase-change energy storage and building-integrated renewable technologies operation under dynamic tariffs," *Energy Conversion and Management*, vol. 291, p. 117 220, 2023. DOI: 10.1016/j.enconman.2023.117220.

[6] **C. Vallianos**, A. Athienitis, and B. Delcroix, "Automatic generation of multi-zone RC models using smart thermostat data from homes," *Energy and Buildings*, vol. 277, p. 112 571, 2022. DOI: 10.1016/j.enbuild.2022.112571.

[7] J. A. Candanedo, **C. Vallianos**, B. Delcroix, J. Date, A. S. Derakhtenjani, N. Morovat, C. John, and A. K. Athienitis, "Control-oriented archetypes: A pathway for the systematic application of advanced controls in buildings," *Journal of Building Performance Simulation*, vol. 15, no. 4, pp. 433–444, 2022. DOI: 10.1080/19401493.2022.2063947.

[8] **C. Vallianos**, A. Athienitis, and J. Rao, "Hybrid ventilation in an institutional building: Modeling and predictive control," *Building and Environment*, vol. 166, p. 106 405, 2019. DOI: 10.1016/j.buildenv.2019.106405.

7.2.2 Conference proceedings

[1] **C. Vallianos**, J. Candanedo, and A. Athienitis, "Large-scale Deployment of Model Predictive Control in the Residential Sector: Proposed Methodology and Assessment of Aggregated Impact," in *17th Conference on Sustainable Development of Energy, Water and Environment Systems (SDEWES)*, Paphos, Cyprus, Nov. 2022.

[2] A.-M. Sigounis, **C. Vallianos**, and A. Athienitis, "Design and control strategies for optimal operation of an air-based BIPV/T system in an institutional net-zero energy building," in *17th Conference on Sustainable Development of Energy, Water and Environment Systems (SDEWES)*, Paphos, Cyprus, Nov. 2022.

[3] A. Maturo, **C. Vallianos**, A. Buonomano, and A. Athienitis, "Model predictive control for energy flexibility of a building coupled with advanced solar and energy storage technologies," in *17th Conference on Sustainable Development of Energy, Water and Environment Systems (SDEWES)*, Paphos, Cyprus, Nov. 2022.

[4] **C. Vallianos**, S. Saeed Hosseini, A. Athienitis, K. Agbossou, B. Delcroix, J. Rao, and N. Henao, "Automated RC Model Generation for MPC Applications to Energy Flexibility Studies in Québec Houses," in *Proceedings of the 5th International Conference on Building Energy and Environment*, L. L. Wang, H. Ge, Z. J. Zhai, D. Qi, M. Ouf, C. Sun, and D. Wang, Eds., Singapore: Springer Nature Singapore, 2023, pp. 1331–1340. DOI: 10.1007/978-981-19-9822-5_73.

[5] S. S. Hosseini, **C. Vallianos**, K. Agbossou, A. Athienitis, B. Delcroix, N. Henao, J. Rao, and S. Kelouwani, "Impact of Zoning Definition on Electrical Heating Systems Flexibility Potential in Residential Buildings: A Québec Case Study," in *Proceedings of the 5th International Conference on Building Energy and Environment*, L. L. Wang, H. Ge, Z. J. Zhai, D. Qi, M. Ouf, C. Sun, and D. Wang, Eds., Singapore: Springer Nature Singapore, 2023, pp. 1331–1340. DOI: 10.1007/978-981-19-9822-5_154.

[6] A.-M. Sigounis, **C. Vallianos**, and A. K. Athienitis, "Modelling and Predictive Control of an Air-Based BIPV/T System for Optimal HVAC Integration," in *Proceedings of the 5th International Conference on Building Energy and Environment*, L. L. Wang, H. Ge, Z. J.

Zhai, D. Qi, M. Ouf, C. Sun, and D. Wang, Eds., Singapore: Springer Nature Singapore, 2023, pp. 1331–1340. DOI: 10.1007/978-981-19-9822-5_138.

[7] A.-M. Sigounis, E. Rounis, A. Athienitis, and **C. Vallianos**, "Control-oriented model for air-based BIPV/T systems," *Journal of Physics: Conference Series*, vol. 2069, no. 1, p. 012 221, Nov. 2021. DOI: 10.1088/1742-6596/2069/1/012221.

7.2.3 Non-refereed contributions

[1] **C. Vallianos**, *Automated multi-zone model generation*, version v1.0, Nov. 2023. DOI: 10.5281/zenodo.10156745.

[2] **C. Vallianos**, J. Candanedo, and A. Athienitis, *North american house thermal models*, version v1.0, Zenodo, Sep. 2023. DOI: 10.5281/zenodo.8347091.

[3] **C. Vallianos**, M. Abtahi, A. Athienitis, B. Delcroix, and L. Rueda, *Experimental House of Building Energetics Model Predictive Control experiment data*, version v1.0, Zenodo, Jun. 2023. DOI: 10.5281/zenodo.8021941.

[4] D. Blum, J. Candanedo, Z. Chen, G. Fierro, V. Gori, H. Johra, H. Madsen, A. Marszal-Pomianowska, Z. O'Neill, O. Pradhan, D. Rovas, F. Sacco, S. Stensson, C. A. Thikler, **C. Vallianos**, J. Wen, and S. D. White, "Data-Driven Smart Buildings (Annex 81): State-of-the-Art Review," International Energy Agency: Energy in Buildings and Communities, Technology Collaboration Programme, 2023.

7.3 Recommendations for future work

Although this thesis has achieved advancements, additional steps are necessary to fully leverage the abundance of measured data that are becoming readily available with the widespread adoption of smart thermostats. Eventually these steps can pave the way for making MPC a commonplace practice in controlling residential buildings.

On an individual level, a home can use multi-zone RC models to perform MPC, ensuring the thermal comfort of the occupants in all zones of the house and fully leveraging its energy flexibility. The automated methodology that has been presented in this thesis can be enhanced further

by incorporating the effect of occupants, electric appliances and internal loads (for example, water heaters can create significant power peaks). The effect of occupants on building models is already the topic of IEA EBC Annex 79: Occupant-centric Building Design and Operation. Since deploying a multitude of sensors in each house in not realistic in the current environment, many of these disturbances would have to be implied by the data itself. This can be done using data-driven techniques that infer the disturbance characteristics (profile, period, magnitude, etc.), or by modeling the unmeasured disturbances in the MPC itself. Another improvement could be the introduction of B-splines for solar factor estimation, which would model the effect of solar radiation on the house in a more accurate way. All these improvements would also make the model more complicated, less interpretable, and much more computationally demanding, opening a discussion concerning the trade-off between accuracy, simplicity, and computational effort.

When it comes to real-time MPC implementation, the first steps of the future work would be to incorporate it on the supervisory control system of the building. That could take the form of a local Raspberry Pi that serves at the "brain" of the system, or eventually it could be directly implemented within the smart thermostats themselves. Including the model and the MPC in the smart thermostat would enable the occasional automatic model recalibration to maintain proper model performance. Instead of using a fixed control horizon, which is usually around 6 hours, a variable one could be implemented, where the model updates its predictions only when it understands that the previous ones are not accurate enough. Furthermore, more insight is needed to understand the effect that weather forecast errors have on different model resolutions and structures, and therefore to real-time MPC.

In the current energy market, MPC can help homeowners reduce their costs by preconditioning their houses and reducing energy consumption during high-price periods. However, MPC does not significantly decrease daily peak power; it effectively shifts it to an earlier time to precondition the house in anticipation to the high-price period. If many customers implement individual MPC, the aggregated shifting effect would only be affected by the effective time constant of the house and would still pose a challenge for the utility grid. Future research can alleviate this problem by focusing on transactive grids, energy aggregators, and aggregated load shaping, which may prove to be necessary with the increasing adoption of electric vehicles and space heating electrification.

Studies into transactive grids, energy aggregators, and aggregated load shaping can benefit

from repositories of building models calibrated with measured data, which can be invaluable for researchers to explore and leverage. The model information and data need to be standardized to enable sharing of knowledge and advance state-of-the-art research. Having models from multiple different sources and infrastructures would minimize bias in the results. Initial steps for such a repository are being made for the conclusion of IEA EBC Annex 81: Data-Driven Smart Buildings.

Diverse repositories of models would enable a deep analysis into what effect certain metadata, like the age of a house or its location, can have on model structure or parameters. Eventually, one could create a representative control-oriented building model just by specifying the metadata of an unknown house. Furthermore, if the time constants of the houses are also estimated and available, there is a potential to find the characteristics that would create a portfolio of houses for a community with diverse time constants, effectively allowing different preheating times and shaving the aggregated peak power demand.

Bibliography

[1] A. Levesque, R. C. Pietzcker, and G. Luderer, "Halving energy demand from buildings: The impact of low consumption practices," *Technological Forecasting and Social Change*, vol. 146, pp. 253–266, 2019. DOI: 10.1016/j.techfore.2019.04.025.

[2] L. Clarke, J. Eom, E. H. Marten, *et al.*, "Effects of long-term climate change on global building energy expenditures," *Energy Economics*, vol. 72, pp. 667–677, 2018. DOI: 10.1016/j.eneco.2018.01.003.

[3] J. A. Dirks, W. J. Gorrissen, J. H. Hathaway, *et al.*, "Impacts of climate change on energy consumption and peak demand in buildings: A detailed regional approach," *Energy*, vol. 79, pp. 20–32, 2015. DOI: 10.1016/j.energy.2014.08.081.

[4] Z. J. Zhai and J. M. Helman, "Implications of climate changes to building energy and design," *Sustainable Cities and Society*, vol. 44, pp. 511–519, 2019. DOI: 10.1016/j.scs.2018.10.043.

[5] M. Gercek and Z. D. Arsan, "Energy and environmental performance based decision support process for early design stages of residential buildings under climate change," *Sustainable Cities and Society*, vol. 48, p. 101 580, 2019. DOI: 10.1016/j.scs.2019.101580.

[6] C.-J. Yang, "Reconsidering solar grid parity," *Energy Policy*, vol. 38, no. 7, pp. 3270–3273, 2010. DOI: 10.1016/j.enpol.2010.03.013.

[7] A. Allouhi, S. Rehman, M. S. Buker, and Z. Said, "Up-to-date literature review on Solar PV systems: Technology progress, market status and R&D," *Journal of Cleaner Production*, vol. 362, p. 132 339, 2022. DOI: 10.1016/j.jclepro.2022.132339.

[8] A. Sow, M. Mehrtash, D. R. Rousse, and D. Haillot, "Economic analysis of residential solar photovoltaic electricity production in Canada," *Sustainable Energy Technologies and Assessments*, vol. 33, pp. 83–94, 2019. DOI: 10.1016/j.seta.2019.03.003.

[9] K. Enongene, F. Abanda, I. Otene, S. Obi, and C. Okafor, "The potential of solar photovoltaic systems for residential homes in Lagos city of Nigeria," *Journal of Environmental Management*, vol. 244, pp. 247–256, 2019. DOI: 10.1016/j.jenvman.2019.04.039.

[10] T. Cui, J. Carr, A. Brissette, and E. Ragaini, "Connecting the Last Mile: Demand Response in Smart Buildings," *Energy Procedia*, vol. 111, pp. 720–729, 2017. DOI: 10.1016/j.egypro.2017.03.234.

[11] U.S. Energy Information Administration, *As solar capacity grows, duck curves are getting deeper in California*, https://www.eia.gov/todayinenergy/detail.php?id=56880, [Online; accessed 01-August-2023], 2023.

[12] H. Québec, "Overview of Hydro-Québec's energy resources: Setting new sights with our clean energy," Hydro Québec, Tech. Rep., 2019.

[13] S. Billimoria, L. Guccione, M. Henchen, and L. Louis-Prescott, "The Economics of Electrifying Buildings: How Electric Space and Water Heating Supports Decarbonization of Residential Buildings," in *World Scientific Encyclopedia of Climate Change*, ch. Chapter 33, pp. 297–304. DOI: 10.1142/9789811213960_0033.

[14] J. Deason and M. Borgeson, "Electrification of Buildings: Potential, Challenges, and Outlook," *Current Sustainable/Renewable Energy Reports*, vol. 6, pp. 131–139, Dec. 2019. DOI: 10.1007/s40518-019-00143-2.

[15] F. Padovani, N. Sommerfeldt, F. Longobardi, and J. M. Pearce, "Decarbonizing rural residential buildings in cold climates: A techno-economic analysis of heating electrification," *Energy and Buildings*, vol. 250, p. 111 284, 2021. DOI: 10.1016/j.enbuild.2021.111284.

[16] P. R. White, J. D. Rhodes, E. J. Wilson, and M. E. Webber, "Quantifying the impact of residential space heating electrification on the Texas electric grid," *Applied Energy*, vol. 298, p. 117 113, 2021. DOI: 10.1016/j.apenergy.2021.117113.

[17] M. Blonsky, A. Nagarajan, S. Ghosh, K. K. McKenna, S. Veda, and B. D. Kroposki, "Potential Impacts of Transportation and Building Electrification on the Grid: A Review of Electrification Projections and their Effects on Grid Infrastructure, Operation, and Planning," *Current Sustainable/Renewable Energy Reports*, vol. 6, Nov. 2019. DOI: 10.1007/s40518-019-00140-5.

[18] Hydro Quebec, *Dynamic pricing — New offerings for winter 2019–2020*, http://www.hydroquebec.com/residential/customer-space/rates/dynamic-pricing.html, [Online; accessed 3-September-2019], 2019.

[19] B. Lehmann, D. Gyalistras, M. Gwerder, K. Wirth, and S. Carl, "Intermediate complexity model for Model Predictive Control of Integrated Room Automation," *Energy and Buildings*, vol. 58, pp. 250–262, 2013. DOI: 10.1016/j.enbuild.2012.12.007.

[20] P. D. Lund, J. Lindgren, J. Mikkola, and J. Salpakari, "Review of energy system flexibility measures to enable high levels of variable renewable electricity," *Renewable and Sustainable Energy Reviews*, vol. 45, pp. 785–807, 2015. DOI: 10.1016/j.rser.2015.01.057.

[21] P. Denholm and M. Hand, "Grid flexibility and storage required to achieve very high penetration of variable renewable electricity," *Energy Policy*, vol. 39, no. 3, pp. 1817–1830, 2011. DOI: 10.1016/j.enpol.2011.01.019.

[22] Y. Liu, N. Yu, W. Wang, *et al.*, "Coordinating the operations of smart buildings in smart grids," *Applied Energy*, vol. 228, pp. 2510–2525, 2018. DOI: 10.1016/j.apenergy.2018.07.089.

[23] M. J. O. Panão, N. M. Mateus, and G. C. da Graça, "Measured and modeled performance of internal mass as a thermal energy battery for energy flexible residential buildings," *Applied Energy*, vol. 239, pp. 252–267, 2019. DOI: 10.1016/j.apenergy.2019.01.200.

[24] S. Ø. Jensen, A. Marszal-Pomianowska, R. Lollini, *et al.*, "IEA EBC Annex 67 Energy Flexible Buildings," *Energy and Buildings*, vol. 155, pp. 25–34, 2017. DOI: 10.1016/j.enbuild.2017.08.044.

[25] A. K. Athienitis, E. Dumont, N. Morovat, K. Lavigne, and J. Date, "Development of a dynamic energy flexibility index for buildings and their interaction with smart grids," in *ACEEE 2020 Summer Study on Energy Efficiency in Buildings*, Pacific Grove, CA, USA, Aug. 2020.

[26] G. M. Huebner, M. McMichael, D. Shipworth, M. Shipworth, M. Durand-Daubin, and A. Summerfield, "The reality of English living rooms – A comparison of internal temperatures against common model assumptions," *Energy and Buildings*, vol. 66, pp. 688–696, 2013. DOI: 10.1016/j.enbuild.2013.07.025.

[27] W. Belazi, S.-E. Ouldboukhitine, A. Chateauneuf, and A. Bouchair, "Experimental and numerical study to evaluate the effect of thermostat settings on building energetic demands during the heating and transition seasons," *Applied Thermal Engineering*, vol. 152, pp. 35–51, 2019. DOI: 10.1016/j.applthermaleng.2019.02.020.

[28] Mission Innovation, *Innovation Challenge 7: Affordable Heating and Cooling of Buildings*, http://mission-innovation.net/our-work/innovation-challenges/affordable-heating-and-cooling-of-buildings/, [Online; accessed 5-September-2019], 2019.

[29] C. I. of Building Services Engineers, *Building control systems*. Routledge, 2000.

[30] A. Afram and F. Janabi-Sharifi, "Theory and applications of HVAC control systems – A review of model predictive control (MPC)," *Building and Environment*, vol. 72, pp. 343–355, Feb. 2014. DOI: 10.1016/j.buildenv.2013.11.016.

[31] Z. Jiang, V. Chinde, A. Kohl, A. G. Kelkar, and S. Sarkar, "Supervisory Control and Distributed Optimization of Building Energy Systems," *Journal of Dynamic Systems, Measurement, and Control*, vol. 142, no. 10, Jun. 2020, 101008. DOI: 10.1115/1.4047448.

[32] F. Oldewurtel, A. Parisio, C. N. Jones, *et al.*, "Use of model predictive control and weather forecasts for energy efficient building climate control," *Energy and Buildings*, vol. 45, pp. 15–27, 2012. DOI: 10.1016/j.enbuild.2011.09.022.

[33] B. Huchuk, S. Sanner, and W. O'Brien, "Development and evaluation of data-driven controls for residential smart thermostats," *Energy and Buildings*, vol. 249, p. 111 201, 2021. DOI: 10.1016/j.enbuild.2021.111201.

[34] S. Seal, B. Boulet, and V. R. Dehkordi, "Centralized model predictive control strategy for thermal comfort and residential energy management," *Energy*, vol. 212, p. 118 456, 2020. DOI: 10.1016/j.energy.2020.118456.

[35] W. J. Cole, K. M. Powell, E. T. Hale, and T. F. Edgar, "Reduced-order residential home modeling for model predictive control," *Energy and Buildings*, vol. 74, pp. 69–77, 2014. DOI: 10.1016/j.enbuild.2014.01.033.

[36] G. Bianchini, M. Casini, A. Vicino, and D. Zarrilli, "Demand-response in building heating systems: A Model Predictive Control approach," *Applied Energy*, vol. 168, pp. 159–170, 2016. DOI: 10.1016/j.apenergy.2016.01.088.

[37] J. Drgoňa, J. Arroyo, I. Cupeiro Figueroa, *et al.*, "All you need to know about model predictive control for buildings," *Annual Reviews in Control*, vol. 50, pp. 190–232, 2020. DOI: 10.1016/j.arcontrol.2020.09.001.

[38] D. Mayne, "Robust and stochastic model predictive control: Are we going in the right direction?" *Annual Reviews in Control*, vol. 41, pp. 184–192, 2016. DOI: 10.1016/j.arcontrol.2016.04.006.

[39] X. Li and J. Wen, "Review of building energy modeling for control and operation," *Renewable and Sustainable Energy Reviews*, vol. 37, pp. 517–537, 2014. DOI: 10.1016/j.rser.2014.05.056.

[40] J. Candanedo, A. Allard, and A. Athienitis, "Predictive Control of Radiant Floor Heating and Transmitted Irradiance in a Room with High Solar Gains," vol. 117, Jan. 2011.

[41] S. Prívara, Z. Váňa, E. Žáčeková, and J. Cigler, "Building modeling: Selection of the most appropriate model for predictive control," *Energy and Buildings*, vol. 55, pp. 341–350, 2012. DOI: 10.1016/j.enbuild.2012.08.040.

[42] G. P. Henze, "Model predictive control for buildings: A quantum leap?" *Journal of Building Performance Simulation*, vol. 6, no. 3, pp. 157–158, 2013. DOI: 10.1080/19401493.2013.778519.

[43] H. Li, H. Johra, F. de Andrade Pereira, *et al.*, "Data-driven key performance indicators and datasets for building energy flexibility: A review and perspectives," *Applied Energy*, vol. 343, p. 121 217, 2023. DOI: 10.1016/j.apenergy.2023.121217.

[44] D. Kanakadhurga and N. Prabaharan, "Demand side management in microgrid: A critical review of key issues and recent trends," *Renewable and Sustainable Energy Reviews*, vol. 156, p. 111 915, 2022. DOI: 10.1016/j.rser.2021.111915.

[45] H. Kazmi, C. Fu, and C. Miller, "Ten questions concerning data-driven modelling and forecasting of operational energy demand at building and urban scale," *Building and Environment*, vol. 239, p. 110 407, 2023. DOI: 10.1016/j.buildenv.2023.110407.

[46] M. Gouda, S. Danaher, and C. Underwood, "Building thermal model reduction using nonlinear constrained optimization," *Building and Environment*, vol. 37, no. 12, pp. 1255–1265, Dec. 2002. DOI: 10.1016/s0360-1323(01)00121-4.

[47] *2017 ASHRAE Handbook: Fundamentals*. American Society of Heating, Refrigeration and Air-Conditioning Engineers, 2017.

[48] S. R. Mohandes, X. Zhang, and A. Mahdiyar, "A comprehensive review on the application of artificial neural networks in building energy analysis," *Neurocomputing*, vol. 340, pp. 55–75, May 2019. DOI: 10.1016/j.neucom.2019.02.040.

[49] H. Gao, C. Koch, and Y. Wu, "Building information modelling based building energy modelling: A review," *Applied Energy*, vol. 238, pp. 320–343, Mar. 2019. DOI: 10.1016/j.apenergy.2019.01.032.

[50] P. Singh and A. Sadhu, "Multicomponent energy assessment of buildings using building information modeling," *Sustainable Cities and Society*, vol. 49, p. 101 603, Aug. 2019. DOI: 10.1016/j.scs.2019.101603.

[51] E. Kamel and A. M. Memari, "Review of BIM's application in energy simulation: Tools, issues, and solutions," *Automation in Construction*, vol. 97, pp. 164–180, Jan. 2019. DOI: 10.1016/j.autcon.2018.11.008.

[52] A. Farzaneh, D. Monfet, and D. Forgues, "Review of using Building Information Modeling for building energy modeling during the design process," *Journal of Building Engineering*, vol. 23, pp. 127–135, May 2019. DOI: 10.1016/j.jobe.2019.01.029.

[53] J. A. Candanedo, C. Vallianos, B. Delcroix, *et al.*, "Control-oriented archetypes: A pathway for the systematic application of advanced controls in buildings," *Journal of Building Performance Simulation*, vol. 15, no. 4, pp. 433–444, 2022. DOI: 10.1080/19401493.2022.2063947.

[54] S. Asadi, E. Mostavi, D. Boussaa, and M. Indaganti, "Building energy model calibration using automated optimization-based algorithm," *Energy and Buildings*, vol. 198, pp. 106–114, 2019. DOI: 10.1016/j.enbuild.2019.06.001.

[55] A. Giretti, M. Vaccarini, M. Casals, M. Macarulla, A. Fuertes, and R. Jones, "Reduced-order modeling for energy performance contracting," *Energy and Buildings*, vol. 167, pp. 216–230, May 2018. DOI: 10.1016/j.enbuild.2018.02.049.

[56] M. H. Kristensen, R. Choudhary, and S. Petersen, "Bayesian calibration of building energy models: Comparison of predictive accuracy using metered utility data of different temporal resolution," in *Energy Procedia*, vol. 122, Elsevier, Sep. 2017, pp. 277–282. DOI: 10.1016/j.egypro.2017.07.322.

[57] M. Royapoor and T. Roskilly, "Building model calibration using energy and environmental data," *Energy and Buildings*, vol. 94, pp. 109–120, May 2015. DOI: 10.1016/j.enbuild.2015.02.050.

[58] S. Prívara, J. Cigler, Z. Váňa, F. Oldewurtel, C. Sagerschnig, and E. Žáčeková, "Building modeling as a crucial part for building predictive control," *Energy and Buildings*, vol. 56, pp. 8–22, 2013. DOI: 10.1016/j.enbuild.2012.10.024.

[59] D. Coakley, P. Raftery, and M. Keane, "A review of methods to match building energy simulation models to measured data," *Renewable and Sustainable Energy Reviews*, vol. 37, pp. 123–141, Sep. 2014. DOI: 10.1016/j.rser.2014.05.007.

[60] E. T. Maddalena, Y. Lian, and C. N. Jones, "Data-driven methods for building control — A review and promising future directions," *Control Engineering Practice*, vol. 95, p. 104 211, 2020. DOI: 10.1016/j.conengprac.2019.104211.

[61] V. Dermardiros, "Modelling and Experimental Evaluation of an Active Thermal Energy Storage System with Phase-Change Materials for Model-Based Control," M.S. thesis, Concordia University, Montreal, Canada, 2015.

[62] G. Mustafaraj, G. Lowry, and J. Chen, "Prediction of room temperature and relative humidity by autoregressive linear and nonlinear neural network models for an open office," *Energy and Buildings*, vol. 43, no. 6, pp. 1452–1460, 2011. DOI: 10.1016/j.enbuild.2011.02.007.

[63] A. Mechaqrane and M. Zouak, "A comparison of linear and neural network ARX models applied to a prediction of the indoor temperature of a building," *Neural Computing & Applications*, vol. 13, no. 1, pp. 32–37, Apr. 2004. DOI: 10.1007/s00521-004-0401-8.

[64] C. Deb, L. S. Eang, J. Yang, and M. Santamouris, "Forecasting diurnal cooling energy load for institutional buildings using Artificial Neural Networks," *Energy and Buildings*, vol. 121, pp. 284–297, 2016. DOI: 10.1016/j.enbuild.2015.12.050.

[65] A. Ruano, E. Crispim, E. Conceição, and M. Lúcio, "Prediction of building's temperature using neural networks models," *Energy and Buildings*, vol. 38, no. 6, pp. 682–694, 2006. DOI: 10.1016/j.enbuild.2005.09.007.

[66] H. U. Frausto and J. G. Pieters, "Modelling greenhouse temperature using system identification by means of neural networks," *Neurocomputing*, vol. 56, pp. 423–428, 2004. DOI: 10.1016/j.neucom.2003.08.001.

[67] M. Nørgaard, O. Ravn, and N. K. Poulsen, "NNSYSID and NNCTRL tools for system identification and control with neural networks," *Computing Control Engineering Journal*, vol. 12, no. 1, pp. 29–36, Feb. 2001. DOI: 10.1049/cce:20010105.

[68] A. Afram, F. Janabi-Sharifi, A. S. Fung, and K. Raahemifar, "Artificial neural network (ANN) based model predictive control (MPC) and optimization of HVAC systems: A state of the art review and case study of a residential HVAC system," *Energy and Buildings*, vol. 141, pp. 96–113, 2017. DOI: 10.1016/j.enbuild.2017.02.012.

[69] J. Drgoňa, D. Picard, M. Kvasnica, and L. Helsen, "Approximate model predictive building control via machine learning," *Applied Energy*, vol. 218, pp. 199–216, 2018. DOI: 10.1016/j.apenergy.2018.02.156.

[70] H. Shah and M. Gopal, "Model-Free Predictive Control of Nonlinear Processes Based on Reinforcement Learning," *IFAC-PapersOnLine*, vol. 49, no. 1, pp. 89–94, 2016. DOI: 10.1016/j.ifacol.2016.03.034.

[71] P. Ferreira, A. Ruano, S. Silva, and E. Conceição, "Neural networks based predictive control for thermal comfort and energy savings in public buildings," *Energy and Buildings*, vol. 55, pp. 238–251, 2012. DOI: 10.1016/j.enbuild.2012.08.002.

[72] F. Ferracuti, A. Fonti, L. Ciabattoni, *et al.*, "Data-driven models for short-term thermal behaviour prediction in real buildings," *Applied Energy*, vol. 204, pp. 1375–1387, Oct. 2017. DOI: 10.1016/j.apenergy.2017.05.015.

[73] C. Finck, R. Li, and W. Zeiler, "Economic model predictive control for demand flexibility of a residential building," *Energy*, vol. 176, pp. 365–379, 2019. DOI: 10.1016/j.energy.2019.03.171.

[74] Nasruddin, Sholahudin, P. Satrio, T. M. I. Mahlia, N. Giannetti, and K. Saito, "Optimization of HVAC system energy consumption in a building using artificial neural network and multi-objective genetic algorithm," *Sustainable Energy Technologies and Assessments*, vol. 35, pp. 48–57, 2019. DOI: 10.1016/j.seta.2019.06.002.

[75] J. Drgoňa, A. R. Tuor, V. Chandan, and D. L. Vrabie, "Physics-constrained deep learning of multi-zone building thermal dynamics," *Energy and Buildings*, vol. 243, p. 110 992, 2021. DOI: 10.1016/j.enbuild.2021.110992.

[76] L. Di Natale, B. Svetozarevic, P. Heer, and C. Jones, "Physically Consistent Neural Networks for building thermal modeling: Theory and analysis," *Applied Energy*, vol. 325, p. 119 806, 2022. DOI: 10.1016/j.apenergy.2022.119806.

[77] A. Athienitis and W. O'Brien, Eds., *Modeling, Design, and Optimization of Net-Zero Energy Buildings*. Berlin, Germany: Wilhelm Ernst & Sohn, Feb. 2015. DOI: 10.1002/9783433604625.

[78] Z. Afroz, G. Shafiullah, T. Urmee, and G. Higgins, "Modeling techniques used in building HVAC control systems: A review," *Renewable and Sustainable Energy Reviews*, vol. 83, pp. 64–84, 2018. DOI: 10.1016/j.rser.2017.10.044.

[79] G. Reynders, J. Diriken, and D. Saelens, "Quality of grey-box models and identified parameters as function of the accuracy of input and observation signals," *Energy and Buildings*, vol. 82, pp. 263–274, 2014.

[80] A. Fonti, G. Comodi, S. Pizzuti, A. Arteconi, and L. Helsen, "Low Order Grey-box Models for Short-term Thermal Behavior Prediction in Buildings," *Energy Procedia*, vol. 105, pp. 2107–2112, May 2017. DOI: 10.1016/j.egypro.2017.03.592.

[81] M. Lauster, J. Teichmann, M. Fuchs, R. Streblow, and D. Mueller, "Low order thermal network models for dynamic simulations of buildings on city district scale," *Building and Environment*, vol. 73, pp. 223–231, 2014. DOI: 10.1016/j.buildenv.2013.12.016.

[82] H. Li, Z. Wang, T. Hong, and M. A. Piette, "Energy flexibility of residential buildings: A systematic review of characterization and quantification methods and applications," *Advances in Applied Energy*, vol. 3, p. 100 054, 2021. DOI: 10.1016/j.adapen.2021.100054.

[83] V. Harish and A. Kumar, "A review on modeling and simulation of building energy systems," *Renewable and Sustainable Energy Reviews*, vol. 56, pp. 1272–1292, Apr. 2016. DOI: 10.1016/j.rser.2015.12.040.

[84] M. Killian and M. Kozek, "Ten questions concerning model predictive control for energy efficient buildings," *Building and Environment*, vol. 105, pp. 403–412, 2016. DOI: 10.1016/j.buildenv.2016.05.034.

[85] K. Arendt, M. Jradi, H. R. Shaker, and C. Veje, "Comparative analysis of white-, gray- and black-box models for thermal simulation of indoor environment: Teaching building case study," in *Proceedings of the 2018 Building Performance Modeling Conference and SimBuild co-organized by ASHRAE and IBPSA-USA, Chicago, IL, USA*, 2018, pp. 26–28.

[86] Y. Li, Z. O'Neill, L. Zhang, J. Chen, P. Im, and J. DeGraw, "Grey-box modeling and application for building energy simulations - A critical review," *Renewable and Sustainable Energy Reviews*, vol. 146, p. 111 174, 2021. DOI: 10.1016/j.rser.2021.111174.

[87] Z. Wang and Y. Chen, "Data-driven modeling of building thermal dynamics: Methodology and state of the art," *Energy and Buildings*, vol. 203, p. 109 405, Nov. 2019. DOI: 10.1016/j.enbuild.2019.109405.

[88] Y. Zong, G. M. Böning, R. M. Santos, S. You, J. Hu, and X. Han, "Challenges of implementing economic model predictive control strategy for buildings interacting with smart energy systems," *Applied Thermal Engineering*, vol. 114, pp. 1476–1486, 2017. DOI: 10.1016/j.applthermaleng.2016.11.141.

[89] Natural Resources Canada, "Energy Fact Book 2020-2021," Natural Resources Canada, Tech. Rep., 2021.

[90] U.S. Energy Information Administration, "Annual Energy Outlook 2021 with projections to 2050," U.S. Department of Energy, Tech. Rep., 2021.

[91] Eurostat, "Energy, transport and environment statistics: 2020 edition," European Comission, Tech. Rep., 2020. DOI: 10.2785/522192.

[92] S. Gyamfi, S. Krumdieck, and T. Urmee, "Residential peak electricity demand response—Highlights of some behavioural issues," *Renewable and Sustainable Energy Reviews*, vol. 25, pp. 71–77, 2013. DOI: 10.1016/j.rser.2013.04.006.

[93] S. Zhan and A. Chong, "Data requirements and performance evaluation of model predictive control in buildings: A modeling perspective," *Renewable and Sustainable Energy Reviews*, vol. 142, p. 110 835, May 2021. DOI: 10.1016/j.rser.2021.110835.

[94] J. Whitmore and P.-O. Pineau, "État de l'énergie au Québec 2023," French, Chaire de gestion du secteur de l'énergie, HEC Montréal, Tech. Rep., 2023.

[95] Hydro-Québec, *Dynamic pricing — residential customers*, [Online; accessed 9-January-2023], 2023.

[96] Y. Q. Ang, Z. M. Berzolla, and C. F. Reinhart, "From concept to application: A review of use cases in urban building energy modeling," *Applied Energy*, vol. 279, p. 115 738, 2020. DOI: 10.1016/j.apenergy.2020.115738.

[97] J. Langevin, J. Reyna, S. Ebrahimigharehbaghi, *et al.*, "Developing a common approach for classifying building stock energy models," *Renewable and Sustainable Energy Reviews*, vol. 133, p. 110 276, 2020. DOI: 10.1016/j.rser.2020.110276.

[98] Y. Ye, C. A. Faulkner, R. Xu, *et al.*, "System modeling for grid-interactive efficient building applications," *Journal of Building Engineering*, vol. 69, p. 106 148, 2023. DOI: 10.1016/j.jobe.2023.106148.

[99] D. Patteeuw, G. P. Henze, and L. Helsen, "Comparison of load shifting incentives for low-energy buildings with heat pumps to attain grid flexibility benefits," *Applied Energy*, vol. 167, pp. 80–92, 2016. DOI: 10.1016/j.apenergy.2016.01.036.

[100] G. Reynders, J. Diriken, and D. Saelens, "Generic characterization method for energy flexibility: Applied to structural thermal storage in residential buildings," *Applied Energy*, vol. 198, pp. 192–202, 2017. DOI: 10.1016/j.apenergy.2017.04.061.

[101] A. Wang, R. Li, and S. You, "Development of a data driven approach to explore the energy flexibility potential of building clusters," *Applied Energy*, vol. 232, pp. 89–100, 2018. DOI: 10.1016/j.apenergy.2018.09.187.

[102] T. Loga, B. Stein, and N. Diefenbach, "Tabula building typologies in 20 european countries—making energy-related features of residential building stocks comparable," *Energy and Buildings*, vol. 132, pp. 4–12, 2016. DOI: 10.1016/j.enbuild.2016.06.094.

[103] B. Glasgo, N. Khan, and I. L. Azevedo, "Simulating a residential building stock to support regional efficiency policy," *Applied Energy*, vol. 261, p. 114 223, 2020. DOI: 10.1016/j.apenergy.2019.114223.

[104] E. J. Wilson, C. B. Harris, J. J. Robertson, and J. Agan, "Evaluating energy efficiency potential in low-income households: A flexible and granular approach," *Energy Policy*, vol. 129, pp. 710–737, 2019. DOI: 10.1016/j.enpol.2019.01.054.

[105] E. J. H. Wilson, A. Parker, A. Fontanini, *et al.*, "End-Use Load Profiles for the U.S. Building Stock: Methodology and Results of Model Calibration, Validation, and Uncertainty Quantification," Tech. Rep., Mar. 2022. DOI: 10.2172/1854582.

[106] P. Westermann and R. Evins, "Surrogate modelling for sustainable building design – A review," *Energy and Buildings*, vol. 198, pp. 170–186, 2019. DOI: 10.1016/j.enbuild.2019.05.057.

[107] I. De Jaeger, G. Reynders, C. Callebaut, and D. Saelens, "A building clustering approach for urban energy simulations," *Energy and Buildings*, vol. 208, p. 109 671, 2020. DOI: 10.1016/j.enbuild.2019.109671.

[108] U. Ali, M. H. Shamsi, C. Hoare, E. Mangina, and J. O'Donnell, "A data-driven approach for multi-scale building archetypes development," *Energy and Buildings*, vol. 202, p. 109 364, 2019. DOI: 10.1016/j.enbuild.2019.109364.

[109] I. De Jaeger, J. Lago, and D. Saelens, "A probabilistic building characterization method for district energy simulations," *Energy and Buildings*, vol. 230, p. 110 566, 2021. DOI: 10.1016/j.enbuild.2020.110566.

[110] C. John, C. Vallianos, J. Candanedo, and A. Athienitis, "Estimating time constants for over 10,000 residential buildings in North America: towards a statistical characterization of thermal dynamics," in *Proceedings of the 7th International Building Physics Conference*, Syracuse, NY, 2018. DOI: 10.14305/ibpc.2018.ps17.

[111] G. Baasch, A. Wicikowski, G. Faure, and R. Evins, "Comparing Gray Box Methods to Derive Building Properties from Smart Thermostat Data," in *Proceedings of the 6th ACM International Conference on Systems for Energy-Efficient Buildings, Cities, and Transportation*, ser. BuildSys '19, New York, NY, USA: Association for Computing Machinery, 2019, pp. 223–232. DOI: 10.1145/3360322.3360836.

[112] M. M. Hossain, T. Zhang, and O. Ardakanian, "Identifying grey-box thermal models with Bayesian neural networks," *Energy and Buildings*, vol. 238, p. 110 836, 2021. DOI: 10.1016/j.enbuild.2021.110836.

[113] A. Doma, M. Ouf, G. Newsham, and H. Knudsen, "Investigating the Thermal Performance of Canadian Houses Using Smart Thermostat Data," *ASHRAE Transactions*, vol. 127, pp. 64–72, 2021.

[114] B. Huchuk, S. Sanner, and W. O'Brien, "Evaluation of data-driven thermal models for multi-hour predictions using residential smart thermostat data," *Journal of Building Performance Simulation*, vol. 15, no. 4, pp. 445–464, 2022. DOI: 10.1080/19401493.2020.1864474.

[115] J. Leprince, H. Madsen, C. Miller, *et al.*, "Fifty shades of grey: Automated stochastic model identification of building heat dynamics," *Energy and Buildings*, vol. 266, p. 112 095, 2022. DOI: 10.1016/j.enbuild.2022.112095.

[116] P. Bacher and H. Madsen, "Identifying suitable models for the heat dynamics of buildings," *Energy and Buildings*, vol. 43, no. 7, pp. 1511–1522, 2011. DOI: https://doi.org/10.1016/j.enbuild.2011.02.005.

[117] J. Leprince, C. Miller, H. Madsen, K. Basu, R. van der Vlist, and W. Zeiler, "Grey-brick buildings, an open data set of calibrated rc models of dutch residential building heat dynamics," in *Proceedings of the 20th ACM Conference on Embedded Networked Sensor Systems*, ser. SenSys '22, Boston, Massachusetts: Association for Computing Machinery, 2023, pp. 1067–1071. DOI: 10.1145/3560905.3567760.

[118] A. Doma and M. Ouf, "Data-driven approach to prioritize residential buildings' retrofits in cold climates using smart thermostat data," *Architectural Science Review*, vol. 66, no. 3, pp. 172–186, 2023. DOI: 10.1080/00038628.2023.2193164.

[119] M. Shin and J. S. Haberl, "Thermal zoning for building HVAC design and energy simulation: A literature review," *Energy and Buildings*, vol. 203, p. 109 429, 2019. DOI: 10.1016/j.enbuild.2019.109429.

[120] E. Žáčeková, Z. Váňa, and J. Cigler, "Towards the real-life implementation of MPC for an office building: Identification issues," *Applied Energy*, vol. 135, pp. 53–62, 2014. DOI: 10.1016/j.apenergy.2014.08.004.

[121] H. Harb, N. Boyanov, L. Hernandez, R. Streblow, and D. Müller, "Development and validation of grey-box models for forecasting the thermal response of occupied buildings," *Energy and Buildings*, vol. 117, pp. 199–207, 2016. DOI: 10.1016/j.enbuild.2016.02.021.

[122] M. Abtahi, A. Athienitis, and B. Delcroix, "Control-oriented thermal network models for predictive load management in Canadian houses with on-Site solar electricity generation: application to a research house," *Journal of Building Performance Simulation*, vol. 15, no. 4, pp. 536–552, 2022. DOI: 10.1080/19401493.2021.1998223.

[123] Z. Wang, Y. Chen, and Y. Li, "Development of RC model for thermal dynamic analysis of buildings through model structure simplification," *Energy and Buildings*, vol. 195, pp. 51–67, 2019. DOI: 10.1016/j.enbuild.2019.04.042.

[124] S. S. Hosseini, C. Vallianos, K. Agbossou, *et al.*, "Impact of Zoning Definition on Electrical Heating Systems Flexibility Potential in Residential Buildings: A Quebec Case Study," in *5th International Conference on Building Energy and Environment*, Jul. 2022.

[125] O. Brastein, D. Perera, C. Pfeifer, and N.-O. Skeie, "Parameter estimation for grey-box models of building thermal behaviour," *Energy and Buildings*, vol. 169, pp. 58–68, 2018. DOI: 10.1016/j.enbuild.2018.03.057.

[126] D. H. Yi, D. W. Kim, and C. S. Park, "Parameter identifiability in Bayesian inference for building energy models," *Energy and Buildings*, vol. 198, pp. 318–328, 2019. DOI: 10.1016/j.enbuild.2019.06.012.

[127] D. H. Yi and C. S. Park, "Model selection for parameter identifiability problem in bayesian inference of building energy model," *Energy and Buildings*, vol. 245, p. 111 059, 2021. DOI: 10.1016/j.enbuild.2021.111059.

[128] C. Agbi, Z. Song, and B. Krogh, "Parameter identifiability for multi-zone building models," in *2012 IEEE 51st IEEE Conference on Decision and Control (CDC)*, Issn: 0743-1546, Dec. 2012, pp. 6951–6956. DOI: 10.1109/cdc.2012.6425995.

[129] L. Ljung, *System Identification: Theory for the User* (Prentice Hall information and system sciences series). Prentice Hall PTR, 1999.

[130] S. Prívara, J. Cigler, Z. Váňa, F. Oldewurtel, and E. Žáčeková, "Use of partial least squares within the control relevant identification for buildings," *Control Engineering Practice*, vol. 21, no. 1, pp. 113–121, 2013. DOI: 10.1016/j.conengprac.2012.09.017.

[131] G. Reynders, J. Diriken, and D. Saelens, "Robustness of reduced-order models for prediction and simulation of the thermal behavior of dwellings," in *Proceedings of BS 2013: 13th Conference of the International Building Performance Simulation Association*, Aug. 2013.

[132] R. D. Coninck, F. Magnusson, J. Åkesson, and L. Helsen, "Toolbox for development and validation of grey-box building models for forecasting and control," *Journal of Building Performance Simulation*, vol. 9, no. 3, pp. 288–303, 2016. DOI: 10.1080/19401493.2015.1046933.

[133] J. Arroyo, F. Spiessens, and L. Helsen, "Identification of multi-zone grey-box building models for use in model predictive control," *Journal of Building Performance Simulation*, vol. 13, no. 4, pp. 472–486, 2020. DOI: 10.1080/19401493.2020.1770861.

[134] R. Gopaluni, R. Patwardhan, and S. Shah, "MPC relevant identification—tuning the noise model," *Journal of Process Control*, vol. 14, no. 6, pp. 699–714, 2004. DOI: 10.1016/j.jprocont.2003.05.001.

[135] R. Quachio and C. Garcia, "MPC relevant identification method for Hammerstein and Wiener models," *Journal of Process Control*, vol. 80, pp. 78–88, 2019. DOI: 10.1016/j.jprocont.2019.01.011.

[136] M. Pčolka, E. Žáčeková, R. Robinett, S. Čelikovský, and M. Šebek, "Bridging the gap between the linear and nonlinear predictive control: Adaptations for efficient building climate control," *Control Engineering Practice*, vol. 53, pp. 124–138, 2016. DOI: 10.1016/j.conengprac.2016.01.007.

[137] A. S. Potts, R. A. Romano, and C. Garcia, "Improving performance and stability of MPC relevant identification methods," *Control Engineering Practice*, vol. 22, pp. 20–33, 2014. DOI: 10.1016/j.conengprac.2013.09.007.

[138] J. Rehor and V. Havlena, "Grey-box model identification – control relevant approach," *IFAC Proceedings Volumes*, vol. 43, no. 10, pp. 117–122, 2010. DOI: 10.3182/20100826-3-TR-4015.00024.

[139] J. Zhao, Y. Zhu, and R. Patwardhan, "Some notes on MPC relevant identification," in *2014 American Control Conference*, 2014, pp. 3680–3685. DOI: 10.1109/acc.2014.6858665.

[140] S. Carlucci, M. De Simone, S. K. Firth, *et al.*, "Modeling occupant behavior in buildings," *Building and Environment*, vol. 174, p. 106 768, 2020. DOI: 10.1016/j.buildenv.2020.106768.

[141] Y. Ma, J. Matusko, and F. Borrelli, "Stochastic Model Predictive Control for Building HVAC Systems: Complexity and Conservatism," *Control Systems Technology, IEEE Transactions on*, vol. 23, pp. 101–116, Jan. 2015. DOI: 10.1109/TCST.2014.2313736.

[142] L. Sha, Z. Jiang, and H. Sun, "A control strategy of heating system based on adaptive model predictive control," *Energy*, vol. 273, p. 127 192, 2023. DOI: 10.1016/j.energy.2023.127192.

[143] H. Akaike, "A new look at the statistical model identification," *IEEE transactions on automatic control*, vol. 19, no. 6, pp. 716–723, 1974.

[144] G. Schwarz, "Estimating the Dimension of a Model," *The Annals of Statistics*, vol. 6, no. 2, pp. 461–464, 1978. DOI: 10.1214/aos/1176344136.

[145] J. E. Cavanaugh and A. A. Neath, "The akaike information criterion: Background, derivation, properties, application, interpretation, and refinements," *WIREs Computational Statistics*, vol. 11, no. 3, e1460, 2019. DOI: 10.1002/wics.1460.

[146] A. A. Neath and J. E. Cavanaugh, "The Bayesian information criterion: background, derivation, and applications," *WIREs Computational Statistics*, vol. 4, no. 2, pp. 199–203, 2012. DOI: 10.1002/wics.199.

[147] M. Bogdan, J. K. Ghosh, and M. Żak-Szatkowska, "Selecting explanatory variables with the modified version of the Bayesian information criterion," *Quality and Reliability Engineering International*, vol. 24, no. 6, pp. 627–641, 2008. DOI: 10.1002/qre.936.

[148] F. Pallonetto, E. Mangina, F. Milano, and D. P. Finn, "SimApi, a smartgrid co-simulation software platform for benchmarking building control algorithms," *SoftwareX*, vol. 9, pp. 271–281, 2019. DOI: 10.1016/j.softx.2019.03.003.

[149] P. Scharnhorst, B. Schubnel, C. Fernández Bandera, *et al.*, "Energym: A Building Model Library for Controller Benchmarking," *Applied Sciences*, vol. 11, no. 8, 2021. DOI: 10.3390/app11083518.

[150] D. Blum, J. Arroyo, S. Huang, *et al.*, "Building optimization testing framework (BOPTEST) for simulation-based benchmarking of control strategies in buildings," *Journal of Building Performance Simulation*, vol. 14, no. 5, pp. 586–610, 2021. DOI: 10.1080/19401493.2021.1986574.

[151] C. Vallianos, A. Athienitis, and B. Delcroix, "Automatic generation of multi-zone RC models using smart thermostat data from homes," *Energy and Buildings*, vol. 277, p. 112 571, 2022. DOI: 10.1016/j.enbuild.2022.112571.

[152] D. Gyalistras, M. Gwerder, F. Oldewurtel, C. Jones, and M. Morari, "Analysis of energy savings potentials for integrated room automation," in *Clima-RHEVA World Congress*, 2010.

[153] S. Freund and G. Schmitz, "Implementation of model predictive control in a large-sized, low-energy office building," *Building and Environment*, vol. 197, p. 107 830, 2021. DOI: 10.1016/j.buildenv.2021.107830.

[154] C. Vallianos, A. Athienitis, and J. Rao, "Hybrid ventilation in an institutional building: Modeling and predictive control," *Building and Environment*, vol. 166, p. 106 405, 2019. DOI: 10.1016/j.buildenv.2019.106405.

[155] A. Foucquier, S. Robert, F. Suard, L. Stéphan, and A. Jay, "State of the art in building modelling and energy performances prediction: A review," *Renewable and Sustainable Energy Reviews*, vol. 23, pp. 272–288, Jul. 2013. DOI: 10.1016/j.rser.2013.03.004.

[156] F. Neirotti, M. Noussan, and M. Simonetti, "Towards the electrification of buildings heating - Real heat pumps electricity mixes based on high resolution operational profiles," *Energy*, vol. 195, p. 116 974, 2020. DOI: 10.1016/j.energy.2020.116974.

[157] R. A. Lara, E. Naboni, G. Pernigotto, *et al.*, "Optimization Tools for Building Energy Model Calibration," *Energy Procedia*, vol. 111, pp. 1060–1069, 2017. DOI: 10.1016/j.egypro.2017.03.269.

[158] A. Cacabelos, P. Eguía, L. Febrero, and E. Granada, "Development of a new multi-stage building energy model calibration methodology and validation in a public library," *Energy and Buildings*, vol. 146, pp. 182–199, 2017. DOI: 10.1016/j.enbuild.2017.04.071.

[159] F. Zhang, C. Deb, S. E. Lee, J. Yang, and K. W. Shah, "Time series forecasting for building energy consumption using weighted Support Vector Regression with differential evolution optimization technique," *Energy and Buildings*, vol. 126, pp. 94–103, 2016. DOI: 10.1016/j.enbuild.2016.05.028.

[160] J. A. Date, "A Study of Impact of Thermal Model Resolution and Zone Set Point Profiles on Peak Heating Load and its Calculation," M.S. thesis, Concordia University, Jul. 2015.

[161] X. Zhang, D. Saelens, and S. Roels, "Estimating dynamic solar gains from on-site measured data: An ARX modelling approach," *Applied Energy*, vol. 321, p. 119 278, 2022. DOI: 10.1016/j.apenergy.2022.119278.

[162] D. Kim, J. Cai, K. B. Ariyur, and J. E. Braun, "System identification for building thermal systems under the presence of unmeasured disturbances in closed loop operation: Lumped disturbance modeling approach," *Building and Environment*, vol. 107, pp. 169–180, 2016. DOI: 10.1016/j.buildenv.2016.07.007.

[163] C. Vallianos, M. Abtahi, A. Athienitis, B. Delcroix, and L. Rueda, "Online model-based predictive control with smart thermostats: Application to an experimental house in Québec," *Journal of Building Performance Simulation*, pp. 1–17, 2023. DOI: 10.1080/19401493.2023.2243602.

[164] A. Murray, T. Schütz, G. Pan, D. Müller, and V. Hagenmeyer, "On modelling effects in the battery and thermal storage scheduling problem," *Journal of Building Performance Simulation*, vol. 14, no. 1, pp. 38–51, 2021. DOI: 10.1080/19401493.2020.1838611.

[165] S. S. Ravi and M. Aziz, "Utilization of Electric Vehicles for Vehicle-to-Grid Services: Progress and Perspectives," *Energies*, vol. 15, no. 2, 2022. DOI: 10.3390/en15020589.

[166] C. Vallianos, S. Saeed Hosseini, A. Athienitis, *et al.*, "Automated RC Model Generation for MPC Applications to Energy Flexibility Studies in Québec Houses," in *Proceedings of the 5th International Conference on Building Energy and Environment*, L. L. Wang, H. Ge, Z. J. Zhai, *et al.*, Eds., Singapore: Springer Nature Singapore, 2023, pp. 1331–1340. DOI: 10.1007/978-981-19-9822-5_73.

[167] M. Fiorentini, L. L. Gomis, D. Chen, and P. Cooper, "On the impact of internal gains and comfort band on the effectiveness of building thermal zoning," *Energy and Buildings*, vol. 225, p. 110 320, 2020. DOI: 10.1016/j.enbuild.2020.110320.

[168] C. Vallianos, J. Candanedo, and A. Athienitis, "Application of a large smart thermostat dataset for model calibration and Model Predictive Control implementation in the residential sector," *Energy*, vol. 278, p. 127 839, 2023. DOI: 10.1016/j.energy.2023.127839.

[169] *SIMEB - Données météo*.

[170] *Solcast, 2019, Global solar irradiance data and PV system power output data, https://solcast.com*, en.

[171] N. Henao, M. Fournier, and S. Kelouwani, "Characterizing smart thermostats' operation in residential zoned heating systems and their impact on energy saving metrics," en-US, ser. eSim, vol. 10, IBPSA-Canada, 2018, pp. 17–25.

[172] A. Alessandri, M. Baglietto, and G. Battistelli, "Moving-horizon state estimation for nonlinear discrete-time systems: New stability results and approximation schemes," *Automatica*, vol. 44, no. 7, pp. 1753–1765, 2008. DOI: 10.1016/j.automatica.2007.11.020.

[173] S. Diamond and S. Boyd, *CVXPY: A Python-Embedded Modeling Language for Convex Optimization*, Number: arXiv:1603.00943 arXiv:1603.00943 [math], Jun. 2016. DOI: 10.48550/arXiv.1603.00943.

[174] H. T. Haider, O. H. See, and W. Elmenreich, "A review of residential demand response of smart grid," *Renewable and Sustainable Energy Reviews*, vol. 59, pp. 166–178, 2016. DOI: 10.1016/j.rser.2016.01.016.

[175] C. Vallianos, M. Abtahi, A. Athienitis, B. Delcroix, and L. Rueda, *Experimental House of Building Energetics Model Predictive Control experiment data*, version v1.0, Zenodo, Jun. 2023. DOI: 10.5281/zenodo.8021941.

[176] F. Mostafavi, M. Tahsildoost, and Z. Zomorodian, "Energy efficiency and carbon emission in high-rise buildings: A review (2005-2020)," *Building and Environment*, vol. 206, p. 108 329, 2021. DOI: 10.1016/j.buildenv.2021.108329.

[177] F. Pelletier and A. Faruqui, "Does dynamic pricing work in a winter-peaking climate? A case study of Hydro Québec," *The Electricity Journal*, vol. 35, no. 2, p. 107 080, 2022. DOI: 10.1016/j.tej.2022.107080.

[178] geopy, *Python client for several popular geocoding web services*, [Online; accessed 8-January-2023], 2023.

[179] Nominatim, *Open-source geocoding with OpenStreetMap data*, [Online; accessed 8-January-2023], 2023.

[180] M. Sengupta, Y. Xie, A. Lopez, A. Habte, G. Maclaurin, and J. Shelby, "The National Solar Radiation Data Base (NSRDB)," *Renewable and Sustainable Energy Reviews*, vol. 89, pp. 51–60, Jun. 2018. DOI: 10.1016/j.rser.2018.03.003.

[181] P. Virtanen, R. Gommers, T. E. Oliphant, *et al.*, "SciPy 1.0: Fundamental Algorithms for Scientific Computing in Python," *Nature Methods*, vol. 17, pp. 261–272, 2020. DOI: 10.1038/s41592-019-0686-2.

[182] J. D. Rhodes, W. J. Cole, C. R. Upshaw, T. F. Edgar, and M. E. Webber, "Clustering analysis of residential electricity demand profiles," *Applied Energy*, vol. 135, pp. 461–471, 2014. DOI: 10.1016/j.apenergy.2014.08.111.

[183] H. Madsen, Ed., *Time Series Analysis*. New York, NY, USA: Chapman and Hall/CRC, Feb. 2007. DOI: 10.1201/97814200596875.

[184] J. Palmer Real, C. Rasmussen, R. Li, *et al.*, "Characterisation of thermal energy dynamics of residential buildings with scarce data," *Energy and Buildings*, vol. 230, p. 110 530, 2021. DOI: 10.1016/j.enbuild.2020.110530.

[185] O. E. Board, *Electricity rates*, [Online; accessed 9-January-2023], 2023.

[186] C. Vallianos, J. Candanedo, and A. Athienitis, "Thermal modeling for control applications of 60,000 homes in north america using smart thermostat data," *Energy and Buildings*, p. 113 811, 2023. DOI: 10.1016/j.enbuild.2023.113811.

[187] L. Gelazanskas and K. A. Gamage, "Demand side management in smart grid: A review and proposals for future direction," *Sustainable Cities and Society*, vol. 11, pp. 22–30, 2014. DOI: 10.1016/j.scs.2013.11.001.

[188] H. Das, M. Rahman, S. Li, and C. Tan, "Electric vehicles standards, charging infrastructure, and impact on grid integration: A technological review," *Renewable and Sustainable Energy Reviews*, vol. 120, p. 109 618, 2020. DOI: 10.1016/j.rser.2019.109618.

[189] Z. Shi and W. O'Brien, "Development and implementation of automated fault detection and diagnostics for building systems: A review," *Automation in Construction*, vol. 104, pp. 215–229, 2019. DOI: https://doi.org/10.1016/j.autcon.2019.04.002.

[190] B. Gunay, B. W. Hobson, D. Darwazeh, and J. Bursill, "Estimating energy savings from hvac controls fault correction through inverse greybox model-based virtual metering," *Energy and Buildings*, vol. 282, p. 112 806, 2023. DOI: https://doi.org/10.1016/j.enbuild.2023.112806.

[191] C. Deb and A. Schlueter, "Review of data-driven energy modelling techniques for building retrofit," *Renewable and Sustainable Energy Reviews*, vol. 144, p. 110 990, 2021. DOI: https://doi.org/10.1016/j.rser.2021.110990.

[192] P. Gunn, H. B. Gunay, P. J. Van Geel, and C. Baldwin, "Development of resistor-capacitor and finite difference models to evaluate green roof thermal performance," *Building and Environment*, vol. 226, p. 109 700, 2022. DOI: https://doi.org/10.1016/j.buildenv.2022.109700.

[193] U. Ali, M. H. Shamsi, C. Hoare, E. Mangina, and J. O'Donnell, "Review of urban building energy modeling (ubem) approaches, methods and tools using qualitative and quantitative analysis," *Energy and Buildings*, vol. 246, p. 111 073, 2021. DOI: https://doi.org/10.1016/j.enbuild.2021.111073.

[194] A. Petrucci, F. K. Ayevide, A. Buonomano, and A. Athienitis, "Development of energy aggregators for virtual communities: The energy efficiency-flexibility nexus for demand response," *Renewable Energy*, vol. 215, p. 118 975, 2023. DOI: https://doi.org/10.1016/j.renene.2023.118975.

[195] C. Vallianos, J. Candanedo, and A. Athienitis, *North american house thermal models*, version v1.0, Zenodo, Sep. 2023. DOI: 10.5281/zenodo.8347091.

[196] Ecobee, *Donate your data*, [Online; accessed 30-June-2023], 2023.

[197] H. E. Beck, N. E. Zimmermann, T. R. McVicar, N. Vergopolan, A. Berg, and E. F. Wood, "Publisher correction: Present and future köppen-geiger climate classification maps at 1-km resolution," *Scientific Data*, vol. 7, no. 1, p. 274, Aug. 2020. DOI: 10.1038/s41597-020-00616-w.

[198] Commission for Environmental Cooperation (CEC), *Climate zones of north america*, Scientific Data 5:180214. Ed. 1.0, Vector digital data [1:10,000,000], arcGIS, 2021.

[199] R Core Team, *R: A language and environment for statistical computing*, R Foundation for Statistical Computing, Vienna, Austria, 2022.

[200] Technical University of Denmark Compute, *Ctsmr: Continuous time stochastic modelling for r*, [Online; accessed 30-June-2023], 2023.

[201] N. R. Kristensen and H. Madsen, "Continous time stochastic modelling: Ctsm 2.3," Technical University of Denmark, Mathematics Guide, 2003.

[202] N. R. Kristensen, H. Madsen, and S. B. Jørgensen, "Parameter estimation in stochastic grey-box models," *Automatica*, vol. 40, no. 2, pp. 225–237, 2004. DOI: 10.1016/j.automatica.2003.10.001.

[203] H. Hofmann, H. Wickham, and K. Kafadar, "Letter-Value Plots: Boxplots for Large Data," *Journal of Computational and Graphical Statistics*, vol. 26, no. 3, pp. 469–477, 2017. DOI: 10.1080/10618600.2017.1305277.

[204] B. C. Ubah, *Control: A control systems toolbox*, 2017.

A Data of EHBE

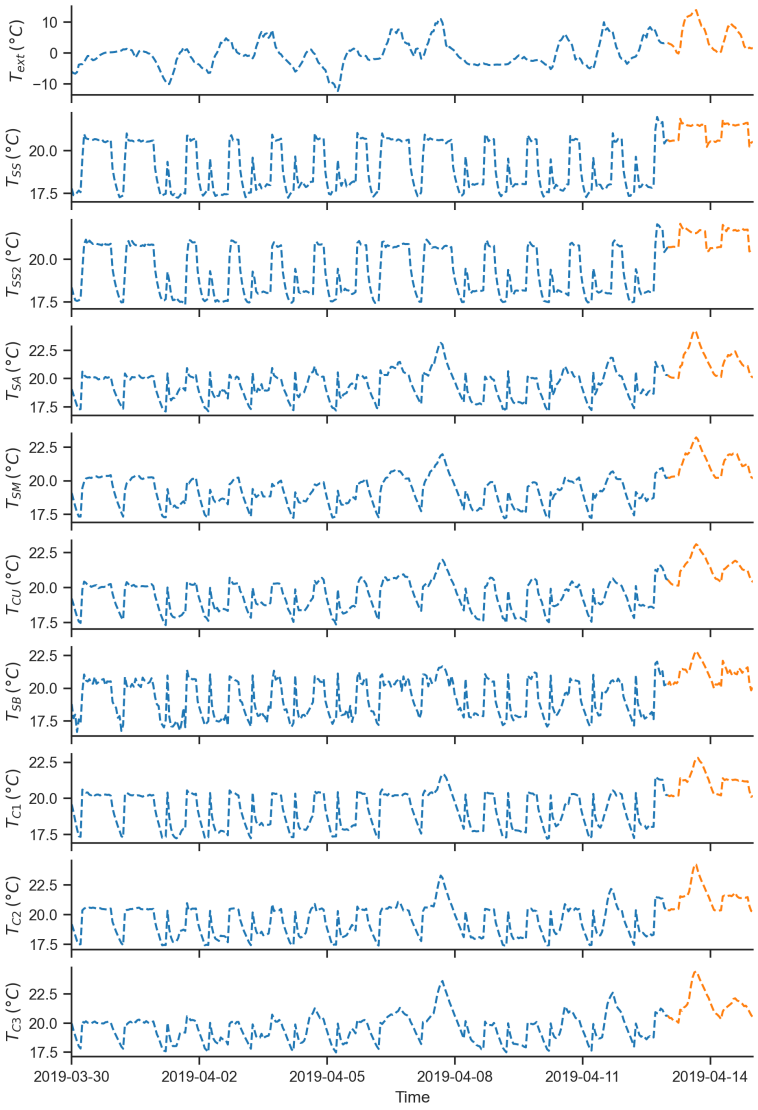

Figure A.1: Measured data of outdoor temperature and zone indoor temperatures of EHBE. The blue line represents the training set used in parameter calibration and the orange one is the test set

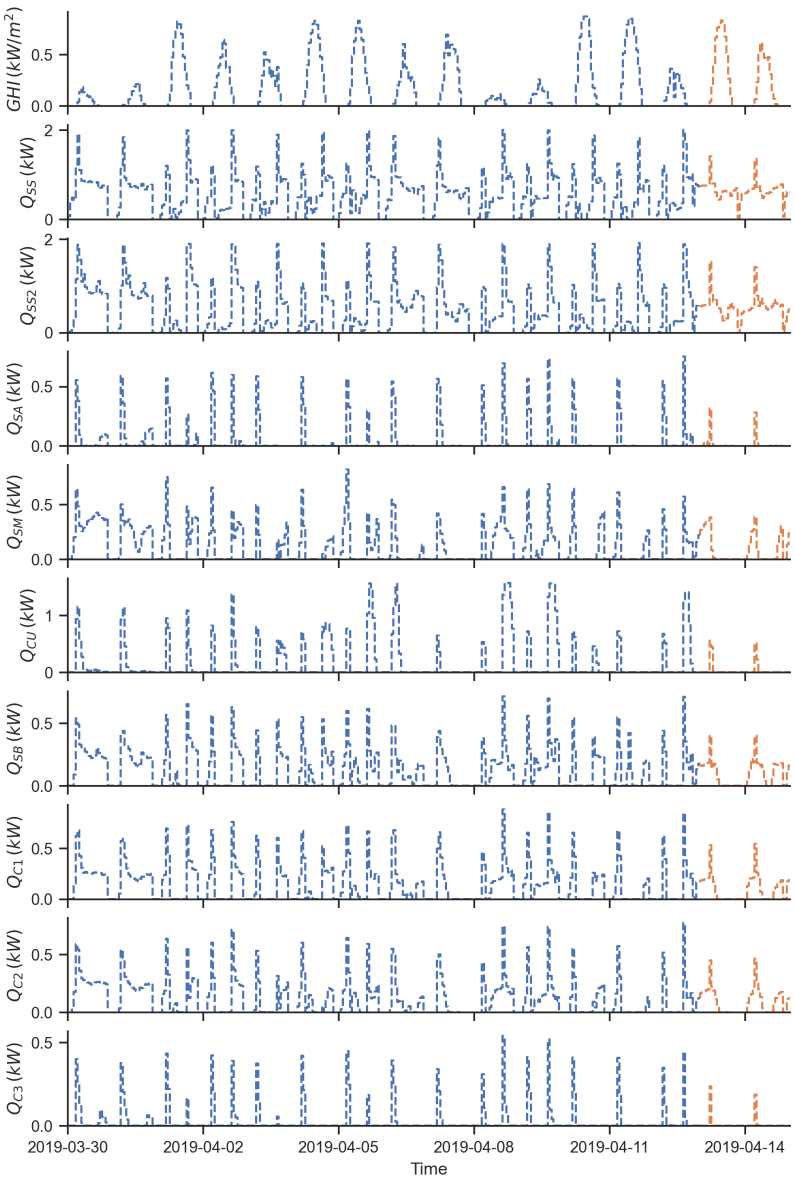

Figure A.2: Measured data of global horizontal irradiance and zone heating of EHBE. The blue line represents the training set used in parameter calibration and the orange one is the test set

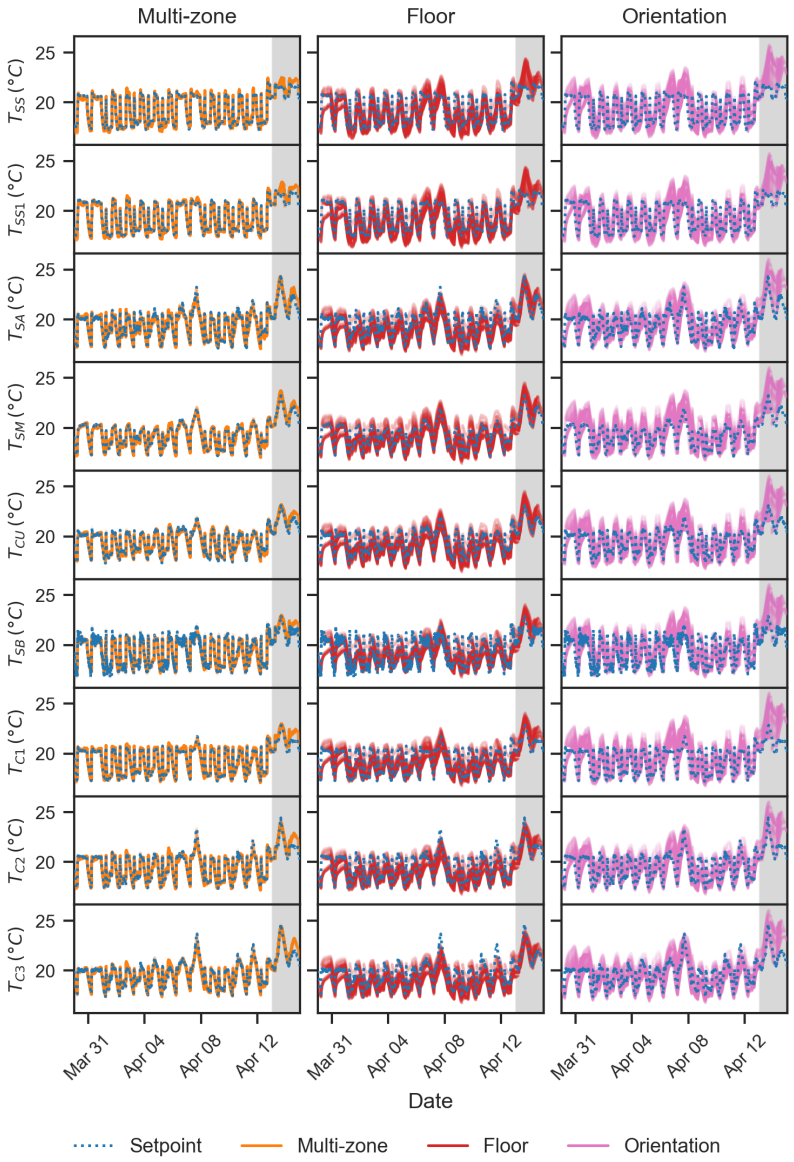

Figure A.3: 24-hour predicted zone temperatures every 15 minutes for each model. The shaded area represents the test set, i.e., data that the models had not seen during the calibration procedure

B Metadata effect on parameters of models calibrated with the Ecobee dataset

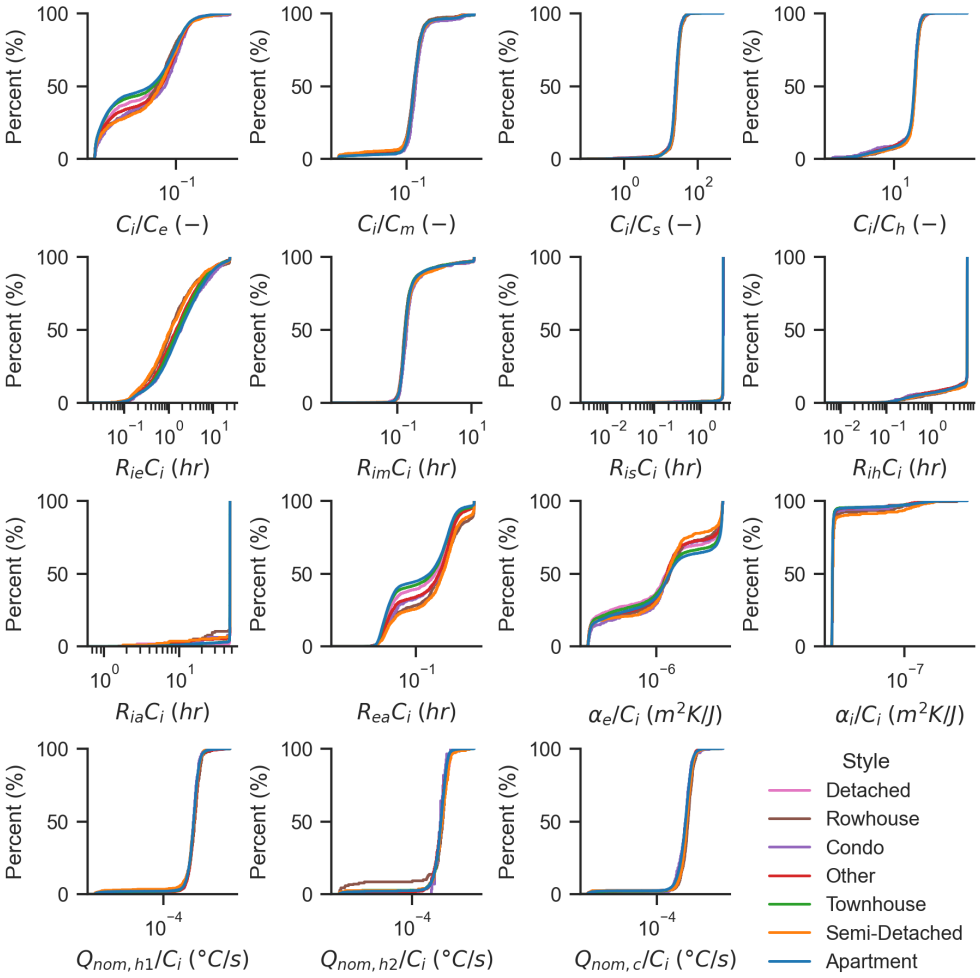

Figure B.1: Cumulative distribution functions of parameters for the different house styles.

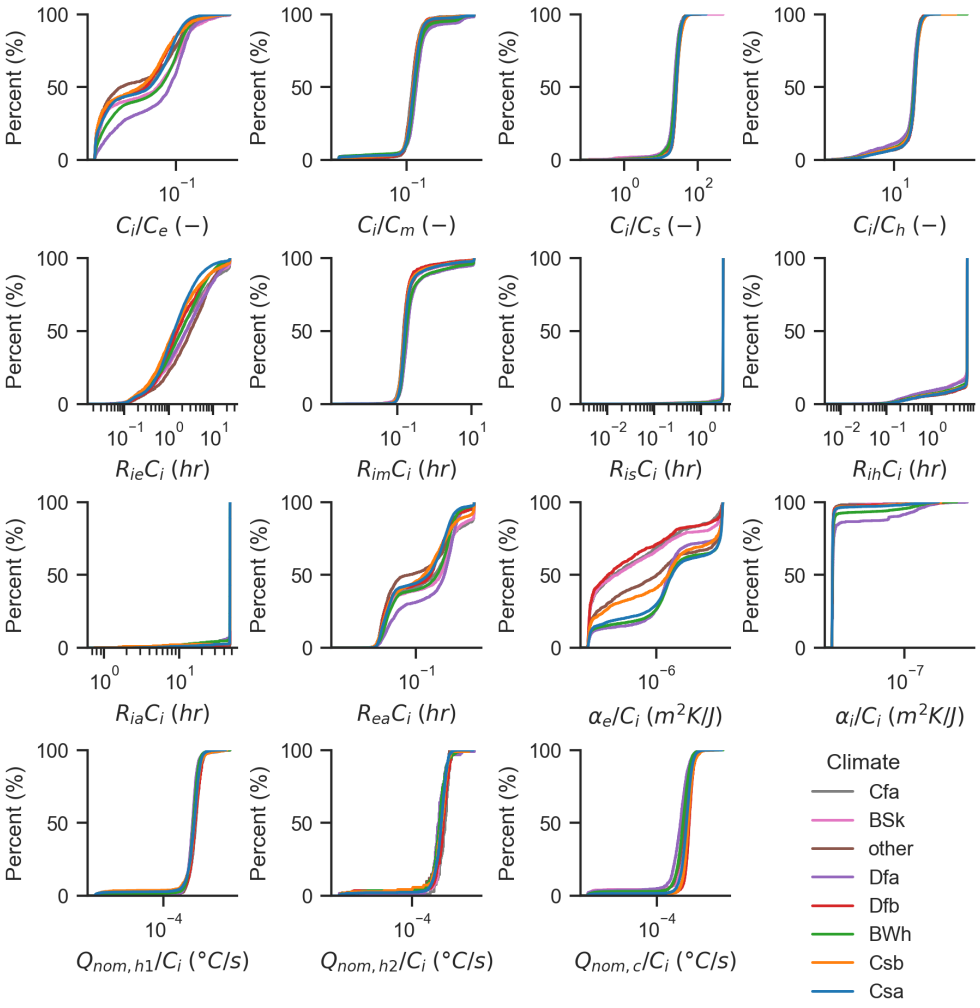

Figure B.2: Cumulative distribution functions of parameters for the different climates.

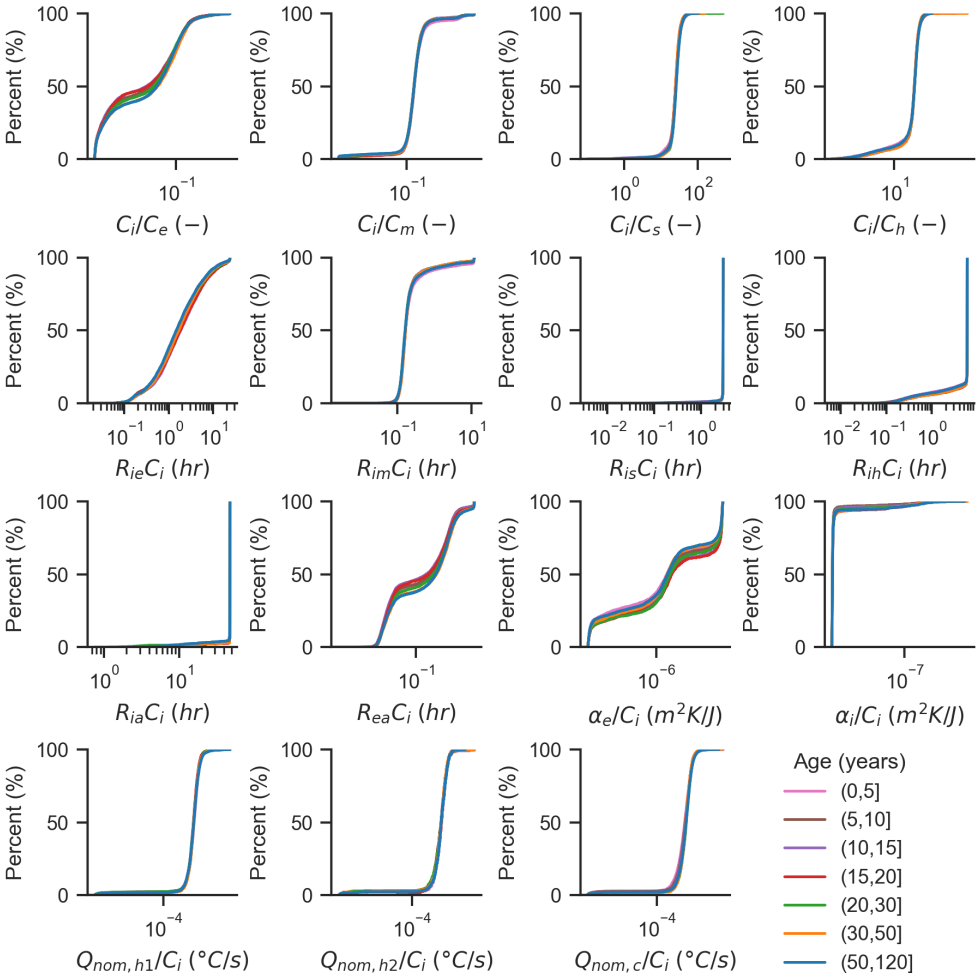

Figure B.3: Cumulative distribution functions of parameters for the different house ages.

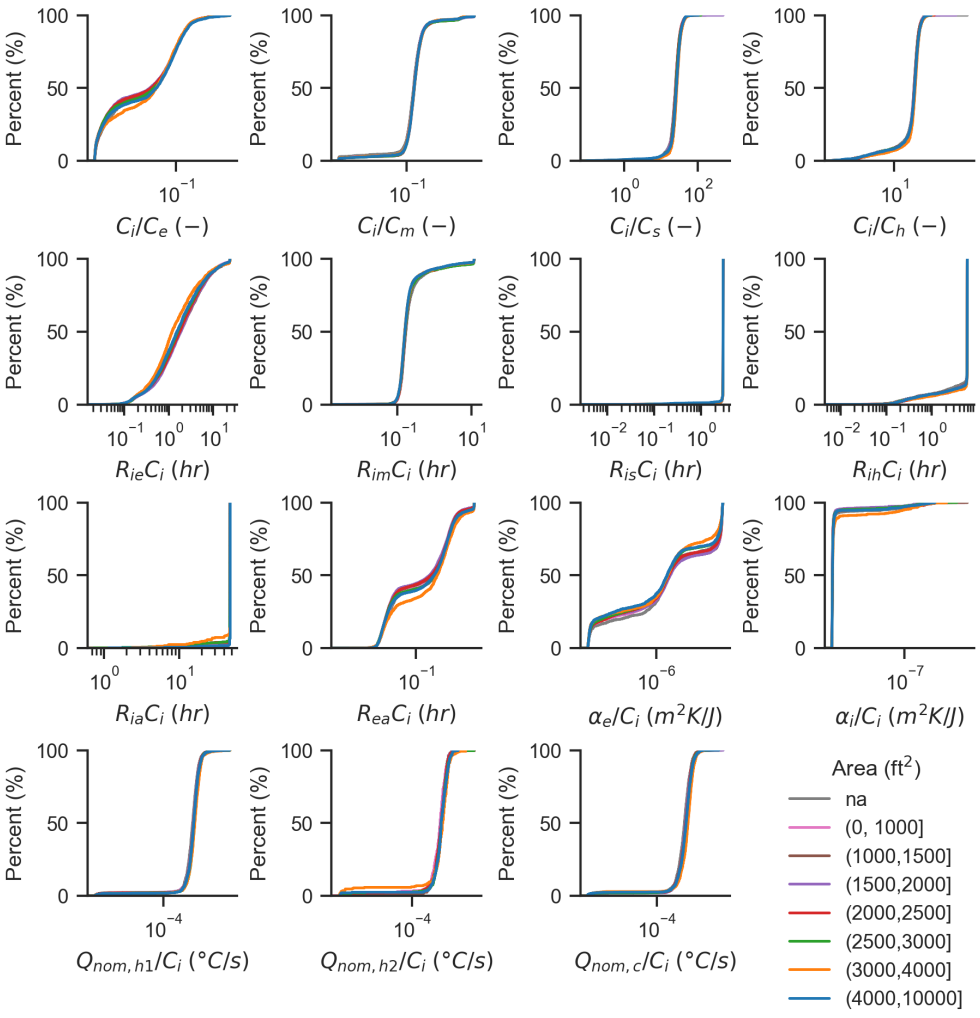

Figure B.4: Cumulative distribution functions of parameters for the different house floor areas.

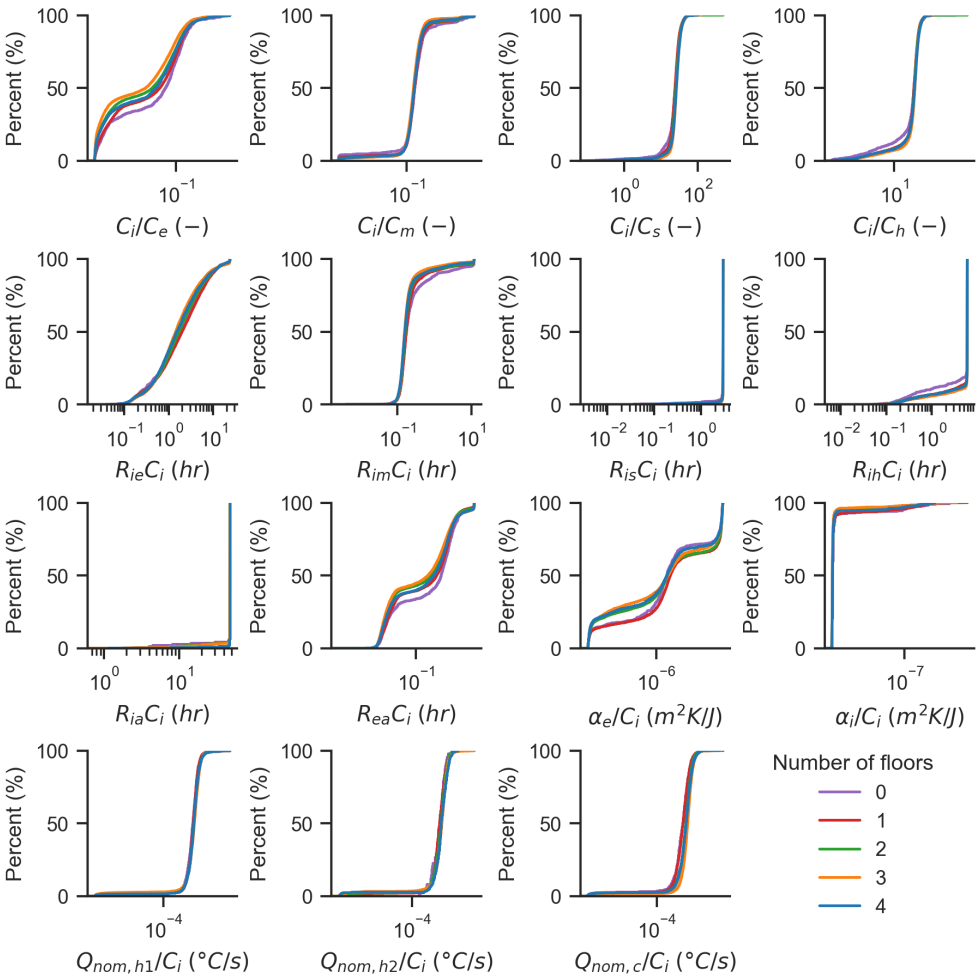

Figure B.5: Cumulative distribution functions of parameters for the different numbers of floors.

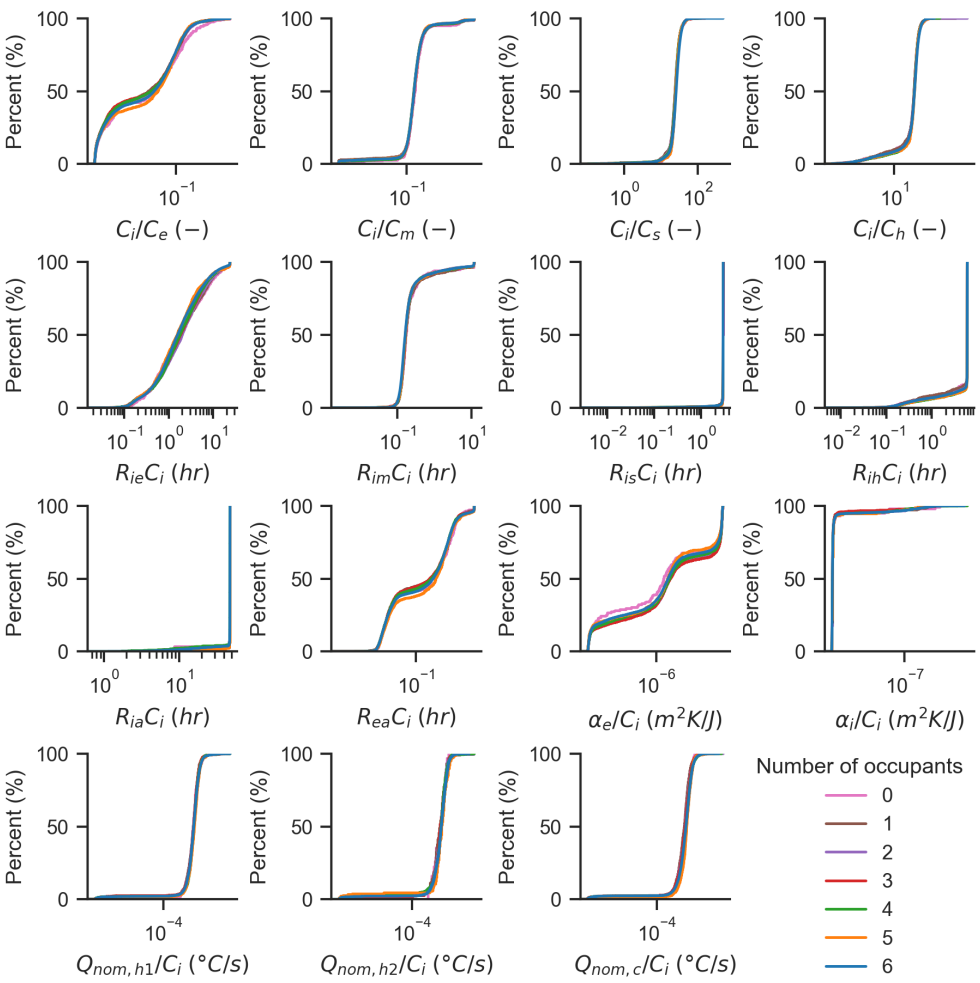

Figure B.6: Cumulative distribution functions of parameters for the different numbers of occupants.